A study of the Transport, Extraction and Co-ordination Chemistry of a number of Thiourea Ligands with a series of Transition and Post-transition metal Ions

by

Michael M. Habtu

Thesis presented in fulfillment of the requirements for the
degree of **Master of Science** at the **University of**
Stellenbosch

Supervisors: ***Professor K. R. Koch*** *and* ***Dr. R. C. Luckay***

December 2003

Declaration

I, the undersigned, hereby declare that the work contained in this thesis is my original work and that I have not previously in its entirety or in part submitted it at any university for a degree.

Signature:

Date:

Abstract

In this study, a number of mono- and di-substituted acyl(aroyl)thioureas were investigated for potential application as specific carriers (ionophores) for the transport and extraction of Ag(I) from a mixture of Co(II), Ni(II), Cu(II), Zn(II), Cd(II), and Pb(II) ions. The experimental arrangement for the transport experiments employed a liquid membrane set up involving a 3-phase system – 2 aqueous phases (source and receiving phase) separated by a chloroform membrane incorporating the ligand. Competitive metal ion transport experiments were conducted using the liquid membrane set up. The aqueous source and receiving phases were analyzed using Atomic Absorption Spectroscopy (AAS) and results were confirmed by Inductively Coupled Plasma-Optical Emission Spectroscopy (ICP-OES). The transport results show that the *N,N*-dialkyl-substituted-*N'*-acyl(aroyl) (HL) thioureas studied, with the exception of the *N,N*-di-(2-hydroxyethyl)-*N'*-benzoylthiourea (HL^3) and *N*-piperidyl-*N'*-4-nitrobenzoylthiourea (HL^9), were efficient and selective for Ag(I). HL^9 was also selective for Ag(I) but not efficient. HL^3 was selective for Cu(II). Under the experimental conditions employed, 13% Cu(II) was transported by HL^3. Among the *N,N*-dialkyl-*N'*-aroylthioureas, maximum Ag(I) transport was obtained by using *N,N*-diethyl-*N'*-4-chlorobenzoylthiourea (HL^5) and *N,N*-di-n-butyl-*N'*-benzoylthiourea (HL^1). Under the experimental conditions employed, the percentages of Ag(I) transported by HL^5 and HL^1 were 48% and 42% respectively.

The transport selectivity and efficiency of 3,3,3',3'-tetraethyl-1,1'-isophthaloylbisthiourea (H_2L^{12}) and *N,N*-diethyl-*N'*-camphanoylthiourea (HL^{13}) for Ag(I) were also studied. We were particularly interested in comparing the Ag(I) transport and extraction efficiency of these ligands with that of the HL and H_2L ligands. The experimental results reveal that, of all the ligands we investigated in this study, HL^{13} was the most efficient and selective carrier for Ag(I) transport. The interesting result is that, depending on the ligand concentration used, HL^{13} transported 71-81% of Ag(I).

Competitive two-phase metal ion solvent extraction experiments were also performed under conditions similar to the transport studies. The results show that by varying the ligand concentration in the membrane phase, up to 100% Ag(I) can be selectively and efficiently extracted from the mixture of the seven metal ions.

Finally, the *N*,*N*-di-(n)-butyl-*N'*-benzoylthiourea (HL^1) ligand and its complex with Ag(I) were synthesized. Single crystals of the complex were grown for X-ray crystallography and the crystal and molecular structure of the complex was determined. The crystal structure showed that Ag(I) is bonded to the deprotonated ligand through the *S*,*O* atoms forming interesting cluster $[Ag\ (L - S,\ O)]_4$ in the solid state. This structure is monoclinic and crystallizes in the space group $P2_1/c$ with a = 17.805 (4) Å, b = 21.759 (4) Å, c = 36.438 (7) Å, β= 96.34(3)^0, Z = 8 and a final R-factor of 5.4%.

Samevatting

In hierdie proefskrif is ‘n aantal mono- en di-gesubstitueerde asiel(ariel) tioureums ondersoek vir moontlike gebruik as ionofore (spesifieke draers) vir die transportasie en ekstraksie van Ag(I) vanuit ‘n mengsel van Co(II), Ni(II), Cu(II), Zn(II), Cd(II), Ag(I) en Pb(II) ione.

‘n Drie-fase selsisteem is gebruik vir die transportasie eksperimente, twee waterige fases (bron- en ontvang-fase) wat geskei is met die chloroform membraan fase wat die ligande bevat. Kompeterende metaalioon transportasie eksperimente is uitgevoer met behulp van hierdie vloeistof membraan stelsel. Die twee waterige fases is deur middel van Atoomabsorpsie Spektroskopie (AAS) ge-analiseer en resultate is bevestig met gebruik van Induktief-gekoppelde Plasma-Optiese Emissie Spektroskopie (IGP-OES). Die resultate het getoon dat elkeen van die *N*,*N*-dialkiel-gesubstitueerde-*N'*-asiel(ariel) (HL) tioureums, met uitsondering van *N*,*N*-di(2-hidroksie-etiel)-*N'*-benzieltioureum(HL^3) en *N*-piperidiel-*N'*-4-nitrobenzieltioureum(HL^9), doeltreffend en selektief was vir Ag(I) transportasie. HL^9 was selektief vir Ag(I), maar die transportasie waarde was nie hoog nie, dws. dit was nie doeltreffend nie. HL^3 was selektief vir Cu(II). Met gebruik van ons eksperimentele kondisies is 13% Cu(II) getransporteer deur HL^3. Van die *N*,*N*-dialkiel-*N'*-ariel tioureums, is maksimum transportasie van Ag(I) verkry met gebruik van *N*,*N*-dietiel-*N'*-4-chlorobenzieltioureum (HL^5) en *N*,*N*-di-n-butiel-*N'*-benzieltioureum (HL^1). Met gebruik van ons eksperimentele kondisies was die persentasie transportasie van Ag(I) deur HL^5 en HL^1 48% en 42% onderskeidelik.

Die selektiwiteit en doeltreffendheid van 3,3,3',3'-tetra-etiel-1,1'-isoftalielbistioureum(H_2L^{12}) en *N*,*N*-di-etiel-*N'*-kamfonieltioureum (HL^{13}) vir Ag(I) transportasie is ook onderneem. Ons was besonder ge-interesseerd om die Ag(I) transportasie en ekstraksie van hierdie ligande te vergelyk met dié van die HL en H_2L tipe ligande. Die eksperimentele resultate het getoon dat van al die ligande wat bestudeer is, HL^{13} die doeltreffendste en mees selektiewe ionofoor was. Van besondere, belang was dat, afhangend van die ligand konsentrasie wat gebruik is, HL^{13} 71-81% Ag(I) getransporteer het.

Kompeterende twee-fase metaalioon vloeistof-vloeistof ekstraksie eksperimente is ook uitgevoer onder toestande soortgelyk aan dié van die transportasie eksperimente. Die resultate toon dat met varierende ligand konsentrasie, tot soveel as 100% Ag(I) selektief en doeltreffend geëkstrakeer word vanuit ,n mengsel van die sewe metaal ione.

N,*N*-di-n-butiel-*N*′-benzieltioureum (HL^1) ligande en die kompleks daarvan met Ag(I) is ook gesintetiseer. Enkel-kristalle van die kompleks is verkry en X-straal kristallografiese analiese is onderneem. Die kristalstruktuur toon hoedat Ag(I) gebind is aan die gedeprotoneerde ligand deur die S en O atome en toon ook interessante $[Ag(L\text{-}S,O)]_4$ groepe in die vaste toestand. Hierdie struktuur is monoklinies en kristaliseer in die ruimtegroep $P2_1/c$ met a = 17.805(4) Á, b = 21.759(4)Á, c = 36.438(7)Á, β = 96.34(3)°, z = 8 en 'n finale R-faktor van 5.4%.

Dedication

To my beloved family

Acknowledgements

I wish to preface this work with many thanks to God, the author and perfector of my faith and whose light shines upon my path always!

This research has benefited from the inputs of many; although my gratitude is to all, I would like to mention some. My deepest appreciation goes to my supervisors, Prof. K. R. Koch and Dr. R. C. Luckay for their expert guidance, continued advice and fruitful suggestions to my work. My gratitude also goes to the following colleagues: Dr. M.W. Esterhuysen for carefully refining my crystal structure and Mr. A. Westra for reading Chapters one and two of my thesis and his constructive comments on them. I would also like to thank Mr. A. Westra and Mr. S. Mtongana for generously providing me their ligands for my research.

A special acknowledgement of gratitude goes to Dr. R. C. Luckay and Dr. S. Cronje for their special love and endless encouragement throughout my stay in Stellenbosch. Many thanks to those who believed in my capabilities, never faltering to be at my side and offer their humble assistance, the result of my hard work and sacrifice is in all modesty, humbly dedicated to them.

Special thanks goes to the government of the State of Eritrea for the scholarship that covered all my academic and living expenses and to Mrs. Lula Gebreyesus for the professional job she did in approving funds related to academic matters as well as for her encouragement and motherly love throughout my study period in South Africa.

Last but not least, to all my family members for their prayers, encouragement and endless love. A special acknowledgement also goes to my sister, *Senait*, for her continual love and encouragement.

Finally, I wish to extend my appreciation to all my friends here in Stellenbosch and all over for their motivation and intellectual stimulation. My indebtedness expressed here goes beyond the confines of the brief way in which they are all noted. I remain entirely grateful.

Michael M. Habtu
December 2003, Stellenbosch

Table of Contents

List of tables

List of Abbreviations

BLM	Bulk liquid membrane
ELM	Emulsion liquid membrane
SLM	Supported liquid membrane
AAS	Atomic Absorption Spectroscopy
ICP	Inductively Coupled Plasma
ICP-OES	Inductively Coupled Plasma-Optical Emission Spectroscopy
$CDCl_3$	Deuterated chloroform
NMR	Nuclear Magnetic Resonance spectroscopy
δ	An NMR chemical shift in parts per million (ppm)
UCT	University of Cape Town
Bu	Butyl
Et	Ethyl
Pr	Propyl
HL	Free ligand with one dissociable proton
H_2L	Free ligand with two dissociable protons
Å	Angstrom 10^{-10} metres
Deg	Degree

Chapter 1

1 Literature review

1.1 Introduction to Membranes

1.1.1 Definition

A membrane can be defined as a semi-permeable barrier between two phases, which permits the migration of metal ions across a concentration gradient. This usually involves the presence of a suitable ligand (ionophore) in the membrane, which acts as a carrier for the transport of metal ions across the membrane. There are two generic types of membranes. These are:

(a) Liquid membranes, and

(b) Polymeric membranes

Liquid membranes offer certain distinct advantages over other conventional chemical separation techniques e.g. low capital costs, space requirements and energy consumption [1]. The effectiveness of membrane transport is determined by the flux of species through the membrane and by the selectivity of the membrane. Compared to polymeric membranes, liquid membranes produce higher flux and selectivity. This study focuses only on liquid membranes.

1.1.2 Liquid membranes

Liquid membranes have been widely used in the area of separation sciences. They are highly selective and with the use of carriers for the transport mechanism, specific metal ion separation can be achieved. The simultaneous extraction and stripping operation is very attractive, because metal ion(s) of interest can be selectively transported from a higher concentration solution to a lower concentration solution by the use of a suitable carrier [2].

Liquid membranes are relatively efficient and as such are being looked into for potential industrial applications in the recovery of metal ions from dilute samples as well as in the treatment of wastewater. Besides these potential applications, there is also a promising avenue for the use of liquid membranes in the biochemical and biological fields. The use of carriers utilizing proteins, antibiotics, or other molecules naturally found in cell membranes provides a wide area of study for the researcher.

1.1.3 Types of liquid membranes

There are three types of liquid membranes that are generally employed in the transport of metal ions. These are: bulk liquid membranes, emulsion liquid membranes and supported liquid membranes. Here is a brief overview of the design and set up of these membranes.

1.1.3.1 Bulk liquid membrane (BLM)

The most common configuration encountered in metal ion transport systems, (see **Fig. 1.1**), involves a three-phase arrangement consisting of two aqueous phases (source and receiving phase) separated by an immiscible (organic) membrane phase [3]. The ligand (carrier) is dissolved in a suitable organic solvent (like $CHCl_3$, CH_2Cl_2, etc.) and is placed in the bottom of the cell. The two aqueous phases are placed on top of the organic phase. A stirrer stirs both the organic and aqueous phases separately at a low speed (10 rpm in most cases) and this maintains the membrane stability. The concentration of the metal ions transported from the source phase into the receiving phase is then determined by spectrometric techniques like ICP or AAS.

In BLM, a relatively thick layer of immiscible liquid is used to separate the source and receiving phases. Due to the thickness of the membrane, the amount of species transported is low. Moreover, the bulk system is not commercially viable, transport rates are small, relatively large data standard deviations are observed, and it is difficult to sort out surface effects in the system. Therefore, BLMs are used in basic laboratory transport experiments and have less potential for separation.

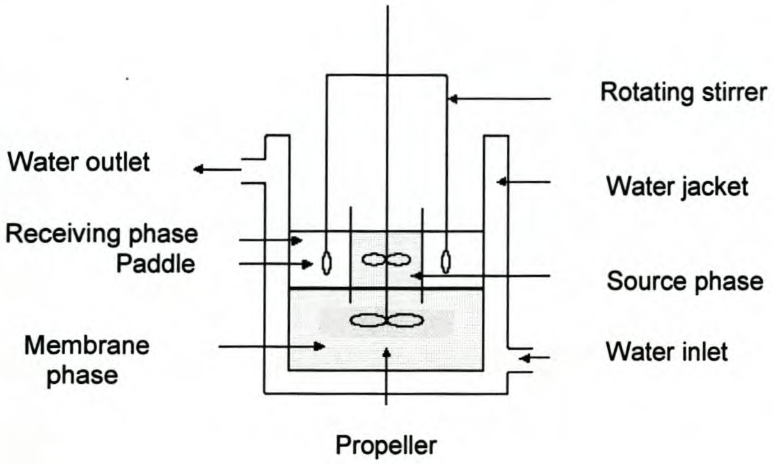

Figure 1.1 : Cell diagram for bulk liquid membrane transport studies.

1.1.3.2 Emulsion liquid membrane (ELM)

Emulsion liquid membranes, also called surfactant liquid membranes, are prepared by dispersing an inner receiving phase in an immiscible liquid membrane phase to form an emulsion. The membrane is very thin and has a large surface area per unit source phase volume, which enhances the transport rate.

The stripping agent is emulsified in the form of fine droplets with the help of a suitable surfactant into the membrane phase consisting of a carrier (extractant) in a diluent. This emulsion is dispersed in the feed solution containing the metal ions to be recovered (removed) in the form of globules and during this process the pertraction (extraction through permeation) takes place. Hence, ELM technology refers to simultaneous extraction and stripping, and in some cases involves carrier-mediated transport.

In the carrier mediated transport shown in **Fig. 1.2**, the metallic element present in the feed solution (source phase) forms a complex with the ligand at the interface of the emulsion globule and the feed phase. The complex formed is then shuttled through the organic membrane phase to the membrane - strip interface and from there it is stripped into the bulk of the encapsulated strip phase. Emulsion stability is maintained by using a moderately hydrophobic membrane solvent and carrier molecules. Furthermore, the ionic strength and pH of the aqueous phases must be closely monitored.

Compared to conventional liquid membrane processes, the liquid emulsion membrane process has some attractive features such as simple operation, high efficiency, larger interfacial area and scope of continuous operation. However, the ELM system has certain disadvantages all having to do with the formation of the emulsion [4]. A serious industrial disadvantage of emulsion liquid membranes is the need to break the emulsion to recover the receiving phase [5]. In comparison to BLM and SLM, ELM has been by far the most industrially used separation technique and has the greatest potential in the immediate future [4].

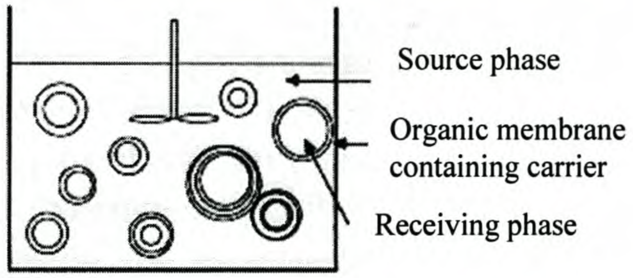

Figure 1.2 : Carrier mediated transport across emulsion liquid membranes.

1.1.3.3 Supported liquid membrane (SLM)

Supported liquid membranes are one of the newly emerging tools well suited as separation methods in which an organic solvent immiscible with water and containing a complexing agent, R, selective towards a target metal, is immobilized on a thin, macroporous, hydrophobic polymeric membrane [4,6]. The membrane is interposed between two aqueous phases (source phase and receiving phase) and the aqueous phases are then gently stirred (see **Fig.1.3**)

In this system, the source phase contains the metal to be transported whereas the receiving (strip) solution contains a complexing agent, R', having a stronger affinity to trap the target metal than R.

In SLMs, the analyte can be concentrated by using a strip solution of much smaller volume than the source solution. This makes SLMs potentially attractive techniques for the separation and concentration of trace elements. Supported liquid membranes can be fabricated in different geometries: flat, spiral wound, etc. The most simplistic in design is the flat supported liquid membrane.

Metal ion transport in SLMs may be proton or counter ion driven. However, the majority of the work reported in the literature is based on the proton driven mechanism, with most applications in industrial separations and recovery of target elements [4-7]. The main advantage of supported liquid membranes over the traditional separation technologies is the low inventory of the organic phase used, hence only small quantities of extractants are required and this allows the use of very selective and expensive extractants [7]. Other advantages include low capital and operating costs, simplicity of operation and low investment costs [7,8]. SLMs can be used in various fields, particularly in industrial, clinical, pharmaceutical and environmental fields. It has been used, for example, in the recovery and enrichment of metals from hydrological samples, extraction of noble metals, and removal of toxic metals and organic pollutants from wastewater [4,9]. A new supported liquid membrane (SLM) system for the selective transport of Ag(I) has also been introduced recently [10]. In this study, the SLM used was a thin porous membrane impregnated with a recently synthesized mixed aza-thioether crown containing a 1,10-phenanthroline sub-unit dissolved in nitrophenyl octyl ether. The study shows a quantitative transport of Ag(I) from a mixture of Co(II), Cu(II), Ni(II), Zn(II), Pb(II), Cd(II) and Ag(I) ions. In a related investigation, a supported liquid membrane (SLM) study involving a di(2-ethylhexyl)phosphoric acid as a carrier for the removal of Ag(I) and Cu(II) ions from acidic thiourea solutions has also been reported [11].

Despite all these advantages, there are a few limitations for SLMs. For instance, the fact that it is difficult to get rid of the carrier or organic liquid in the pores of the supporting membrane after the transport has been accomplished. However, there are two possible ways to overcome this limitation. One is through carrier or solvent evaporation, and the other is by creating a large pressure difference across the membrane, effectively pushing the fluid out. The other limitation is that SLMs, like BLMs, can only be utilized for laboratory scale. This method cannot be scaled up for industrial purposes.

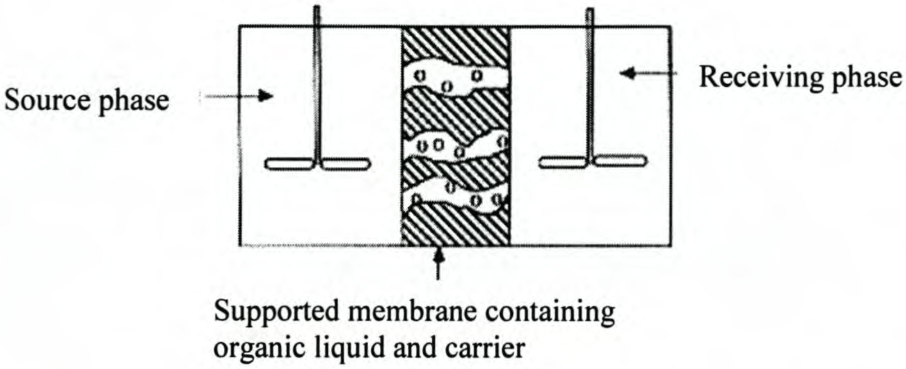

Figure 1.3: Carrier mediated transport across supported liquid membranes.

1.2 Carrier mediated liquid membrane transport and extraction studies using synthetic ionophores

The literature contains a wide range of studies on the selective transport of metal cations through liquid membranes using synthetic ionophores. Such ionophores include macrocyclic [12-14] as well as open chain (acyclic) derivatives [15-18] of varying structure and donor atoms. In particular, macrocyclic ligands have been the subject of great interest to many researchers due to their unique properties such as their capacity to bind selectively to a particular metal ion [19] as well as their tendency to form both kinetically and thermodynamically stable metal complexes [20,21]. These studies employed a systematic variation of the macrocyclic ring size, the donor atoms present and/or the degree of substitution of the parent ring structure to tune the affinity of these ligands for the specific metal ion(s) of interest [21,22]. For example, macrocyclic crown [7] and aza-crown ethers [23] have been extensively used as carriers for the selective transport of transition metal ions as well as heavy metal ions in liquid membranes [7-8, 24-26]. However, the complexing ability of crown ethers towards soft heavy metal ions is quite low [19] and therefore, in order to circumvent this problem, some of the oxygen atoms of the crown ethers have been substituted by sulfur atoms. This has resulted in a considerable increase in the transport rate of soft metal ions such as Ag(I) and Hg(II). Sulfur containing crown ethers (thiacrown ethers) are hydrophobic and they have high bonding affinities to soft metal ions [27]. Thus, in recent years, some thiacrown ethers have been of common use as carriers in liquid membrane transport and extraction studies [19, 28-30].

Liquid membrane transport and extraction of Ag(I) from a mixture of interfering metal ions has also been a subject of interest in the last few years due to the widespread use of silver in different areas of technology and due to its toxicity [31-33]. The results obtained in such studies vary with the type of ligands and experimental conditions employed. Recently, a facilitated counter-transport of Ag(I) and Cu(II) ions, both in acidic thiourea medium, across a supported liquid membrane by using di-(2-ethylhexyl)phosphoric acid as carrier has been investigated [11]. The fundamental parameters influencing the transport of Ag(I) and Cu(II) have been determined. These include: thiourea concentration in the source phase, pH of the source phase, pH of the receiving phase, Ag(I) and Cu(II) concentration in the source phase, temperature of the system and membrane support characteristics. According to this study, thiourea can form complexes with both ions that are less mobile than the free metal ion. The study also showed that the transport flux (J value) of Ag(I) and Cu(II) ions decreases when the concentration of the thiourea in the source phase increases. However, by taking advantage of the optimisation of the different parameters, separation of Ag(I) and Cu(II) in the presence of thiourea was achieved. The selectivity of the transport achieved, J (Ag(I)/Cu(II)), was 1.96.

1.3 The chemistry of *N,N*-dialkyl-(HL) and *N*-alkyl-*N'*-(H_2L) acyl(aroyl) thiourea ligands

1.3.1 Introduction

There is a large body of information in the literature on the synthesis, properties, co-ordination chemistry and industrial application of *N,N*-dialkyl-(HL) and *N*-alkyl-*N'*-(H_2L) acyl(aroyl)thiourea ligands [34-38]. In particular, the co-ordination chemistry of these ligands with platinum group metals has been studied in detail [35-38]. These ligands can be generally represented as:

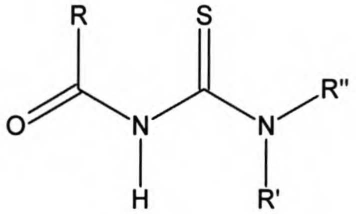

If R = C_6H_5 and R', R" are alkyl groups, then it is *N,N*-dialkyl-*N'*-aroylthiourea – *HL*.

If R, R' and R" are alkyl groups, then it is *N,N*-dialkyl -*N'*- acylthiourea – *HL*.

If R = C_6H_5, R' = alkyl group and R" = H, then it is *N*-alkyl-*N'*-aroylthiourea – *H_2L*.

If R and R' are alkyl groups and R" = H, then it is *N*-alkyl-*N'*-acylthiourea – *H_2L*.

1.3.2 Ligand synthesis, properties and structure

Although the HL and H_2L ligands were first prepared by Neucki in 1873 [36], their coordination chemistry and potential applications have only been explored to some extent in the last three decades. The facile synthesis of HL and H_2L, reported by Douglas and Dains [39], from readily available and inexpensive starting materials is one of the interesting features of these ligands. In general, ligands of the type HL that are derived from benzoyl chloride are very stable and relatively hydrophobic [39]. This property makes these ligands suitable for transport and extraction studies.

The proton on the amido ---C(O)NHC(S)--- moiety is weakly acidic. The acid dissociation constants, $pK_{a(NH)}$ for a series of hydrophilic *N*,*N*-dialkyl-*N'*-aroylthioureas have been reported to range from 7.5 to 10.9 in water-dioxane mixtures [40]. In the presence of certain acceptors, the charge on the sulfur donor atom of these ligands can be increased by means of resonance effects. The combination of high charge density at the donor atoms with a relatively high NH acidity has the effect that almost all complexes of these ligands are formed in acidic media [41]. In acidic conditions it is only the platinum group metals, gold, silver and mercury that are complexed as a result of their specific acceptor properties [41]. Therefore, it is possible to carry out separations within this group of thiophilic elements by adjusting the acid concentration, the ligand dose, and by exploiting kinetic effects.

1.3.3 Conformational studies

The X-ray diffraction studies done by Koch [40] reveal a significant influence of intra-molecular hydrogen bonding on the structure of H_2L ligands and this leads to differences in the preferred conformation as well as the co-ordination chemistry between the *N*,*N*-dialkyl-substituted, HL and the *N*-alkyl-substituted, H_2L ligands.

For *N*-alkyl-substituted (H_2L) ligands, the intra-molecular hydrogen bonding between the thiourea --C(S)NHR--moiety and the oxygen atom of the amidic group locks the ---C(O)NHC(S)NHR unit into a planar six-membered ring [35,40,42]. In contrast, the corresponding *N*,*N*-dialkyl substituted (HL) ligand assumes a twisted conformation in the solid state with the sulphur and oxygen atoms pointing approximately in opposite directions (see **Fig. 1.4**).

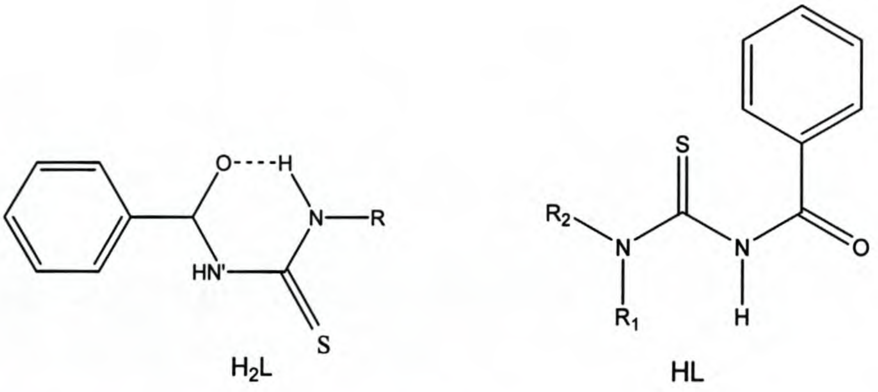

H_2L HL

Figure 1.4: The effect of the intra-molecular hydrogen bonding on the preferred conformation of H_2L ligands.

The ^1H and ^{13}C NMR spectra of *N,N*-dialkyl-*N'*-aroyl, HL, thioureas show separate resonances for the two methylene groups of the $(S)CN(CH_2)_2$--- moiety in $CDCl_3$ at room temperature [40] and this indicates that the (S)C---N(R/H) bond has a partial double bond character.

1.3.4 The co-ordination chemistry of HL and H_2L ligands

The simple monodentate thiourea has played a great role in the development of the co-ordination chemistry of the transition metals, particularly in the case of the noble metals, as well as gold and silver [36]. However, the coordination chemistry of HL and H_2L ligands differs significantly from that of simple thioureas.

Beyer and Hoyer [36] were the first authors to review the co-ordination chemistry of *N,N*-dialkyl-*N'*-aroylthioureas with a number of first and second row transition metal ions such as Ni(II), Co(II), Zn(II), Pd(II), Ag(I) and Cd(II). However, a detailed review of the co-ordination chemistry of *N,N*-dialkyl-*N'*- (HL) and *N*-alkyl-*N'*-acyl(aroyl)thioureas (H_2L) with Pt(II), Pd(II) and Rh(III) has only been done recently by Koch [40]. This study showed that the mode of co-ordination of HL and H_2L ligands differs significantly for these ligands in some important aspects. In general, the HL ligand co-ordinates to d^8 metal ions in a *cis* bidentate manner through the *S*, *O* atoms with the loss of a proton. It has been reported that the simple *N,N*-disubstituted-*N'*-acyl(aroyl)thioureas (HL) readily coordinate to Pt(II) in this fashion to give neutral square planar complexes with 2:1 ligand to metal stoichiometry i.e. $[Pt(L\text{-}S,O)_2]$ [40,43]. However, in the case of H_2L, the ---C(O)NHC(S)-moiety does not participate in bidentate *S,O* coordination because the oxygen atom of the ligand is locked into a stable intermolecular hydrogen bond [35,44]. In HCl solutions these ligands coordinate to Pt(II) or Pd(II), but only via their sulfur atoms and without dissociation of the NH hydrogens. Under these conditions, the complexes formed are usually of the type $[M(H_2L)_2Cl_2]$ [45].

These differences have been ascribed to lower solubility of the *N'*-alkyl substituted - H_2L ligands as well as differing electronic effects in which the + I substituent effect of the alkyl moieties is invoked to lead to enhanced electron densities at the *S* and *O* donor atoms of the ligands [46].

1.3.5 The co-ordination chemistry of bipodal *N'*-acyl(aroyl)thioureas

The bipodal *N'*-acyl(aroyl)thioureas are ligands which have two-C(O)-NH-C(S)- moieties linked to each other with an aliphatic or aromatic spacer group (see **Fig. 1.5**). With rigid or short chain spacer groups, the two chelating moieties of these ligands co-ordinate to different metal centers.

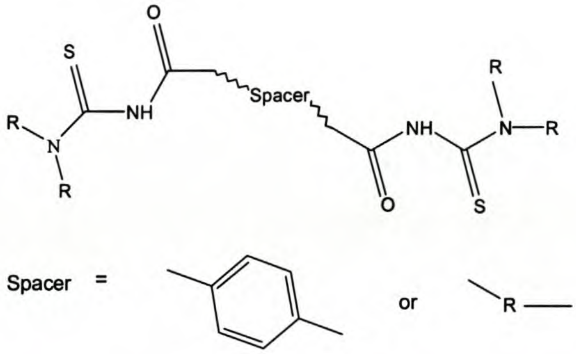

Figure 1.5: Structure of bipodal *N'*-acyl(aroyl)thioureas with aliphatic (aromatic) spacers. R represents an aliphatic group.

A survey of the published literature [47] revealed that these ligands co-ordinate to Pt(II) and Pd(II) in a *cis* bidentate *S,O* chelating fashion in an overall metal to ligand stoichiometry of 1:1. On the other hand, it has also been reported that the bipodal ligand 3,3',3'-tetraethyl-1,1'-isophthaloylbisthiourea, H_2L^{12}, coordinates to Ag(I) in a different coordination mode in which only the sulfur atoms of the ligands are coordinated forming an infinite one-dimensional chain leaving each Ag(I) coordinated in a highly distorted tetrahedral fashion [48].

1.3.6 Potential industrial application of these ligands

The specific arrangement of the heteroatoms of the thiourea group of *N*,*N*-dialkyl-*N'*-benzoylthioureas leads to a series of significant changes in the chemical properties that can be exploited for analytical purposes. *N*,*N*-dialkyl-*N'*-aroylthioureas have proved to be particularly successful as selective complexing agents for heavy metals [49] and for the enrichment of the platinum group metals even from strongly interfering matrices [41,50]. The *N*,*N*-dialkyl-*N'*-aroylthioureas posses an unusually high redox stability and favourable toxicological properties that makes them important for industrial applications [51]. Some of the applications are: for the removal of harmful toxic compounds from organisms and for the detoxification of waste waters containing complexable heavy metals. These ligands also find potential applications in the solvent extraction [46,52] and chromatographic separation of PGMs as well as several 'soft' transition metal ions, notably Cu(II), Hg(II) and Au(III) [40,43,53].

1.4 Atomic Absorption Spectroscopy (AAS) and Inductively Coupled Plasma - Emission Spectroscopy (ICP-ES) as basic analytical tools

1.4.1 Atomic absorption spectroscopy

1.4.1.1 Background

The phenomenon of atomic absorption (AA) was observed a long time ago with the discovery of the Fraunhofer lines in the sun's spectrum. Later, in 1955, an Australian physicist Alan Walsh demonstrated that atomic absorption could be used as a quantitative analytical tool [54]. Since then, atomic absorption spectroscopy has been used more widely as an analytical tool in various fields.

Atomic absorption analysis involves two steps:

1. Measuring the absorption of light by vaporized ground state atoms, and
2. Relating the absorption to concentration.

1.4.1.2 Introduction

Atomic absorption spectroscopy (AAS) is a fairly universal analytical technique for the determination of metallic elements or ions when present in trace or major concentrations. Ions in a sample must first undergo desolvation and vaporization in a high-temperature source such as a flame or graphite furnace before analysis. Based on their methods of vaporizing the sample, we can distinguish between two types of atomic absorption spectroscopy. These are:

(a) Flame atomic absorption spectroscopy, and

(b) Graphite furnace atomic absorption spectroscopy

1.4.1.3 Flame atomic absorption spectroscopy

In this technique, the sample is aspirated into a 1700 - 3150 °C flame using a nebulizer. The flame is lined up in a beam of radiation of the appropriate wavelength and this causes the atoms to undergo a transition from the ground state to the first excited state. The light beam is generated by a hollow cathode lamp that is specific for a target metal. The lamp is perfectly aligned in such a way that the beam crosses the hottest part of the flame and travels into the detector (see **Fig. 1.6**). The reduction in intensity of the light due to the absorption is then detected by means of a suitable detector. However, it is important to mention here that if the flame and analytical conditions are not properly optimized, chemical and ionization interferences can occur.

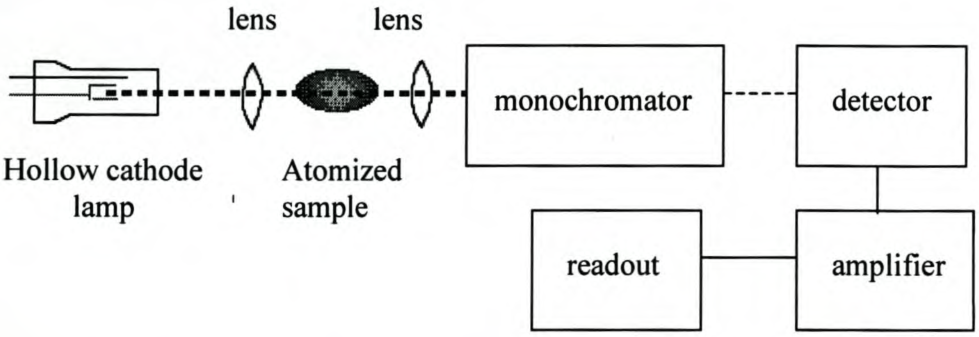

Figure 1.6: Schematic diagram of a flame atomic absorption spectrometer

1.4.1.4 Graphite furnace atomic absorption spectroscopy

This spectroscopic technique uses a graphite tube with a strong electric current to vaporize the sample. Samples are placed directly into the graphite furnace and the furnace is then heated electrically in several steps to dry the sample and then vaporize the analyte atoms or ions in the sample. The advantage of this technique over flame atomic absorption spectroscopy is that it can atomize solutions, slurries, or solid samples in very small quantities more efficiently than flame atomic absorption spectroscopy.

Graphite furnace atomic absorption spectroscopy is applicable for relatively pure samples and it has extremely low detection limits.

1.4.1.5 Interferences

Any factors that affect the ground state population of the analyte element can be classified as interferences. The most common interferences are discussed below.

(a) Spectral interferences

Spectral interferences are the result of radiation overlapping with that of the source light. The interference radiation may be an emission line of another element or compound, or general background radiation from the flame, solvent, or analytical sample. This usually occurs when using organic solvents. Spectral interferences also result from the presence of either molecular combustion products that exhibit broad-band absorption or particulate products that scatter radiation. In general, interferences due to overlapping of lines are rare in AAS because the emission lines of hollow cathode sources are very narrow [55,56].

(b) Chemical interferences

These interferences, also called matrix interferences, are due to differences between surface tension and viscosity of the test solution and standards. Chemical interferences are relatively common in AA, especially with graphite furnace AA, but may be minimized with chemical modifiers and by a suitable choice of instrument operating conditions.

(c) Ionization interferences

Ionization of the analyte reduces signal intensity. This commonly happens in AAS when measuring certain group II elements in a nitrous oxide flame. An ionisation buffer such as Cs, Li or K can be added to both samples and standards to minimize this effect [56,57].

(d) Physical interferences

These interferences relate to the different properties of various samples that can affect sample uptake and droplet formation. These kinds of interferences are common in AAS.

(e) Formation of compounds that do not dissociate in the flame

The sample solution may contain a chemical, usually an anion that can form a refractory (heat-stable) compound with the test element in the flame. The most common example is the formation of calcium and strontium phosphates. Refractory compound formation can be avoided by chemical competition or by the use of a high-temperature flame [57].

1.4.2 Inductively Coupled Plasma - Emission Spectroscopy (ICP-ES)

1.4.2.1 Background

The basis for all emission spectrometry is that atoms or ions in an excited state spontaneously revert to a lower energy state and in so doing emit a photon of energy. To this end, the inductively coupled argon plasma (ICP) is an effective excitation source of atomic emission, which can in principle, be used for the determination of all elements other than argon. Calibration curves relating the analyte concentration with the instrumental response (signal intensity) are linear, typically over five orders of magnitude. Besides this, the fact that any element can have many wavelengths of choice of varied sensitivity makes the ICP-ES suitable for the determination of any element at a concentration ranging from ultra trace levels to major components. A schematic diagram of the plasma is shown in **Fig. 1.7**.

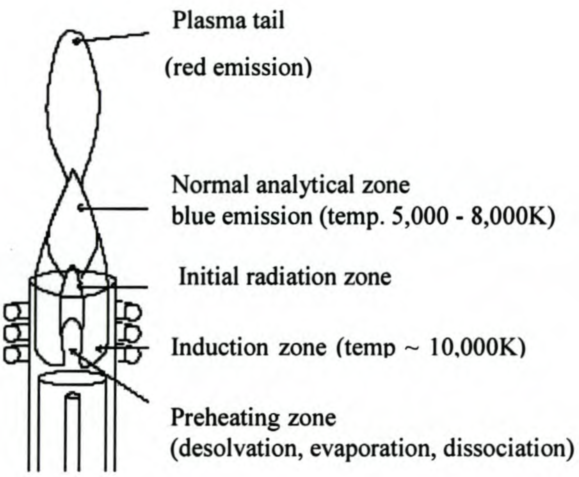

Figure 1.7: Plasma used for emission spectroscopy [58].

1.4.2.2 Historical development

The development of a new analytical technique does not often involve the development of fundamentally new technology; rather it relies on the application and utilization of an existing concept. In this context, the ICP-ES spectroscopy is not an exception. The analytical application of ICP-ES dates back to the early 1960's. The ICP-ES was first established as an analytical tool by Greenfield *et al* and it is the application and refinement of the ideas developed in their work which is now used as the basis of quantitative ICP source spectroscopy [58].

1.4.2.3 Instrumentation

The major constituent parts of an ICP system can be identified as:

1. Sample introduction system (nebulizer)
2. ICP torch
3. High frequency generator
4. Spectrometer
5. Interface and computer

In the simplest form of the equipment, a sample solution of an element whose concentration is to be determined is introduced into the ICP torch as aqueous aerosol by means of a suitable nebulizer. The torch ignites the sample aerosol and this eventually leads to the excitation of the atoms or ions in the sample. The light emitted in the ICP is converted into an electrical signal by a photomultiplier in the spectrometer. The intensity of this electrical signal is then compared to a previously measured intensity of a known concentration of the element, and a concentration is computed.

1.4.2.4 Compromise operating conditions of ICP-ES

The subject of optimisation of ICP systems has been of great debate in the last few years. This is because the analytical characteristics of the ICP method depends on a rather complicated manner of adjusting parameters such as argon flow rate, torch geometry, viewing height, RF power, sample uptake rate, etc. The fact that all elements do not generally have identical sets of optimal parameters, and that various analytical characteristics for a particular element may optimise at different points in the parameter space, complicate the task of optimisation. Changing some of these parameters may improve the sensitivity for one element while certainly degrading it for the other. However, it is usually possible to alter the argon flow rates, the solution uptake rate and the observation height for our needs depending on the type and concentration of our sample.

In conclusion, it is advisable to find a single set of compromise operating conditions that can be used as fixed instrumental settings to obtain excellent analytical results.

1.4.2.5 Instrument limitations

Despite the theoretical scope of this technique, not all elements can be conveniently determined by ICP-ES. For example, the unstable elements need special facilities for handling the radioactive fume from the plasma. Again, the determination of fluorine, chlorine and bromine requires special optics for the transmission of the very short wavelengths. Furthermore, interference effects, although generally small and easily manageable, sometimes have to be taken into account.

1.4.2.6 Interferences

Many new analytical techniques have been introduced as ‘free from interferences’. However, when applied to routine analysis of real samples few of these claims have survived intact. Interferences do occur unless we find a proper way to avoid them. These interferences can be categorized as follows.

(a) Spectral overlaps

In ICP-ES the vast amount of spectra present in the plasma means that there is a greater possibility of spectral interference. Spectral resolutions of 0.010 nm or better are required to resolve nearby interfering lines from the atomic and ionic analytical emission signals of interest. However, when serious spectral interferences occur in ICP, the only satisfactory way to avoid it is to use an alternative line.

(b) Chemical interferences

ICP-ES is almost free from chemical interferences [57]. The chemical bonds that still exist at below 3000 °C are completely ruptured at above 6000 °C. The high temperatures reached in the plasma eliminate chemical interferences, which accounts (for the most part) for the better detection limits achieved for refractory elements. However, these interferences do exist to some extent even in ICP-ES and can never be completely ignored.

(c) Ionization interferences

The ICP contains a large number of free electrons, so ionization interferences for most applications are virtually nonexistent. Ionization interferences can be encountered when determining elements in matrices that contain very high concentrations of Group I elements (e.g. Na & K). However, optimizing the plasma viewing height can minimize these effects.

(d) Physical interferences

As previously explained, these interferences are the result of variations in sample properties such as viscosity. ICP tends to be more susceptible to such interferences because of the smaller droplet size required and lower transport efficiency.

1.5 Comparing AAS with ICP-ES

This section discusses the main differences between the two techniques and the considerations that we need to take into account before choosing the best analytical technique for our particular needs.

The basic difference between the two techniques is that the AAS relies upon an atomic absorption process while the ICP-ES is an atomic (ionic) emission spectroscopic technique. The next essential difference is the means by which the atomic or ionic species are generated. A combustion flame or graphite furnace is typically used for AA while ICP-ES uses a plasma. The typical maximum temperature for an air/acetylene flame is 2300 °C while for nitrous oxide acetylene, it is 2900 °C. Temperatures as high as 10000 °C can be reached in an argon plasma [57,58].

The comparison of the detection limits of the two techniques highlights the following differences:

(a) Furnace AA detection limits are generally better in all cases where the element can be atomized.

(b) Detection limits for Group I elements (e.g. Na, K) are generally better by flame AAS than by ICP.

(c) Detection limits for refractory elements (e.g. B, Ti,V, Al) are better by ICP than by flame AAS.

(d) Non-metals such as sulfur, nitrogen, carbon, and the halogens (e.g. I, Cl, Br) can only be determined by ICP by using special optics for the transmission of the very short wavelengths. Keeping all these factors in mind we still need to consider a few more analytical requirements before deciding which technique to use. These requirements include:

1. The number of elements to be analyzed in each sample. The ICP-ES has proved to be a powerful and versatile technique for multi element analysis [57,59].
2. How much sample volume do we have? ICP-ES normally consumes higher sample volumes than AAS.
3. What concentration ranges are present in the sample? ICP-ES allows a much wider linear dynamic range of about 10^5. For example, copper can be measured at the 324.75 nm wavelength from its detection limit of about 0.002 ppm to over 200 ppm [59]. In ICP, extrapolation of two point calibrations can be accurately used to

achieve orders of magnitude above the top standard. This compares to a linear dynamic range of typically 10^3 for AAS [58].

4. Is an internal standard required? For instance, when our sample viscosity is not uniform we need to use an internal standard.
5. What precision are we looking for? For AAS a precision of 0.1-1% is typical for the short term, but recalibration is required over a longer period [58]. With ICP-ES the short-term precision is typically 0.3-2%, but precisions of 2-5% can be achieved over 8 hour periods without recalibration [58,59].

Answering these questions helps us decide which technique is preferred. In some special cases, it would also be advisable to use one technique to confirm the analysis result of the other.

1.6 Objectives of the research

Metal ion transport and extraction using macrocyclic and open-chain polydentate ligands has been a subject of great interest in recent years. Industries require selective and efficient transporting/extracting agents for the recovery of precious and toxic metal ions from industrial effluents. However, to my knowledge, there is not a single study published in the literature on the transport of metal ions by acyl(aroyl)thiourea ligands of the type described in **section 1.3**. Therefore, this project will focus on the examination of bulk liquid membrane (BLM) transport and extraction of some transition and post transition metal ions using a series of acyl(aroyl)thiourea ligands. This study will pave a way to the design and synthesis of more efficient, selective and commercially viable ligands that will meet the demands of the industry.

- The first part of this study concerns transport. One of the basic requirements for systems designed for metal ion transport across membranes is selectivity. Therefore, we have aimed at achieving high selectivity with our transport model. The other important requirement is that the ligand must efficiently complex to the metal ion while still allowing for the metal to be quantitatively stripped into the receiving phase. In order to achieve these requirements, pH of the source phase, pH of the receiving phase and concentration of the ligand will be optimized.

- The second part of the study concerns extraction. Selective metal ion extraction is a topic of wide commercial interest. The traditional methods of obtaining pure metals from their ores are based upon pyrometallurgy with thermal processes such as smelting. These methods are environmentally unfriendly since the use of carbon to reduce metal oxides results in the release of toxic gases like carbon monoxide. Metals that exist as sulfide ores will give off sulfur dioxide, which is again one of the principal gases that cause the acid rain phenomenon. Therefore, nowadays, there is a lot of active research related to the investigation of new methods of hydrometallurgy in aqueous medium. The added advantages of these methods are that we can work at much lower metal concentrations and also that it is more cost effective than the traditional methods. Therefore, to meet such advantages in the future, preliminary competitive metal ion extraction experiments involving the ligands that we employed in the transport study will be performed. We will use pH = 5.0 buffer containing the metal ions as the source phase and concentration of the ligand will be optimized.

Analysis of the aqueous source phase as well as the aqueous receiving phase will be done by atomic absorption spectroscopy (AAS) and the results obtained will later be confirmed by Inductively Coupled Plasma-Optical emission Spectroscopy (ICP-OES). The obtained transport and extraction results will be rationalized by using classical co-ordination chemistry arguments.

Finally, an attempt will be made to grow single crystals of silver (I) complex with *N*,*N*-di-n-butyl-*N'*-benzoylthiourea. The crystal structure will be solved, and the coordination geometry around the Ag(I) can be determined.

Chapter 2

2 Experimental

2.1 The synthesis and characterisation of ligands

2.1.1 Introduction

The ligand *N*,*N*-di-n-butyl-*N'*-benzoyl thiourea was synthesized by the author according to the method described by Douglass and Dains [39]. All other ligands used in this investigation (**Table 2.1**) had been previously synthesized by senior PGM research group members and were kindly donated to the author. Prior to their use, the identity and purity of the ligands was verified with the help of melting point determination (**section 2.1.4**), ^{1}H and ^{13}C {^{1}H} NMR spectra (**section 2.1.5**) and elemental (C, H, N and S) analysis (**section 2.1.5**).

2.1.2 Synthesis of *N*,*N*-di-n-butyl-*N'*-benzoylthiourea (HL^1) ligand

A pre-dried potassium thiocyanate (3.00 g, 30.9 mmol) was dissolved in 75 ml of anhydrous acetone in a two-necked round-bottomed flask under a nitrogen atmosphere. Benzoyl chloride (4.34 g, 30.9 mmol) was separately dissolved in the same volume of anhydrous acetone and then added drop-wise into the stirring potassium thiocyanate solution through a dropping funnel. After the addition was complete, the reaction mixture was heated to reflux for 45 minutes. Under these reaction conditions, the formation of benzoylthiocyanate was complete [39]. The crude benzoyl isothiocyanate was cooled to room temperature and insoluble potassium chloride was observed settling at the bottom of the flask. Dibutylamine (3.99 g, 30.9 mmol) was weighed, dissolved in 75 ml of anhydrous acetone and added drop-wise into the stirring benzoyl isothiocyanate solution with minimum exposure to air. At this stage, it was not necessary to separate the potassium chloride salt from the reaction mixture since it does not take part in any secondary reaction with the secondary amine [60]. The reaction mixture was heated to reflux for a further 45 minutes with stirring. The mixture was then cooled to room temperature and poured into an open beaker containing 100 ml of water. The water had the dual purpose of dissolving the potassium chloride salt and precipitating the water insoluble organic product. The beaker was left in a fume cupboard until about 200 ml of the acetone had evaporated. The resulting crude product was then collected by filtration, washed with water to remove any trapped salts and finally recrystallized from the acetone/water mixture. White crystals were obtained. In order to remove all the solvent, the pure recrystallized product was dried under vacuum at room temperature and was finally identified and characterized by means of melting point determination, ^{1}H, ^{13}C{^{1}H} NMR spectra and elemental (C, H, N and S) analysis (see **section 2.1.5**). Since benzoyl chloride is moisture sensitive, all the reactions were carried out under a nitrogen atmosphere. The synthetic reaction scheme for *N*,*N*-di-n-butyl-*N'*-benzoylthiourea is shown in **Fig. 2.1**.

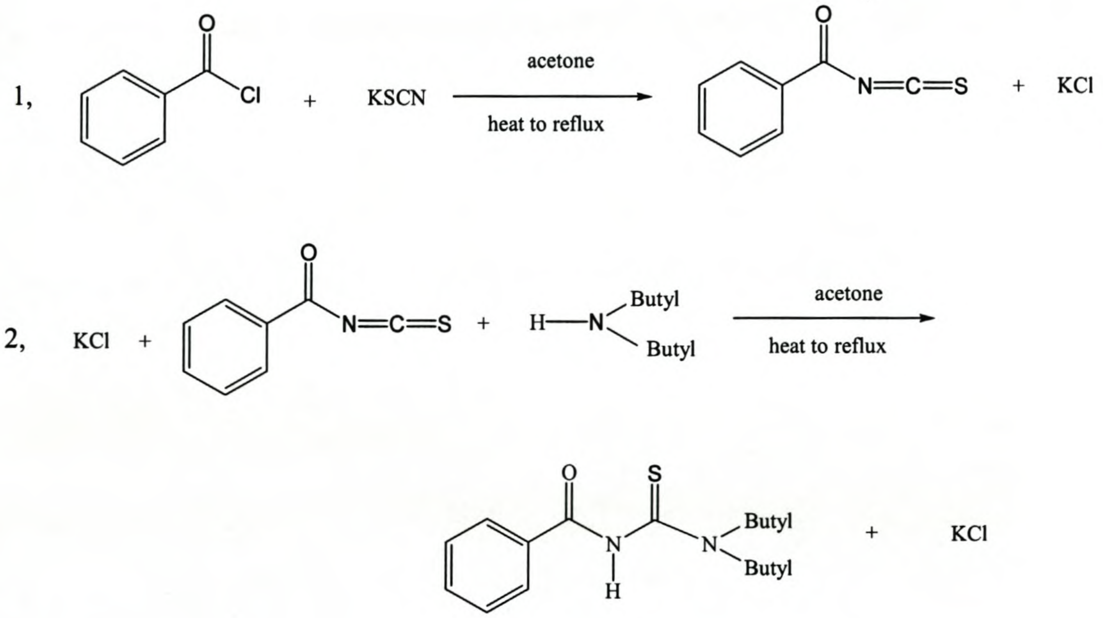

Figure 2.1: A reaction scheme for the one-pot synthesis of *N*,*N*-di-n-butyl-*N'*-benzoylthiourea (HL^{1}).

2.1.3 Structure of the ligands studied

HL^1

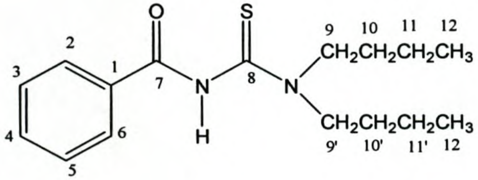

HL^4

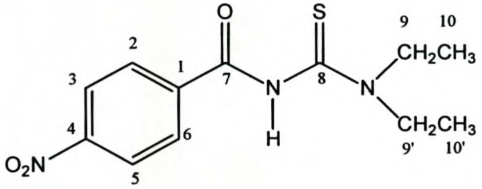

HL^7

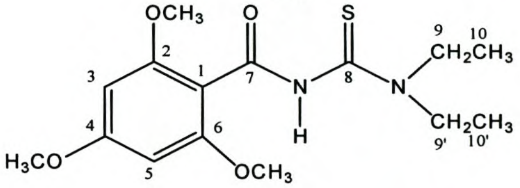

HL^2

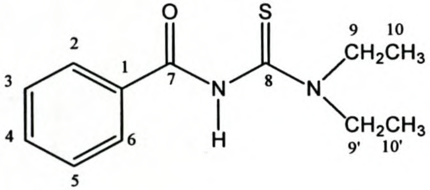

HL^5

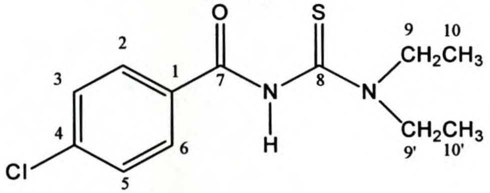

HL^8

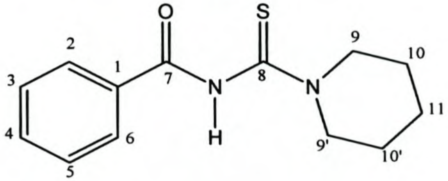

HL^3

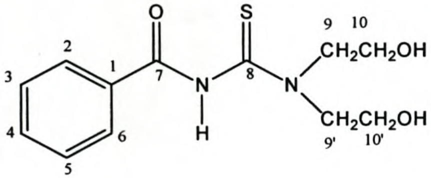

HL^6

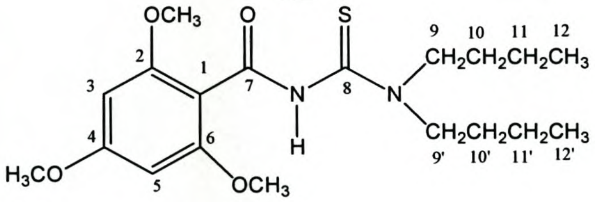

HL^9

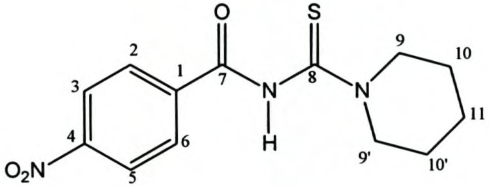

2.1.3 Continued: structure of the ligands studied

HL^{10}

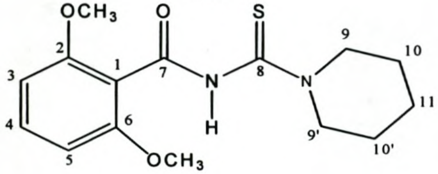

HL^{11}

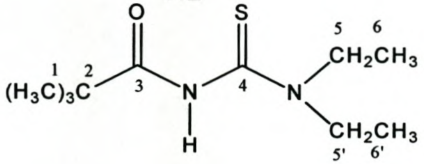

H_2L^1

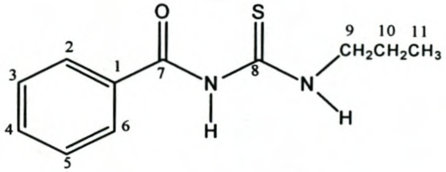

HL^{13}

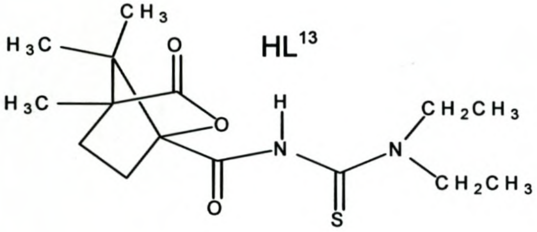

H_2L^{12}

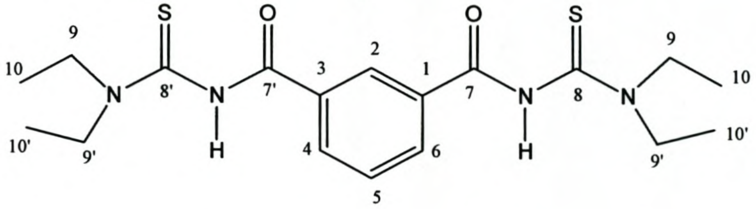

H_2L^3

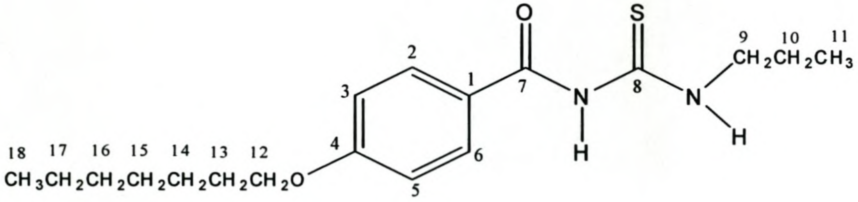

H_2L^2

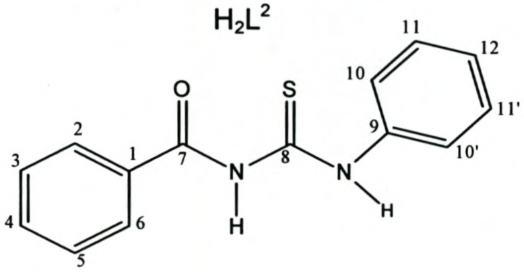

2.1.4 Melting points

Table 2.1: Melting Points of *N,N*-dialkyl-*N'*-aroylthioureas

Ligand Structure	Melting Point (°C)
HL^1 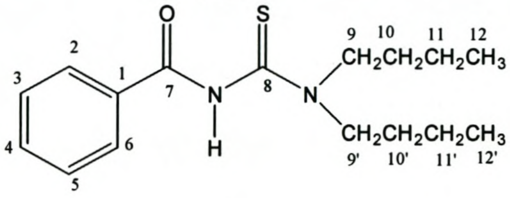	89 - 91
HL^2 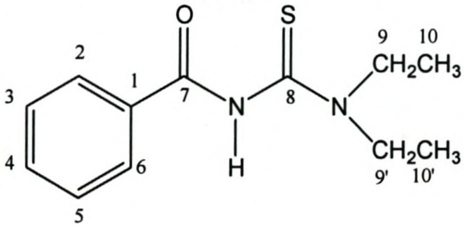	98 - 100
HL^3 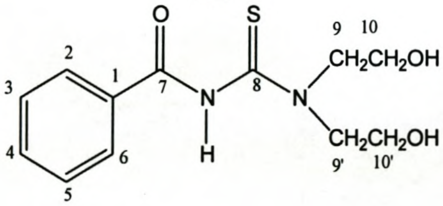	124 - 126
HL^4 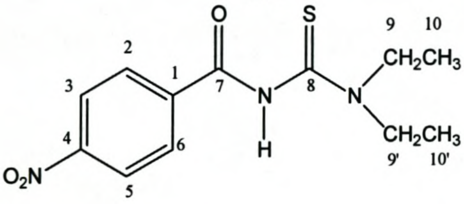	165 - 167
HL^5 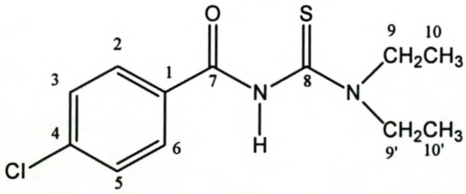	148 - 150

Table 2.1: Continued (Melting Points of *N,N*-dialkyl-*N'*-aroylthioureas)

Ligand Structure	Melting Point (°C)
HL^6 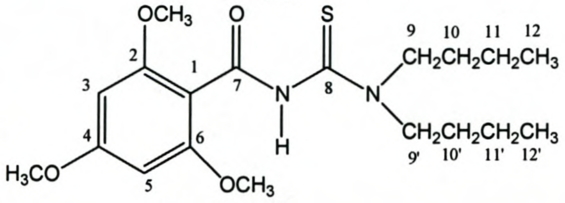	91 - 93
HL^7 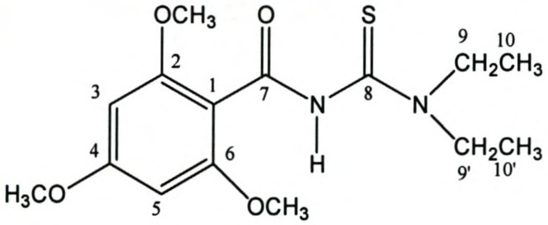	153 - 155
HL^8 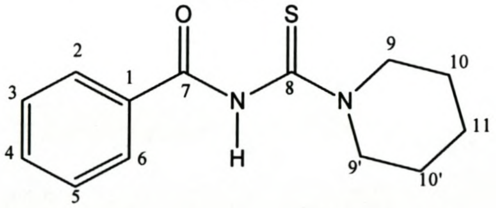	123 - 126
HL^9 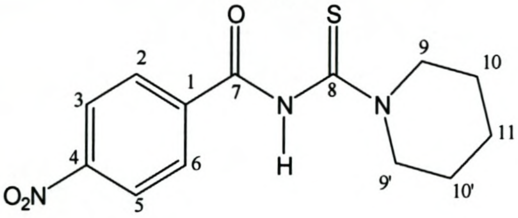	114-116
HL^{10} 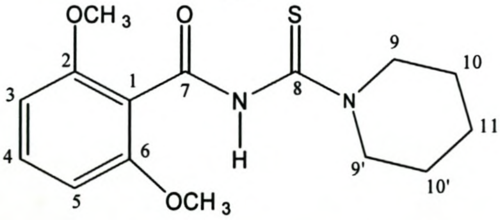	157-159

Table 2.2: Melting point of *N,N*-diethyl-*N'*-2,2-dimethylpropanoylthiourea

Ligand Structure	Melting Point (°C)
HL^{11} 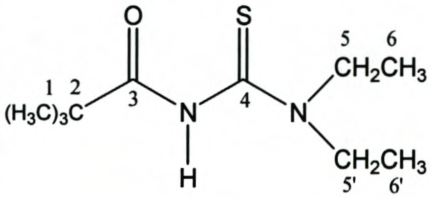	89 - 91

Table 2.3: Melting Points of *N*-substituted-*N'*-aroylthioureas

Ligand Structures	Melting Point (°C)
H_2L^1 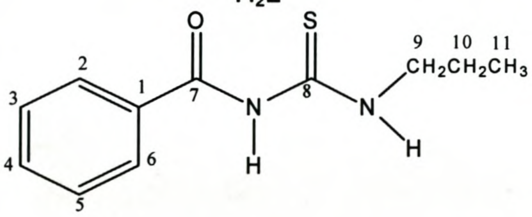	131 - 133
H_2L^{12} 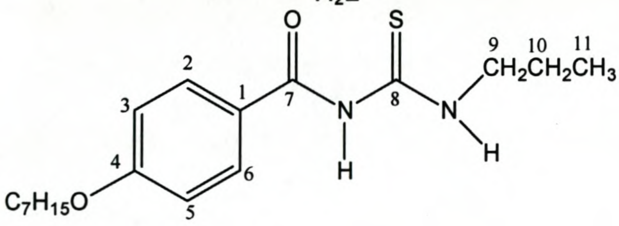	76 - 78
H_2L^3 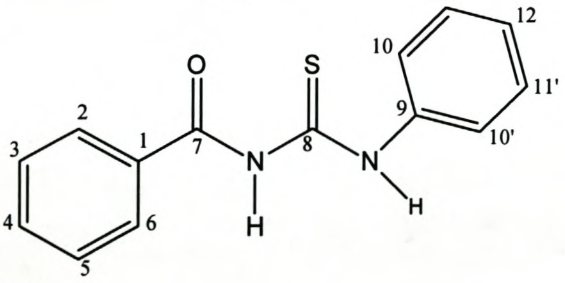	136 - 138

Table 2.4: Melting points of 3,3,3',3'-tetraethyl-1,1-isophthaloylbisthiourea and *N,N*-diethyl-*N'*-camphanoylthiourea

Ligand structures	Melting Point (°C)
H_2L^{12} 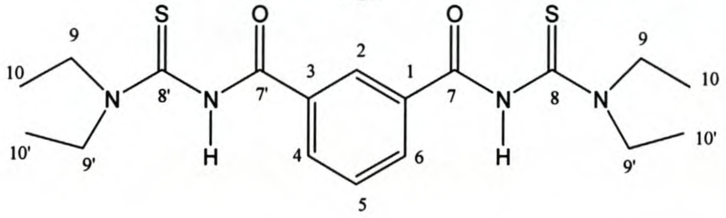	136-138
HL^{13} 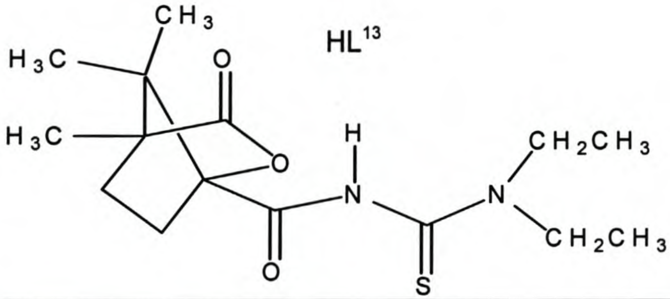	140 -142

2.1.5 Experimental Details

All reagents were commercially available and used without further purification. Melting points were determined using a Gallenkamp melting point apparatus in open capillaries. All ^1H and ^{13}C nuclear magnetic resonance spectra were measured at 25 °C in 5 mm NMR tubes in $CDCl_3$ solution. The chemical shifts (δ) were referenced to tetramethylsilane (TMS) as an internal standard. The instruments used were a Varian Unity 300 and INOVA 600 spectrometer operating at 300 MHz and 600 MHz for proton spectra or at 75 and 150 MHz for ^{13}C spectra. The elemental (C, H, N, and S) analysis was carried out using a Heraeus CHN rapid combustion analyzer.

Although these ligands were previously characterized, we have however checked their purity using melting point determination, ^1H and ^{13}C NMR spectroscopy, and elemental (C, H, N and S) analysis.

N,N-di-n-butyl-*N'*-benzoylthiourea, HL^1

After recrystallization, a yield of (6.1g, 0.023 mol, 75%) was recovered. Mp: 89-91 °C (lit. [61]: 93 °C). (Found: C, 65.71; H, 8.24; N, 9.60; S, 10.99%; $C_{16}H_{24}N_2SO$ required C, 65.72; H, 8.26; N, 9.58; S, 10.97%); δ_H (300MHZ, $CDCl_3$) 0.86 and 0.94 (6H, t, $C_{12/12'}$), 1.23 and 1.39 (4H, m, $C_{11/11'}$), 1.62 and 1.73 (4H, m, $C_{10/10'}$), 3.51 and 3.95 (4H, t, $C_{9/9'}$), 7.46 (2H, t, $C_{3/5}$), 7.57 (1H, t, C_4), 7.84 (2H, d, $C_{2/6}$), 8.37 (1H, s, NH); δc (75MHz, $CDCl_3$) 13.4 and 13.6 ($C_{12/12'}$), 19.8 ($C_{11/11'}$), 28.3 and 28.9 ($C_{10/10'}$), 52.9 and 53.1 ($C_{9/9'}$), 127.9($_{C3/5}$), 129.0 ($C_{2/6}$), 132.8 (C_4), 133.0 (C_1) 163.8(C_7), 180.0 (C_8).

N,N-diethyl-*N'*-benzoylthiourea, HL^2

Mp: 98-100 °C (lit. [61]: 98 °C). (Found C, 60.91; H, 6.82; N, 11.85; S, 13.34%; $C_{12}H_{16}N_2SO$ required C, 60.99; H, 6.82; N, 11.85; S, 13.57%); δ_H (300MHz, $CDCl_3$) 1.33 (6H, t, $C_{10/10'}$), 3.62 and 4.03 (4H, q, $C_{9/9'}$), 7.55 (2H, t, $C_{3/5}$), 7.57 (1H, t, C_4), 7.83 (2H, d, $C_{2/6}$), 8.35 (1H, s, NH); δc (75MHz, $CDCl_3$) 11.5 and 13.2 ($C_{10/10'}$), 47.8 ($C_{9/9'}$), 127.8($C_{3/5}$), 128.9 ($C_{2/6}$), 132.8 (C_1), 132.9 (C_4), 163.8(C_7), 179.4 (C_8).

N,N-di-(2-hydroxyethyl)-*N'*-benzoylthiourea, HL^3

Mp: 124-126 °C. δ_H (300MHz, $CDCl_3$) 3.91 (4H, m, $C_{9/9'}$), 3.93 (4H, m, $C_{10/10'}$), 7.50 (2H, m, $C_{3/5}$), 7.62 (1H, m, C_4), 7.82 (2H, d, $C_{2/6}$), 9.13 (1H, s, NH), 11.03 (2H, s, OH); δc (75MHz, $CDCl_3$) 47.65 ($C_{9/9'}$), 60.67 ($C_{10/10'}$), 127.62 (C_1), 129.26 ($C_{3/5}$), 131.87 (C_4), 133.74 ($C_{2/6}$), 167.13 (C_7), 180.96 (C_8).

N,N-diethyl-*N'*- 4-nitrobenzoylthiourea, HL^4

Mp: 165-167 °C. (Found: C, 51.22; H, 5.35; N, 14.97; S, 11.03%; $C_{12}H_{15}N_3SO_3$ required C, 51.23; H, 5.37; N, 14.94; S, 11.40%); δ_H (300MHz, $CDCl_3$) 1.29 and 1.31 (6H, t, $C_{10/10'}$), 3.56 and 3.98 (4H, q, $C_{9/9'}$), 8.02 (2H, d, $C_{2/6}$), 8.31 (2H, d, $C_{3/5}$), 8.47 (1H, s, NH); δc (75MHZ, $CDCl_3$) 11.2 and 13.0 ($C_{10/10'}$), 46.6 and 47.9($C_{9/9'}$), 124.1($C_{3/5}$), 129.2 ($C_{2/6}$), 138.3(C_1), 150.5(C_4), 162.6 (C_7), 179.6 (C_8).

N,N-diethyl-*N'*-4-chlorobenzoylthiourea, HL^5

Mp: 148-150 °C. (Found: C, 52.95; H, 5.65; N, 10.08; S, 11.78%; $C_{12}H_{15}N_2SOCl$ required C, 52.84; H, 5.54; N, 10.27; S, 11.76%); δ_H (300MHz, $CDCl_3$) 1.32 (6H, t, $C_{10/10'}$), 3.60 and

4.02 (4H, q, $C_{9/9'}$), 7.44 (2H, d, $C_{2/6}$), 7.77 (2H, d, $C_{3/5}$), 8.33 (1H, s, NH); δc (75MHz, $CDCl_3$) 11.5 and 13.2 ($C_{10/10'}$), 47.9 ($C_{9/9'}$), 129.1 ($C_{3/5}$), 129.2 ($C_{2/6}$), 139.2 (C_1), 139.3 (C_4), 162.8 (C_7), 179.1 (C_8).

_N,N_-dibutyl-_N'_-2,4,6-trimethoxybenzoylthiourea, HL^6

Mp: 91-93 °C. (Found C, 59.99; H, 8.30; N, 7.40; S, 7.90%; $C_{19}H_{30}N_2SO_4$ required C, 59.69; H, 7.85; N, 7.33; S, 8.38%); δ_H (300MHz, $CDCl_3$) 1.06 and 1.14 (6H, t, $C_{12/12'}$), 1.44 and 1.60 (4H, m, $C_{11/11'}$), 1.80 and 1.96 (4H, m, $C_{10/10'}$), 3.68 and 4.15 (4H, t, $C_{9/9'}$), 4.07 (9H, s, methoxy substituents at C_2, C_4 and C_6), 7.47 (2H, s, $C_{3/5}$), 9.06 (1H, s, NH); δc (75MHz, $CDCl_3$) 13.44 and 13.60 ($C_{12/12'}$), 19.76 and 19.80 ($C_{11/11'}$), 28.22 and 29.91 ($C_{10/10'}$), 52.69 and 52.94 ($C_{9/9'}$), 50.30 (methoxy substituents at C_2 and C_6), 60.80 (methoxy substituent at C_4), 105.27 ($C_{3/5}$), 127.57 (C_1), 142.24 ($C_{2/6}$), 153.29 (C_4), 163.44 (C_7), 180.37 (C_8).

_N,N_-diethyl-_N'_-2,4,6-trimethoxybenzoylthiourea, HL^7

Mp: 153-155 °C. (Found C, 55.21; H, 6.75; N, 8.59; S, 9.82%); $C_{12}H_{15}N_3SO_3$ required (C, 55.46; H, 7.00; N, 8.68; S, 9.45%); δ_H (300MHz, $CDCl_3$) 1.46 and 1.53 (6H, t, $C_{10/10'}$), 3.75 and 4.22 (4H, q, $C_{9/9'}$), 4.08 (9H, s, protons of the three methoxy substituents), 7.48 (2H, s, $C_{3/5}$), 9.03 (1H, s, NH); δc (75MHZ, $CDCl_3$) 11.14 and 13.02 ($C_{10/10'}$), 47.49 and 47.61($C_{9/9'}$), 56.27 (methoxy substituents at C_2 and C_6), 60.80 (methoxy substituent at C_4), 105.24 ($C_{3/5}$), 127.49 (C_1), 142.21 ($C_{2/6}$), 153.35 (C_4), 163.56 (C_7), 179.87 (C_8).

_N_-Piperidyl-_N'_-benzoylthiourea, HL^8

Mp: 123-126 °C (lit. [62]: 126 - 128 °C) ; δ_H (600MHZ, $CDCl_3$) 1.68 (2H, m, C_{11}), 2.13 (4H, m, $C_{10/10'}$), 3.60 and 4.16 (4H, m, $C_{9/9'}$), 7.47 (2H, m, $C_{3/5}$), 7.58 (2H, m, C_4), 7.83 (2H, d, $C_{2/6}$), 8.44 (1H, s, NH); δc (150MHz, $CDCl_3$) 23.65 (C_{11}), 25.06 and 25.84 ($C_{10/10'}$), 52.66 and 52.97 ($C_{9/9'}$), 126.89 ($C_{3/5}$), 127.94 ($C_{2/6}$), 129.01 (C_4), 133.10 (C_1), 163.43 (C_7), 178.49 (C_8).

_N_-Piperidyl-_N'_-4-nitrobenzoylthiourea, HL^9

Mp: 114-116 °C; δ_H (300MHz, $CDCl_3$) 1.73 (2H, t, C_{11}), 2.18 (4H, m, $C_{10/10'}$), 3.60 and 4.19 (4H, t, $C_{9/9'}$,), 8.00 (2H, m, $C_{2/6}$), 8.35 (2H, d, $C_{3/5}$), 8.78 (1H, s, NH); δc (75MHz, $CDCl_3$)

23.75 (C_{11}), 25.24 and 26.02 ($C_{10/10'}$), 52.87 ($C_{9/9'}$), 123.96 ($C_{3/5}$), 129.10 ($C_{2/6}$), 137.97 (C_1), 150.32 (C_4), 161.39 (C_7), 177.33 (C_8).

N-Piperidyl-*N'*-2,6-dimethoxybenzoylthiourea, HL^{10}

Mp: 157-159 °C; δ_H (300MHz, $CDCl_3$) 1.32 (2H, m, C_{11}), 3.60 (4H, m, $C_{10/10'}$), 3.89 (6H, s, methoxy substituents), 4.02 (4H, t, $C_{9/9'}$), 7.06 (3H, m, C_4 and $C_{3/5}$), 8.53 (1H, s, NH); δc (75MHz, $CDCl_3$) 11.4 and 13.2 ($C_{10/10'}$), 47.7 ($C_{9/9'}$), 55.4 and 61.0 (methoxy substituents), 105.3 ($C_{3/5}$), 127.5 (C_1), 142.2 (C_4), 153.2 ($C_{2/6}$), 163.3(C_7), 179.5 (C_8).

N,N-Diethyl-*N'*-2,2-dimethylpropanoylthiourea, HL^{11}

Mp: 89-91 °C. (Found C, 55.80, H, 9.19; N, 12.76; S, 14.66%); $C_{10}H_{20}N_2SO$ required (C, 55.52; H, 9.32; N, 12.95; S, 14.82%); δ_H (400MHz, $CDCl_3$) 1.24 (15H, s, C_1 and $C_{6/6'}$), 3.50 and 3.95 (4H, q, $C_{5/5'}$), 7.64 (1H, s, NH); δc (100MHz, $CDCl_3$) 11.50 and 13.10 ($C_{6/6'}$), 27.1 (C_1), 39.60 (C_2), 47.50 and 48.0 ($C_{5/5'}$), 174.70 (C_3), 179.70 (C_4).

3,3,3',3'-Tetraethyl-1,1'-isophthaloylbisthiourea, H_2L^{12}

Mp: 136-138 °C (lit. [47]:136 – 138 °C); δ_H (300MHz, $CDCl_3$) 1.30 (12H, t, $C_{10/10'}$), 3.58 and 4.00 (8H, q, $C_{9/9'}$), 7.53 (2H, t, C_5), 7.96 and 7.99 (2H, d, $C_{4/6}$), 9.17 (1H, s, C_2), 8.26 (2H, s, NH's); δc (75MHz, $CDCl_3$) 11.21 and 13.10 ($C_{10/10'}$), 47.45 and 47.78 ($C_{9/9'}$), 126.76 (C_5), 129.63 (C_2), 132.69 ($C_{4/6}$), 133.16 ($C_{1/3}$), 163.49 ($C_{7/7'}$), 179.44 ($C_{8/8'}$).

N-Propyl-*N'*-benzoylthiourea, H_2L^1

Mp: 131-133 °C (lit [63]: 133 - 134 °C); δ_H (600MHz, $CDCl_3$) 0.98 (3H, t, C_{11}), 1.70 (2H, m, C_{10}), 3.63 (2H, m, C_9), 7.49 (2H, m, $C_{3/5}$), 7.60 (1H, m, C_4), 7.82 (2H, d, $C_{2/6}$), 9.14 (1H, s, NH located between C_7 and C_8), 10.76 (1H, s, NH located between C_8 and C_9); δc (150MHz, $CDCl_3$) 11.12 (C_{11}), 21.33 (C_{10}), 47.45 (C_9), 127.52 ($C_{3/5}$), 129.25 ($C_{2/6}$), 132.0 (C_1), 133.65 (C_4), 167.21 (C_7), 180.05 (C_8).

N-Piperidyl-*N'*-4-heptoxybenzoylthiourea, H_2L^2

Mp: 76-78 °C; δ_H (600MHz, $CDCl_3$) 0.89 (3H, t, C_{18}), 1.02 (2H, m, C_{17}), 1.08 (3H, m, C_{11}), 1.31 (2H, m, C_{16}), 1.34 (2H, m, C_{15}), 1.45 (2H, m, C_{14}), 1.74 (2H, m, C_{10}), 1.79 (2H, m, C_{13}), 3.66 (2H, m, C_9), 4.01 (2H, t, C_{12}), 6.96, (2H, d, $C_{2/6}$), 7.78 (2H, d, $C_{3/5}$), 8.91 (1H, s, NH located between C_7 and C_8), 10.80 (1H, s, NH located between C_8 and C_9); δ_C (100MHz, $CDCl_3$) 11.43 (C_{11}), 14.02 (C_{18}), 21.56 (C_{10}), 22.54 (C_{17}), 25.87 (C_{16}), 29.00 (C_{15}), 30.90 (C_{14}), 31.69 (C_{13}), 47.51 (C_9), 68.43 (C_{12}), 114.77 ($C_{3/5}$), 123.36 (C_1), 129.47 ($C_{2/6}$), 163.46 (C_4), 166.23 (C_7), 179.88(C_8).

N-Phenyl-*N'*-benzoylthiourea, H_2L^3

Mp: 136-138 °C; δ_H (300MHz, $CDCl_3$) 7.43 (2H, m, $C_{3/5}$), 7.55 (1H, t, C_4), 7.89 (2H, d, $C_{2/6}$), 7.29 (1H, m, C_{12}), 7.66 (2H, m, $C_{11/11'}$), 7.74 (2H, d, $C_{10/10'}$), 9.10 (1H, s, NH located between C_7 and C_8), 12.60 (1H, s, NH located between C_8 and C_9); δ_C (75MHz, $CDCl_3$) 124.25 ($C_{12/12'}$), 127.05 ($C_{11/11'}$), 129.05 ($C_{10/10'}$), 137.78 (C_9), 127.62 ($C_{3/5}$), 129.37 ($C_{2/6}$), 131.80 (C_1), 133.91 (C_4), 167.20 (C_7), 178.7 (C_8).

N,N-Diethyl-*N'*-camphanoylthiourea, HL^{13}

The method of synthesis and full characterization of the ligand is discussed in detail in reference [64].

2.2 Synthesis and characterization of Ag (I) complex with *N,N*-di-n-butyl-*N'*-benzoylthiourea ligand

The ligand (0.10 g, 0.34 mmol) was dissolved in a 30 ml solvent mixture of acetonitrile-water in a volume ratio of (5:1) respectively. Sodium acetate (0.09 g, 0.684 mmol), dissolved in a minimum volume of water, was added to the ligand solution and the resulting reaction mixture was heated to reflux in an oil bath at 50 °C for 45 minutes. Under these reaction conditions, the weakly acidic proton on the amido-moiety of the ligand is deprotonated and the ligand is therefore ready to form a complex with an incoming metal ion. The use of excess sodium acetate ensures that the deprotonation is complete. (0.06 g, 0.34 mmol) of silver nitrate, dissolved in a minimum volume of water, was added drop-wise to the deprotonated ligand solution and the mixture was refluxed at 60 °C for 1 hour. At this stage, the colour of the reaction mixture (silver-ligand complex) was milky and acetonitrile was added slowly until the solution turned colourless. The reaction mixture was left to stir at room temperature and while cooling excess water (about 20 ml) was added to the flask. The water has a dual purpose of precipitating the complex as well as dissolving the acetate salt. A milky slurry was obtained, left overnight in a refrigerator, and then centrifuged off. A white precipitate was obtained which was filtered and recrystallised from an acetonitrile-chloroform (1:1) solvent mixture. White colourless crystals were obtained after 4 days of slow evaporation of the solvent mixture at room temperature. The crystals were characterized by melting point determination, elemental (C, H, N and S) analysis and X-ray crystal and molecular structure determination.

Mp: 113 -114 °C. (Found: C, 48.44, H, 5.83; N, 7.03; S, 7.73%; $C_{16}H_{23}N_2SOAg$ required C, 48.13; H, 5.81; N, 7.02; S, 8.03%). The crystal structure of the silver complex with *N,N*-di-n-butyl-*N'*-benzoylthiourea is discussed in chapter 5.

2.3 Competitive transport and extraction experiments

2.3.1 Reagents and Chemicals

Analytically pure (AR-grade) chloroform, obtained from Merck, was used in all transport and extraction experiments. Reagent grade $AgNO_3$, $Cu(NO_3)_2.3H_2O$, $Cd(NO_3)_2.4H_2O$, $Zn(NO_3)_2.6H_2O$, $Co(NO_3)_2.6H_2O$, $Ni(NO_3)_2.6H_2O$ and $Pb(NO_3)_2$ salts were all obtained from Merck and used without further purification. AR-grade HNO_3 (55 % w/v) was obtained from Merck and after proper dilution used as a receiving (stripping) solution in the transport experiments. Reagent grade sodium hydroxide and sodium acetate were used in the preparation of buffer solutions. All aqueous solutions were prepared using deionised water.

2.3.2 Preparation of solutions

Three separate source phase buffers (CH_3COOH/CH_3COONa) were prepared. These were: pH = 5.0, pH = 5.5 and pH = 6.0. The recipe for preparing these buffers is summarized in **Table 2.5** [65].

Table 2.5: Sodium acetate, acetic acid buffer (20 °C). The buffer contains x ml of 2M NaOAc and (10-x) ml of 2 M acetic acid, diluted to 100 ml with distilled water.

pH	x
5.0	6.95
5.5	8.75
6.0	9.5

A solution of metal ions was prepared from the nitrate salts of the seven metal ions (see **section 2.3.1**) using deionised water in which the metal ions were each at a concentration of 0.2M. This solution was divided into three flasks and the contents in each flask were diluted with the buffer solutions (pH = 5.0, 5.5 or 6.0) prepared earlier to give a final concentration of each metal ion of 1×10^{-2} mol dm^{-3}. These solutions were used as source phases in the transport experiments.

The aqueous receiving phase used in the transport experiments was either a pH = 3 buffer of HCOOH/HCOONa or a solution of HNO_3 (0.01M, 0.1M, 0.5M or 1.0M) prepared from an AR-grade 55% w/v HNO_3. The pH = 3.0 buffer was prepared by mixing 56.6 ml of HCOOH (1.0M) with 10 ml of NaOH (1.0M) made up to a final volume of 100 ml with deionised water.

The pH of the buffer solutions were measured using a Corning 425 pH meter with a combination glass electrode. The pH meter was calibrated before use by using pH 4.0 and pH 7.0 standard buffer solutions.

The chloroform membrane in the transport experiments contained the ligand (see **section 2.1.3**) and hexadecanoic acid (4×10^{-3} M). The concentration of the ligand was systematically varied between 1×10^{-3} M and 4×10^{-3} M.

2.3.3 Bulk Liquid membrane transport experiments

The metal ion transport arrangement used in the present investigation is represented schematically in **Fig. 1.1**. The study involved metal ion transport from an aqueous source phase containing an equi-molar mixture of the seven metal ions (see **section 2.3.1**) into an aqueous receiving phase, against a back gradient of protons.

An aqueous source phase (10 cm^3) and an aqueous receiving phase (30 cm^3) were bridged by a presaturated chloroform membrane phase that contained the ligand (50 cm^3). The source/organic and organic/receiving phase contact areas were 4.52 and 16.7 cm^2 respectively. Before any transport experiment was conducted, the cells were soaked overnight in 2M HNO_3 solution, rinsed with water and dried with acetone under the hood. The membrane phase, the source phase and the receiving phase were then gently transferred in this respective order into the cells. The cells were thermostated at 25°C and stirred at 10 rpm by means of a coupled single geared synchronous motor.

Under these conditions, not only was the stirring process consistent, but also the interfaces between the organic membrane and the two aqueous phases remained flat and well defined. The cells were first covered with cover slips in order to prevent evaporation of solvents over the 24-hour period and then entirely covered by aluminium foil in order to prevent the light-induced reduction of Ag(I) in the source phase. All transport runs were terminated after 24 hours and the amount of metal ion transported from the source phase to the receiving phase over this period was determined by atomic absorption spectroscopy (AAS). The experimental results obtained by AAS were reproduced by another technique-inductively coupled plasma-optical emission spectroscopy (ICP-OES). The experimental results obtained from both techniques did not differ by more than 4%.

2.3.3.1 Analysis of solutions

Samples were taken from both the source and receiving phases of each duplicate run after each experiment and diluted to the required concentration range with 0.1 M HNO_3. Both the AAS as well as the ICP-OES were calibrated by standards containing the seven metal ions that were prepared from the metal salts described in **section 2.3.1** by proper dilution with 0.1 M HNO_3. The average flux rate, J (mol/hr), for each transport experiment was calculated based on the quantity of metal ions transported into the receiving phase in a 24-hour period. The transport results are quoted as the average values obtained from the duplicate runs carried out in parallel; in all cases the values did not differ by more than 5%. J values equal to or less than 2.2×10^{-8} mol/24 hr were assumed to be within experimental error of zero and have been ignored in the analysis of results.

2.3.4 Extraction experiments

The procedure employed involved 'competitive' metal ion extraction experiments from an aqueous phase into a chloroform phase. The chemical reagents used were identical to those employed in the transport experiments. The aqueous phase was buffered at pH = 5.0 with sodium acetate/acetic acid buffer and contained equal concentrations (1×10^{-2} mol dm^{-3}) of cobalt (II), copper (II), lead (II), silver (I), cadmium (II), zinc (II) and nickel (II) as their respective nitrate salts. The chloroform membrane contained the ligand (**section 2.1.3**) at a concentration varying from 5×10^{-4} mol dm^{-3} to 3×10^{-3} mol dm^{-3}. The aqueous source phase (3 ml) and the chloroform membrane (15 ml) were contained in a sealed polytop vial. Each two-phase solution in the vials was capped tightly, wrapped with parafilm and shaken at 120 cycles per minute for 24 hours on a labcon-oscillating shaker.

Extraction was performed at 25 °C. Throughout the extraction process, the polytop vials were covered with aluminum foil to prevent light-induced reduction of Ag(I). The analyses of metal ions were performed by AAS, while the ICP-OES was used to confirm the results. The results are quoted as the average value obtained from duplicate runs. Any apparent extraction of a metal ion of less than 2.0% was assumed to be within the experimental error of zero and hence ignored in the treatment of the results. In all cases, the values between any two duplicate runs did not differ by more than 2%.

2.4 Instrumentation

2.4.1 Atomic absorption spectrometry (AAS)

2.4.1.1 Instrument set up

The atomic absorption spectrometer used was a Varian model, AA-1275. A specific wavelength at which each metal absorbs and is free from spectral interferences was selected for the analyses (see **Table 2.6**). An acetylene-air gas mixture was used as the flame source for the burner. By running a blank and a series of standard solutions in the linear response range of the detector, a standard calibration curve was drawn. For this specific instrument, calibration curves were found to be linear up to an absorbance reading of 1.0. As the analyte concentration increases, deviation in the instrument response from linearity increases (**Fig. 2.2)**. This deviation could be due to various factors, such as unabsorbed radiation, stray light, or disproportionate decomposition of molecules.

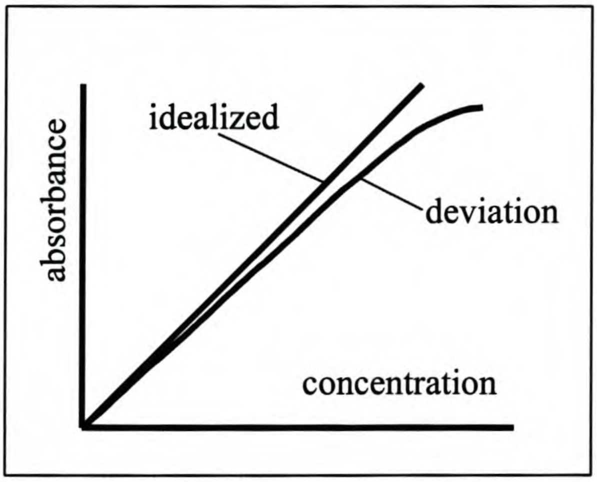

Figure 2.2: The response of the detector as a function of analyte concentration

Table 2.6: Optimum experimental conditions for obtaining a linear dynamic response (as recommended by instrument supplier) [66].

Element	λ(nm)	Spectral band pass (nm)	Optimum working range (ppm)
Ag	328.1	0.5	1 – 5
	338.3	0.5	3 – 12
Cd	228.8	0.5	0.5 – 2.0
	326.1	0.5	25 – 100
Co	240.7	0.2	3 – 12
	304.4	0.5	50 – 200
Cu	324.7	0.5	2 – 8
	327.4	0.2	6 – 24
	218.2	0.2	20 – 80
Ni	232.0	0.2	3 – 12
	341.5	0.2	15 – 60
Pb	217.0	1.0	5 – 20
	283.3	0.5	10 – 40
Zn	213.9	1.0	0.4 – 1.6

2.4.1.2 Chemical interferences

There are no chemical interferences reported for Ag, Cd, Co and Zn in the air-acetylene flame. For Copper, some signal depression at high Zn/Cu ratios has been reported. This can be minimized by the use of a lean air-acetylene flame or a nitrous oxide-acetylene flame. For lead, no cationic interferences have been reported. However, some anionic interferences have been reported [66]. Phosphates, carbonates, iodides, fluorides and acetates suppress lead absorbance significantly at anionic concentrations ten times greater than lead. These interferences can be overcome by adding an EDTA solution to the sample. For nickel, non-atomic species in the flame absorb strongly. If the sample has high concentration of total dissolved solids, it is necessary to correct for non-atomic absorption by using the 231.7 nm nickel non-absorbing line.

2.4.2 Inductively Coupled Plasma-Optical Emission Spectrometry (ICP-OES)

2.4.2.1 Instrument set up

A Varian Liberty II type ICP spectrometer with radially viewed plasma was used to confirm results obtained by the AAS. The operating conditions for the instrument were set by the instrument manufacturer. However, some of the parameters have been optimized to obtain best performance from the ICP-OES system. The final instrument operating conditions used are listed in **Table 2.7**.

Table 2.7: Instrument operating conditions

Power	1.1 kW
Plasma gas flow	15.0 L/min
Auxiliary gas flow	1.5 L/min
Vertical viewing height	8 mm
Pump rate	15.0 rpm
Nebulizer gas flow	15.0 L/min
Internal standard	Not used.
Sample uptake delay	30 s
Rinse time	0 s
Peak tracking window	0.04 nm
Stabilization delay	15.0 min
Replicates	4.0
Auto sampler	Varian SPS-5
Background correction	Polynomial

Before any measurements were recorded, the instrument was calibrated using the external standard calibration method. Very straight calibration curves were obtained. The recommended wavelengths (λ's) and detection limits for the elements analyzed by this technique are summarized in **Table 2.8**.

Table 2.8: Detection limit of elements analyzed at the specific wavelength by ICP-OES [67].

Element	λ (nm)	Instrument detection limit (ppm)
Ag	328.07	2.0
Cd	228.80	1.2
Co	232.89	4.0
Cu	324.75	1.5
Ni	231.60	5.0
Pb	220.35	11.0
Zn	213.86	0.8

Chapter 3

3 Competitive metal-ion bulk membrane transport studies involving *N,N*-dialkyl-*N'*-acyl(aroyl) thioureas

3.1 Introduction

In this chapter, a comparative study of the transport properties of various thiourea ligands (**section 2.1.3**) with a number of transition and post transition metal ions (**section 2.3.1**) is presented.

The ligands are grouped into six sections according to their structural similarities. The discussion of the results obtained for each group of ligands is presented after each section. Finally, a concluding discussion on the overall transport results obtained is made towards the end of the chapter.

3.2 Background

If a ligand is to qualify as a suitable metal ion carrier in a liquid membrane system, it should fulfil certain conditions. These conditions are:

a. It should be selective

b. It should display rapid metal exchange kinetics

c. It should be sufficiently lipophilic [18] (and preferentially of lower molecular weight) to avoid leaching into the aqueous source and receiving phases.

d. It has to have a moderately high formation constant with the target metal ion to be transported [23].

According to Pearson's hard – soft – acid – base (HSAB) principle [68], Ag(I) and Pb(II) are classified as soft acids whereas Co(II), Ni(II), Cu(II), Zn(II) and Cd(II) are classified as borderline acids. The soft acids are the electronegative metals. They are characterized by quite high Pauling electronegativities for metals, generally in the range of 1.9 to 2.54. Gold is the most electronegative metal and hence the softest. Therefore, according to this principle, Ag(I) is softer that Pb(II) because the electronegativity of Ag(I) (1.93) is higher than that of Pb(II) (1.87). The HSAB principle can be restated as: Softer Lewis bases tend to combine with softer Lewis acids [69]. Since the donor atoms of the most common Lewis bases have electronegativities increasing in the order S < Br < N < Cl < O < F, Ag(I) should be transported with sulfur-containing ligands better than any of the other six metal ions. Similarly, ligands containing oxygen or nitrogen as their donor atoms tend to combine with the harder metal ions as both the oxygen and nitrogen atoms are harder compared to sulfur. Therefore, the presence of the sulfur donor atom in the *N*,*N*-dialkyl-*N'*-acyl(aroyl)thioureas could make these ligands selective for Ag(I).

3.3 The mechanism of transport

The following mechanism (**scheme. 3.1**) can be proposed for the transport of a metal ion (M^{n+}) from the source phase into the receiving phase by *N*,*N*-dialkyl-*N'*-benzoyl thiourea ligands.

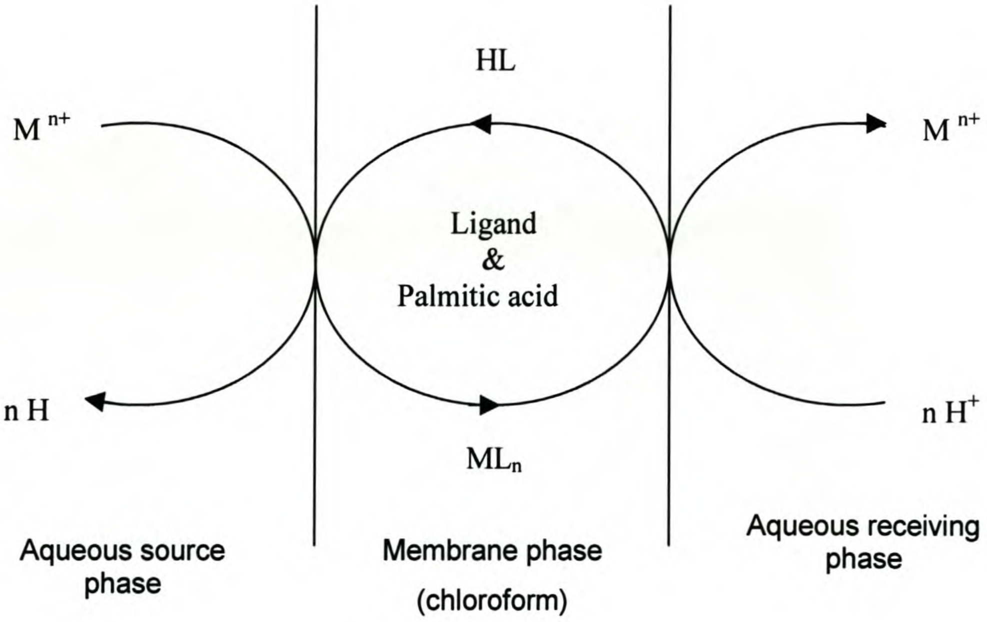

Scheme 3.1: A schematic representation of the mechanism of transport of a metal ion across a chloroform membrane.

The metal ion in the aqueous source phase comes into contact with the ligand at the source phase / organic phase interface. At this interface, the ligand is deprotonated and a neutral complex is formed with the metal ion to be transported. The metal -ligand complex then diffuses through the organic phase until it comes into contact with the receiving phase. At the membrane / receiving phase interface, the ligand is again protonated by the more acidic solution (receiving phase) and in so doing releases the metal ion into the receiving phase, a process called 'stripping'. The protonated form of the ligand then diffuses back across the membrane to the source phase / membrane phase interface to repeat the cycle. The direction of the proton transport is in the opposite direction to that of the metal ions. Interestingly, metal ion transport can be driven past the 50% mark by maintaining the required pH gradient between the source phase and the receiving phase [23].

3.4 Assessment of errors in experimental data

There are two types of error that can affect the precision and accuracy of a measured quantity; namely, determinate errors and indeterminate errors.

3.4.1 Determinate errors

Determinate errors have a definite source that can usually be identified. They cause all the results from replicate measurements to be either high or low. Because they are unidirectional, determinate errors are also called systematic errors. The effect of such type of errors may be either constant or proportional. The magnitude of a constant error does not depend on the size of the quantity measured. However, proportional errors increase or decrease in proportion to the size of the sample taken for analysis. The main cause of proportional errors is the presence of interfering contaminants in the sample.

Sources of determinate errors

There are three types of determinate error. These are:

1. Human errors are the most serious errors of an analyst. Such errors result from the carelessness, inattention, or personal limitations of the experimenter.
2. Systematic instrument errors are caused by imperfections in measuring devices and instabilities in their power supplies.
3. Method errors arise from non-ideal chemical or physical behavior of analytical systems.

3.4.2 Indeterminate errors

Indeterminate errors, also called random errors, arise when a system of measurement is extended to its maximum sensitivity. They are caused by the many uncontrollable variables that are an inevitable part in every physical or chemical measurement. There are many sources of indeterminate errors, but none can be positively identified or measured because most of them are so small that they are undetectable. The cumulative effect of the individual indeterminate errors, however, causes the data from a set of replicate measurements to fluctuate randomly around the mean of the set.

3.5 Experimental conditions and calculations

The following experimental conditions were used throughout the transport experiments.

The aqueous source phase: 10 ml, contained the seven metal ions each at an initial concentration of 0.01M prepared in a buffer solution (CH_3COOH/CH_3COONa) of pH = 5.0, 5.5 or 6.0. The method of preparation of the metal ion salt solutions and the recipe of the buffer solutions are discussed in section **2.3.2**.

The membrane (chloroform) phase: 50 ml, contained palmitic acid and the ligand. The concentration of the palmitic acid was 4×10^{-3} M throughout all the experiments while the ligand concentration was varied between 0.001 and 0.004 M.

The aqueous receiving phase: (30 ml), was in most cases dilute HNO_3 solution prepared by proper dilution of an analytically pure (55% w/v) HNO_3 solution and in some cases, pH = 3.0 buffer was used (for preparation of this buffer, see **section 2.3.2**).

The transport experiments are 'competitive' because all the seven metal ions were initially contained in the source phase. All three phases were stirred independently for 24 hours at 25 °C at a speed of 10 rpm.

The cation flux, J - values, were calculated using the relation:

$$J = \frac{C_{(receiving)} \times V}{t}$$

$C_{(receiving)}$ is the concentration of the cation in the receiving phase (mol/dm^3), V is the volume of the receiving phase (dm^3) and t is the transport time in hours. The percentage of metal ion(s) transported from the aqueous source phase to the aqueous receiving phase, (T%), was calculated using the relation:

$$(T\,\%) = (n_r / n_i) \times 100$$

Where n_r and n_i represent the number of moles of the metal ion transported into the receiving phase and the initial number of moles of the metal ion in the source phase respectively.

Blank experiment was carried out for the transport studies in which the membrane phase contained palmitic acid (4 x 10^{-3} M) without the carrier (ligand). No leakage of cation(s) from source phase into the organic phase was observed. The transport experiments were carried out in duplicate to check reproducibility. All duplicate runs were within 5 -6% of one another. Errors (both determinate and indeterminate) that were introduced throughout the experiments were assumed to be within ± 5% of the results.

3.6 Terminologies and abbreviations

Throughout this chapter, the term **'% metal transported'** refers to the percentage of the metal ion transported from the aqueous source phase to the aqueous receiving phase. The following abbreviations are also used.

$^{Ag}T_r$ % = Percentage of Ag (I) transported into the receiving phase.

$^{Ag}T_M$ %= Percentage of Ag (I) transported into the membrane phase.

$^{Cu}T_r$ % = Percentage of Cu (II) transported into the receiving phase.

$^{Cu}T_M$ %= Percentage of Cu (II) transported into the membrane phase.

In the context of transport behaviour, 'efficiency' is synonymous with high mass transfer of the species being transported. The efficiency of transport set up shown in **Fig. 1.1** is determined by two physical parameters. These are: the physical dimension of the transport cell and the rate of stirring of the solutions. Efficiency can be enhanced by increasing the interfacial contact area between the membrane and the aqueous phases. However, stirring the organic and aqueous phases at a higher rate (>10 rpm) is not recommended as it may cause complete mixing of the two phases.

The other terminology is 'selectivity. In the context of transport, the term 'selective' means that the ligand selects one metal over the other by a relatively large percentage difference. A parameter called "selectivity factor of Ag(I) to Cu(II)", η(Ag(I)/Cu(II)), has also been defined for comparing the selectivity of a specific ligand for Ag(I) over that of Cu(II) as follows:

$$\boxed{\eta\,(\mathrm{Ag(I)/Cu(II)}) = \frac{{}^{Ag}T_r\,\%}{{}^{Cu}T_r\%}}$$

3.7 Experimental results

3.7.1 Metal ion transport by *N,N*-di-n-butyl-*N'*-benzoylthiourea (HL^1), *N,N*-diethyl-*N'*-benzoylthiourea (HL^2) and *N,N*-di-(2-hydroxyethyl)-*N'*-benzoylthiourea (HL^3) ligands.

In this section, HL^1, HL^2 and HL^3 are grouped together. These ligands all posses a benzoyl group and a thiourea motif in their structures but differ in their substituent groups. Competitive metal ion transport experiments involving these ligands were conducted and the results are summarized in **Fig. 3.1 – 3.6** and **Table 3.1**.

For HL^1 and HL^2, a source phase pH of 5.5 and a receiving phase pH of 1.0 were adopted as optimum conditions, so that the effect of varying the ligand concentration from 1 x 10^{-3} to 2 x 10^{-3} M on the transport efficiency and selectivity for Ag(I) could be studied. For HL^3, we have studied the effect of varying the ligand concentration as well as pH of the source phase, and the results are summarized in **Fig. 3.3 and 3.4**.

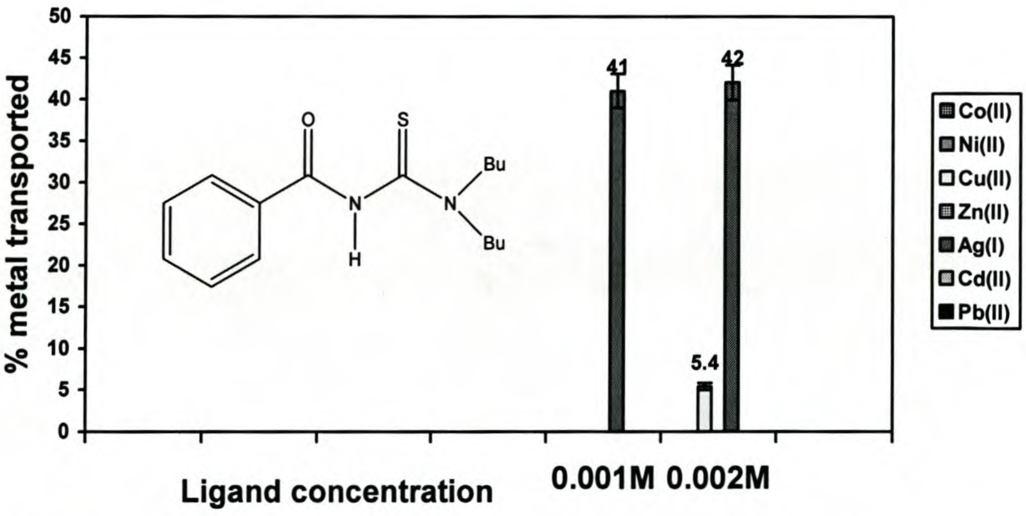

Fig. 3.1: Comparison of the percentage transport of Ag(I) in a competitive transport study involving **HL^1.** The experimental conditions were: **source phase pH = 5.5** and **receiving phase pH = 1.0**. The **ligand concentration** was varied from **1 x 10^{-3} M** to **2 x 10^{-3} M**.

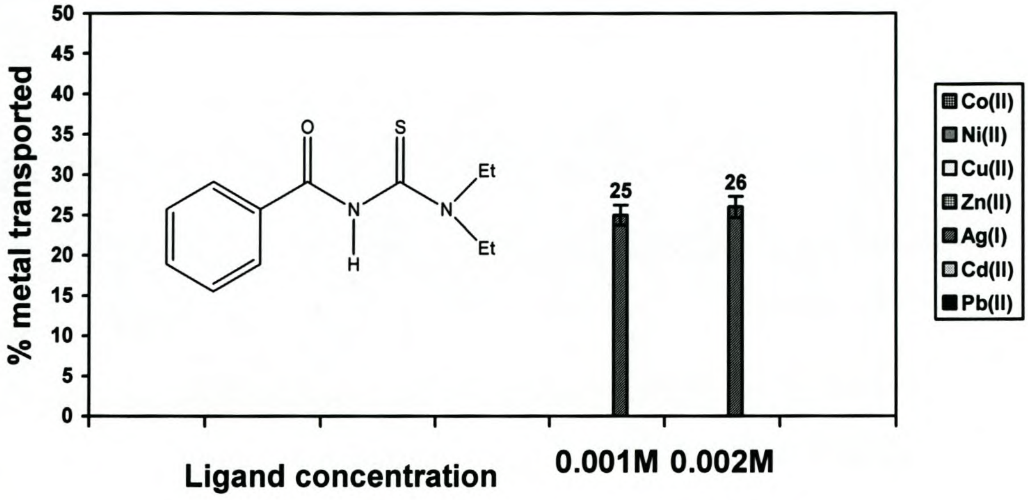

Fig. 3.2: Comparison of the percentage transport of Ag(I) in a competitive transport study involving **HL^2**. The experimental conditions were: **source phase pH = 5.5** and **receiving phase pH = 1.0**. The **ligand concentration** was varied from **1 x 10 $^{-3}$ M** to **2 x 10 $^{-3}$ M**.

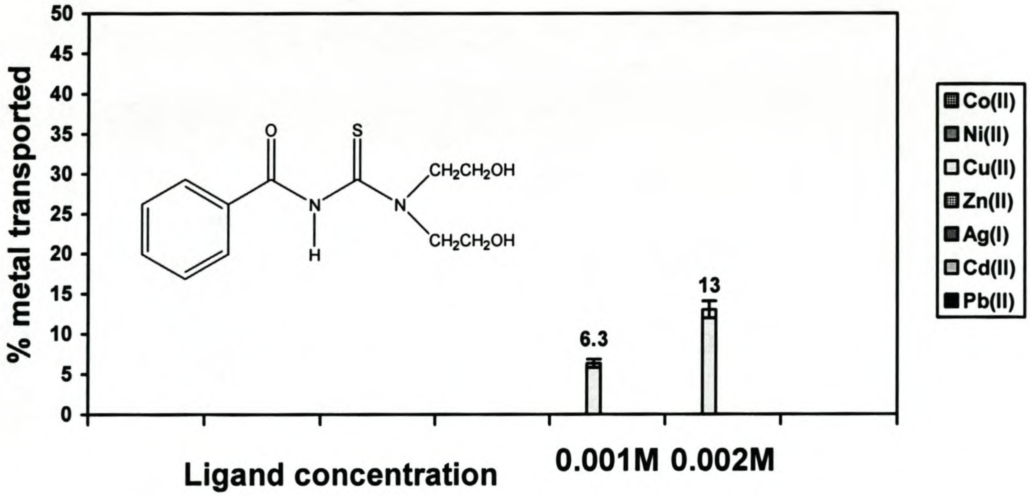

Fig. 3.3: Comparison of the percentage transport of Cu(II) in a competitive transport study involving **HL^3**. The experimental conditions were: **source phase pH = 5.5** and **receiving phase pH = 1.0**. The **ligand concentration** was varied from **1 x 10 $^{-3}$ M** to **2 x 10 $^{-3}$ M**.

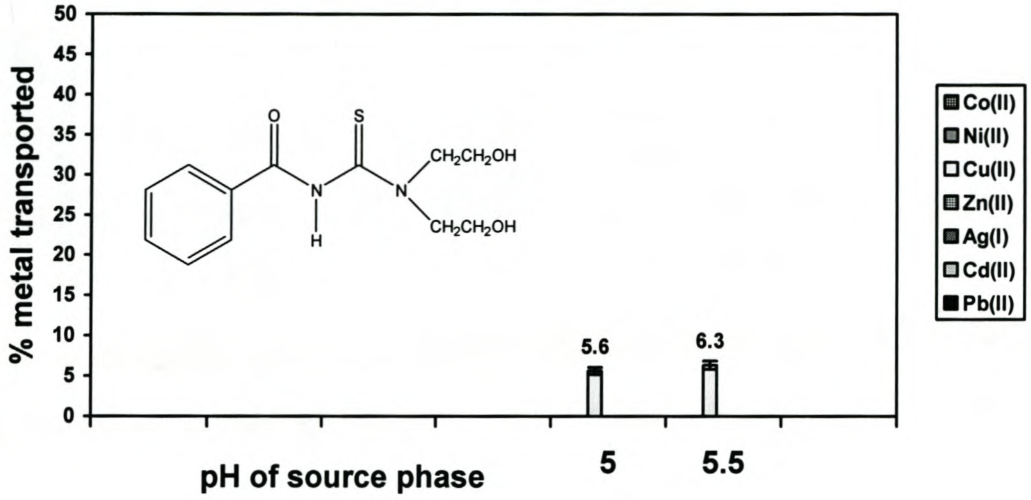

Fig. 3.4: Comparison of the percentage transport of Cu(II) in a competitive transport study involving **HL^3**. The experimental conditions were: **receiving phase pH = 1.0** and **$[HL^3]$ = 1 x 10^{-3} M**. In this case, the **source phase pH** was varied from **5.0** to **5.5**.

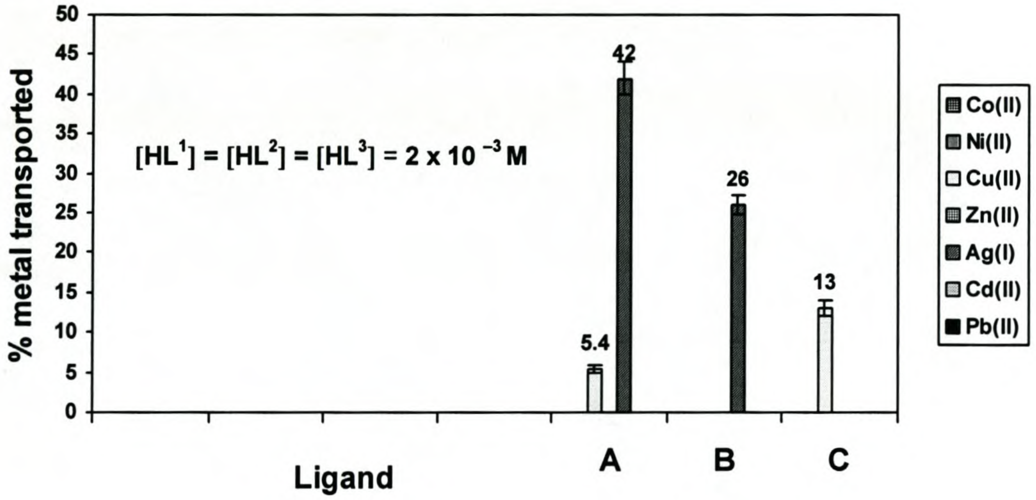

Fig. 3.5: Comparison of the percentage transport of Ag(I) and Cu(II) ions in a competitive transport study involving **HL^1, HL^2 and HL^3** ligands. **A** refers to **HL^1**, **B** refers to **HL^2** and **C** refers to **HL^3**. In all cases, the experimental conditions were the same: **source phase pH = 5.5, receiving phase pH = 1.0** and **$[HL^1]$ = $[HL^2]$ = $[HL^3]$ = 2 x 10^{-3} M**.

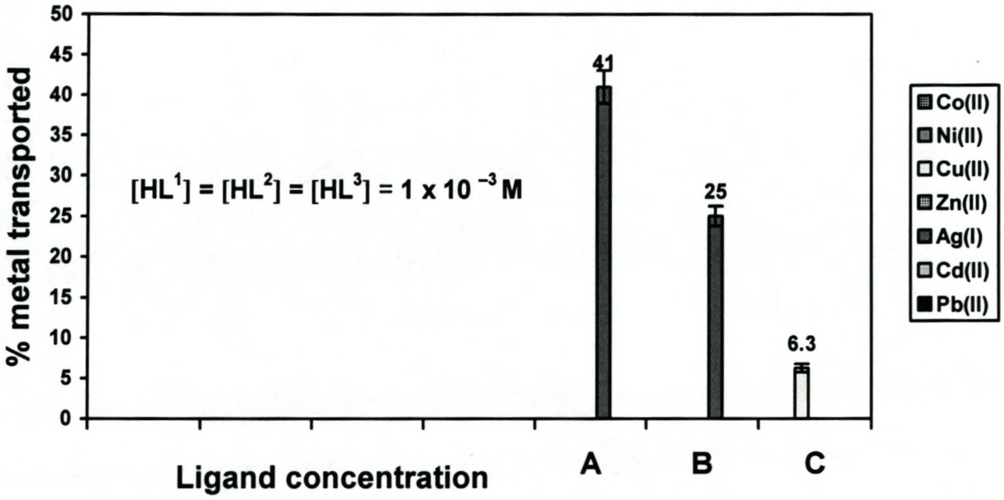

Fig. 3.6: Comparison of the percentage transport of Ag(I) and Cu(II) ions in a competitive transport study involving **HL^1, HL^2 and HL^3**. **A** refers to **HL^1**, **B** refers to **HL^2** and **C** refers to **HL^3**. In all cases, the experimental conditions were the same: **source phase pH = 5.5, receiving phase pH = 1.0** and **$[HL^1] = [HL^2] = [HL^3] = 1 \times 10^{-3}$ M**.

Table 3.1: J-values for the competitive metal ion transport studies involving HL^1 – HL^3 (data includes ± 5% experimental error). The experimental conditions were: pH of source phase = 5.5, pH of receiving phase = 1.0 and concentration of ligand = 0.002 M.

Metal ion transport (J values) in (mol/hr x 10^{-7})			
	HL^1	**HL^2**	**HL^3**
Co(II)	-	-	-
Ni(II)	-	-	-
Cu(II)	2.2	-	5.4
Zn(II)	-	-	-
Ag(I)	18	11	-
Cd(II)	-	-	-
Pb(II)	-	-	-
$^{Ag}T_r$ %	42	26	-
$^{Ag}T_M$ %	43	57	95
$^{Cu}T_r$ %	5.4	-	13
$^{Cu}T_M$%	-	2.5	16
η (Ag(I) / Cu(II))	7.8	$\eta \rightarrow \infty$	$\eta = 0$

3.7.2 Comparison of metal ion transport by *N,N*-di-n-butyl-*N'*-benzoylthiourea (HL^1), *N,N*-diethyl-*N'*-benzoylthiourea (HL^2) and *N,N*-di-(2-hydroxyethyl)-*N'*-benzoylthiourea (HL^3).

Under the experimental conditions employed, HL^1 and HL^2 are selective for Ag(I) whereas HL^3 selectively transports Cu(II). **Fig. 3.1** shows an increase in η (Ag(I) / Cu(II)) with a decrease in the concentration of HL^1. It can also be seen from **Fig. 3.5 - 3.6 and Table 3.1** that the percentage transport of Ag(I) by HL^1 is higher than that of HL^2. The sum ($^{Ag}T_r$ % + $^{Ag}T_M$ %), which is a measure of the interaction between the ligands and Ag (I), is higher for HL^1 than HL^2. HL^1 is more soluble in chloroform compared to HL^2, so the higher percentage transport of Ag(I) by HL^1 can be the result of an increased lipophilicity of the ligand because of its longer alkyl substituents (butyl groups) compared to that of HL^2 where the substituents are ethyl groups.

The fact that HL^3 is selective for Cu(II) compared with Ag(I) can be attributed to the presence of the two – OH groups attached to the alkyl end of the ligand. For HL^3, the sum ($^{Ag}T_r$ % + $^{Ag}T_M$ %) is greater than ($^{Cu}T_r$ % + $^{Cu}T_M$ %). When we look into the metal ions transported by HL^3, it is only Cu(II) that is transported into the receiving phase and not Ag (I). This suggests that although about 95% of Ag(I) is extracted from the source phase into the membrane phase, it is not stripped into the receiving phase at pH = 1.0 (see **Table 3.1**). On the other hand, although Cu(II) was not transported into the membrane phase as efficiently as Ag(I), about 13% of the total Cu(II) that was originally present in the source phase was transported into the receiving phase. Therefore, it appears that the formation constant of HL^3 must be substantially higher for Ag(I) than Cu(II), not allowing the release of Ag(I) from the membrane phase into the receiving phase. Hence, HL^3 is a better transport ionophore for Cu(II) compared to Ag(I).

From the transport results obtained, an attempt is made to predict the coordination chemistry of HL^3 with Ag(I) and Cu(II) ions. The prediction is based on the experimental transport results reported in **Table 3.1**. As can be seen from the table, the sum: ($^{Cu}T_r$% + $^{Cu}T_M$% + $^{Ag}T_M$%) exceeds 100%. This indicates that HL^3 must be simultaneously coordinating with both Ag(I) and Cu(II) ions, thus transporting Cu(II) into the receiving phase while simultaneously extracting Ag(I) into the membrane phase. Therefore, we predict that the ligand may be binding to Ag(I) ion through the sulfur and oxygen donor atoms of the thiourea moiety, and to Cu(II) through the oxygen atoms of the two –OH groups forming two stable five membered chelate rings as shown in **scheme 3.1**.

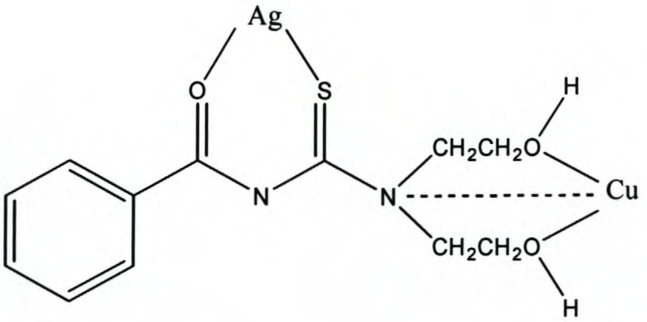

Scheme 3.1: Shows the predicted co-ordination mode of Ag(I) and Cu(II) ions with HL^3. The two five membered chelate rings formed during complex formation are also shown.

3.7.3 Metal ion transport by *N,N*-diethyl-*N'*-4-nitrobenzoylthiourea (HL^4) and *N,N*-diethyl-*N'*-4-chlorobenzoylthiourea (HL^5) ligands.

Competitive metal ion transport experiments involving HL^4 and HL^5 as ionophores have been conducted under conditions where the pH of the source phase, pH of the receiving phase and concentration of the ligand were systematically varied and the results are summarized in **Fig. 3.7 – 3.13.**

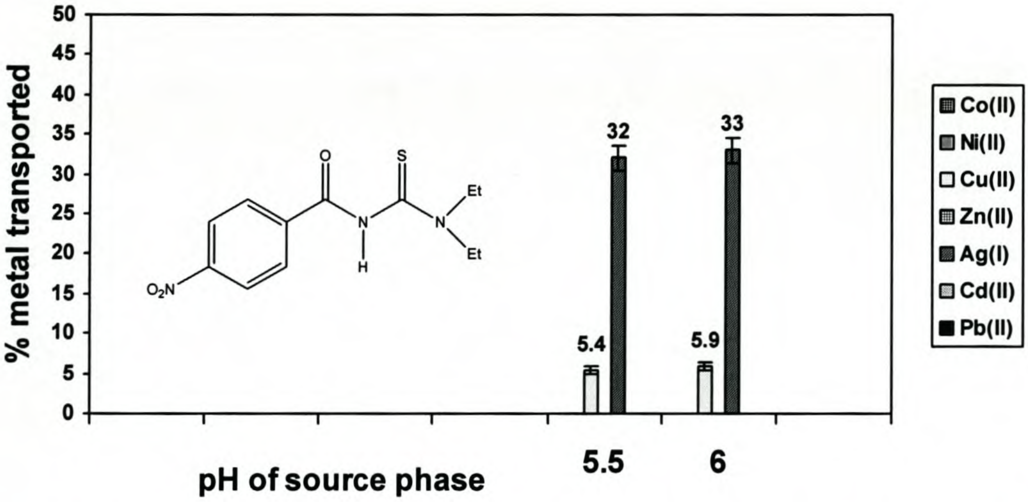

Fig. 3.7: Comparison of the percentage transport of Ag(I) and Cu(II) ions in competitive transport studies involving $\mathbf{HL^4}$. The experimental conditions were: **receiving phase pH = 0.3** and **[HL^4] = 2×10^{-3} M**. The **pH of the source phase** was varied from **5.5** to **6.0** as shown in the above figure.

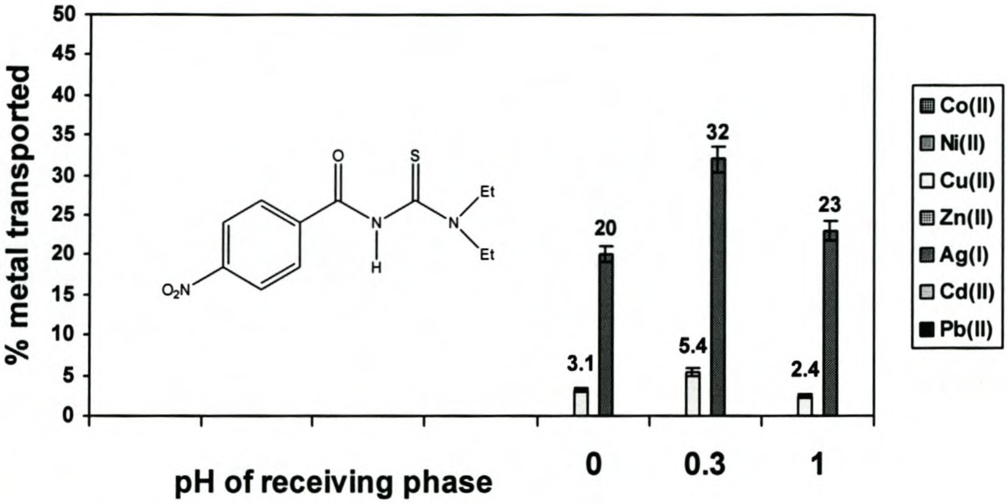

Fig. 3.8: Comparison of the percentage transport of Ag(I) and Cu(II) ions in competitive transport studies involving **HL^4**. The experimental conditions were: **source phase pH = 5.5** and [**HL^4**] = **2 x 10^{-3} M**. The **pH of the receiving phase** was varied from **0** to **1.0** as shown in the above figure.

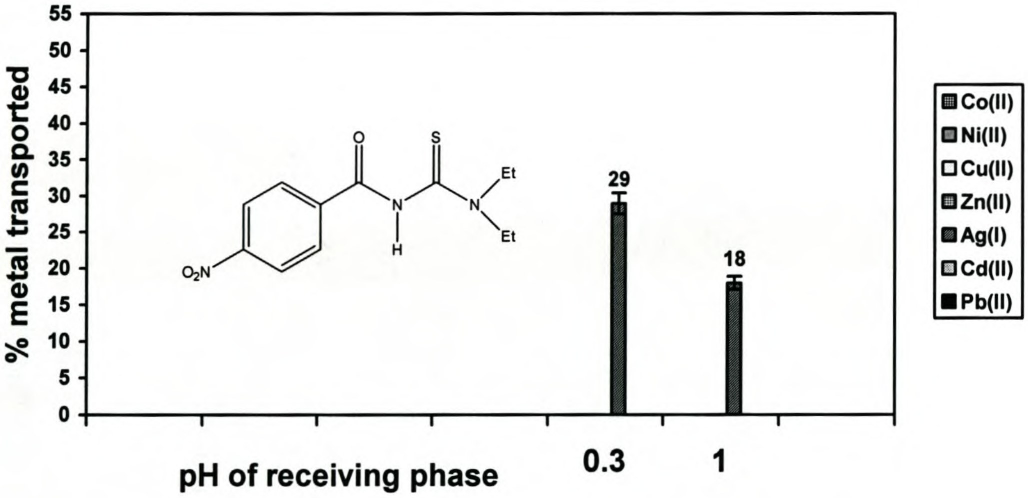

Fig. 3.9: Comparison of the percentage transport of Ag(I) ion in competitive transport studies involving **HL^4**. The experimental conditions were: **source phase pH = 5.5** and [**HL^4**] = **1 x 10^{-3} M**. The **pH of the receiving phase** was varied from **0.3** to **1.0** as shown in the above figure.

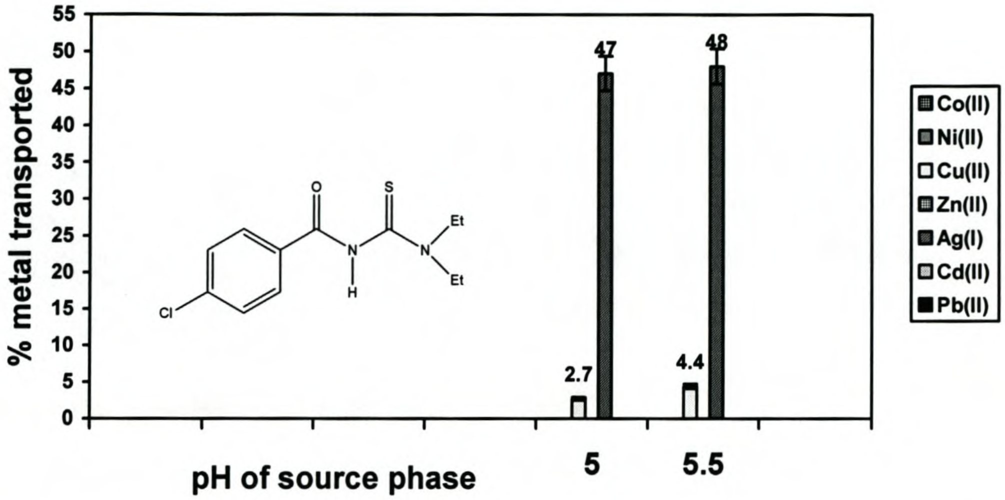

Fig. 3.10: Comparison of the percentage transport of Ag(I) and Cu(II) ions in competitive transport studies involving **HL^5**. The experimental conditions were: **receiving phase pH = 1.0** and [**HL^5**] = **2 x 10^{-3} M**. The **pH of the source phase** was varied from **5.0** to **5.5** as shown in the above figure.

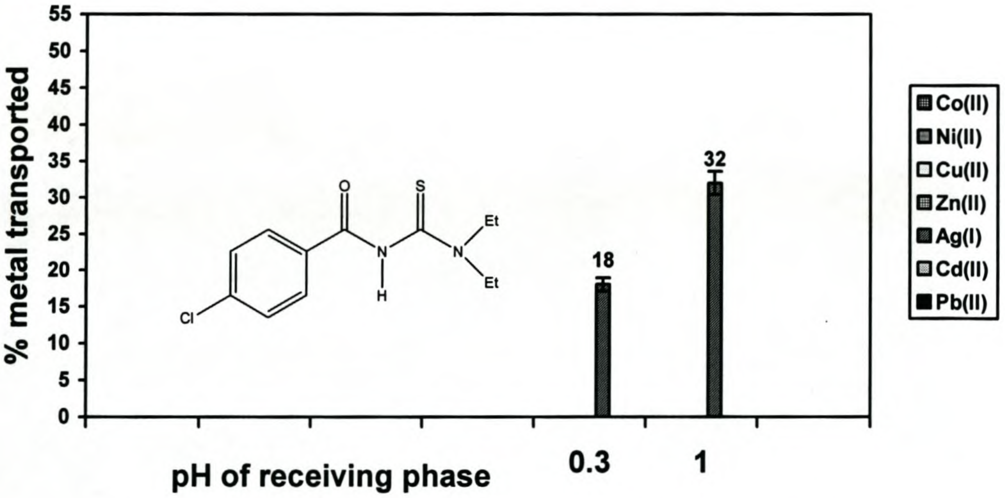

Fig. 3.11: Comparison of the percentage transport of Ag(I) and Cu(II) ions in competitive transport studies involving **HL^5**. The experimental conditions were: **source phase pH = 5.5** and [**HL^5**] = **1 x 10^{-3} M**. The **pH of the receiving phase** was varied from **0.3** to **1.0** as shown in the above figure.

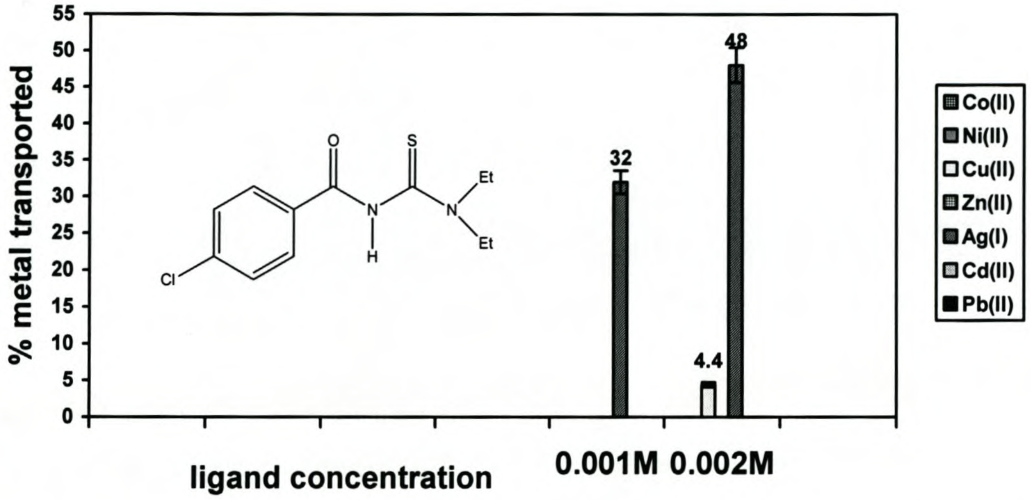

Fig. 3.12: Comparison of the percentage transport of Ag(I) and Cu(II) ions in competitive transport studies involving **HL^5**. The experimental conditions were: **source phase pH = 5.5** and **receiving phase pH = 1.0**. The **ligand concentration** was varied from **1 x 10 $^{-3}$ M** to **2 x 10 $^{-3}$ M** as shown in the above figure.

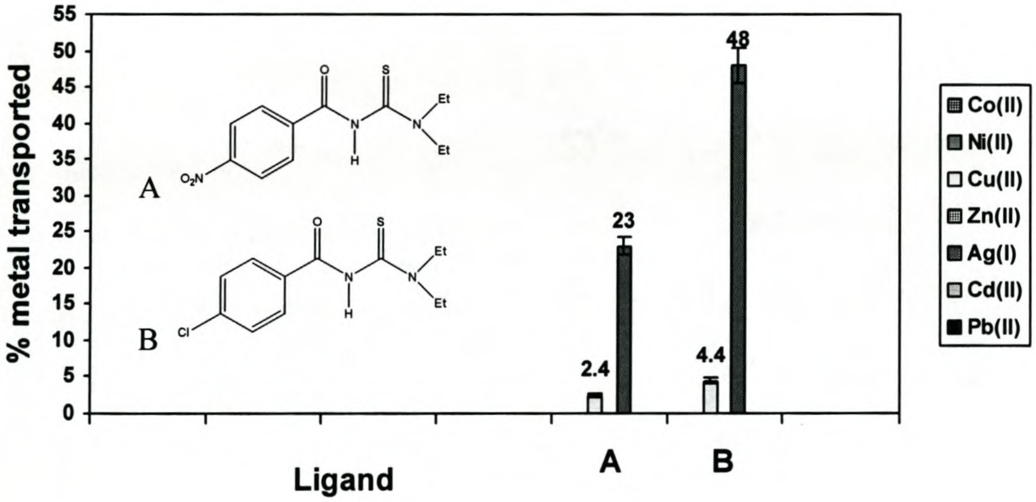

Fig. 3.13: Comparison of the percentage transport of Ag(I) and Cu(II) ions in competitive transport experiments involving **HL^4** and **HL^5** ligands. **A** refers to HL^4 and **B** refers to HL^5. In both experiments, **source phase pH = 5.5, receiving phase pH = 1.0** and **ligand concentration** = **2 x 10^{-3} M**.

Table 3.2: J - values for the competitive metal ion transport studies involving HL^4 and HL^5 ligands (data includes ± 5% experimental error). The experimental conditions were: pH of source phase = 5.5, pH of receiving phase = 1.0 and concentration of ligand = 0.002 M.

Metal ion transport (J values) in (mol/hr x 10^{-7})		
	HL^4	**HL^5**
Co(II)	-	-
Ni(II)	-	-
Cu(II)	1.0	1.8
Zn(II)	-	-
Ag(I)	9.8	20
Cd(II)	-	-
Pb(II)	-	-
$^{Ag}T_r$ %	23	48
$^{Ag}T_M$ %	41	36
$^{Cu}T_r$ %	2.4	4.4
$^{Cu}T_M$%	4.2	-
η (Ag(I)/Cu(II))	9.6	11

3.7.4 Comparison of metal ion transport by *N,N*-diethyl-*N'*-4-nitrobenzoylthiourea (HL^4) and *N,N*-diethyl-*N'*-4-chlorobenzoylthiourea (HL^5) ligands.

HL^4 and HL^5 are grouped together because of their similar structures. These ligands, however, differ greatly in their solubility in chloroform. HL^5 is very soluble, whereas HL^4 is only slightly soluble in chloroform. The difference in solubility behavior is directly related to the polarity and lattice energy. However, other physical properties of the ligands related to solubility may have an influence on transport efficiency of the ligands.

Both ligands are selective to Ag(I), with only a small percentage of Cu(II) being transported along with Ag(I). However, comparison of the results of the rate of transport (J values) of Ag(I) by HL^4 and HL^5 ligands **(Table 3.2)** shows that HL^5 has a higher efficiency and better selectivity for Ag (I) than HL^4 under the same experimental conditions.

It is evident from **Fig. 3.7 – 3.9** that the transport of Ag(I) by HL^4 reads a maximum when the pH of the source phase and pH of the receiving phase are set to 6.0 and 0.3 respectively. Increasing the pH of the source phase from 5.5 to 6.0 resulted in a slight increase in Ag(I) and Cu(II) transport. However, lowering the pH of the receiving phase from 0.3 to 0 resulted in a decrease in the transport percentage of Ag(I) from 29% to 18%. This was expected, as at pH = 0, it was observed that a portion of the yellow colored ligand (HL^4) was bleeding into the receiving phase thereby changing the color of the receiving phase into yellow. This indicates that the ligand may be bleeding into the receiving phase. On the other hand, increasing the pH of the receiving phase from 0.3 to 1.0 resulted in a decrease in percentage of Ag(I) transported by HL^4. This suggests that the stripping process of Ag(I) requires a moderately acidic strippant (see **Fig. 3.8 and 3.9**).

At a ligand concentration of 2 x 10^{-3} M, the optimum pHs of the source phase and the receiving phase which result in a selective and efficient transport of Ag(I) by HL^5 were found to be 5.5 and 1.0 respectively. Decreasing the pH of the source phase from 5.5 to 5.0 did not bring a significant change in Ag(I) transport (**Fig. 3.10**).

Comparison of the sum of the percentage Ag (I) transported into the membrane phase "$^{Ag}T_M$%" and percentage of Ag(I) transported into the receiving phase "$^{Ag}T_r$%" by HL^4 and HL^5 ligands (see **Table 3.2)** shows that, Ag(I) can have a higher formation constant with HL^5 than HL^4. It is also evident that, at the pH conditions reported in **Table 3.2**, the efficiency of the ligands for transporting Ag(I) follows the order: $\mathbf{HL^5} > \mathbf{HL^4} > \mathbf{HL^2}$.

The effect of varying the ligand concentration on Ag(I) transport by HL^4 and HL^5 was also studied. For both ligands, doubling the ligand concentration from 1 x 10^{-3} M to 2 x 10^{-3} M resulted in an increase in efficiency for Ag(I) transport. However, when the ligand concentration was doubled, a small percentage of Cu(II) was transported with Ag(I).

3.7.5 Metal ion transport by *N,N*-dibutyl-*N'*-2,4,6-trimethoxybenzoylthiourea (HL^6) and *N,N*-diethyl-*N'*-2,4,6-trimethoxybenzoylthiourea (HL^7) ligands.

Competitive metal ion transport experiments involving HL^6 and HL^7 as ionophores were conducted under conditions where pH of the source phase, pH of the receiving phase and concentration of the ligand were optimized and the results are presented in **Fig. 3.14- 3.18.**

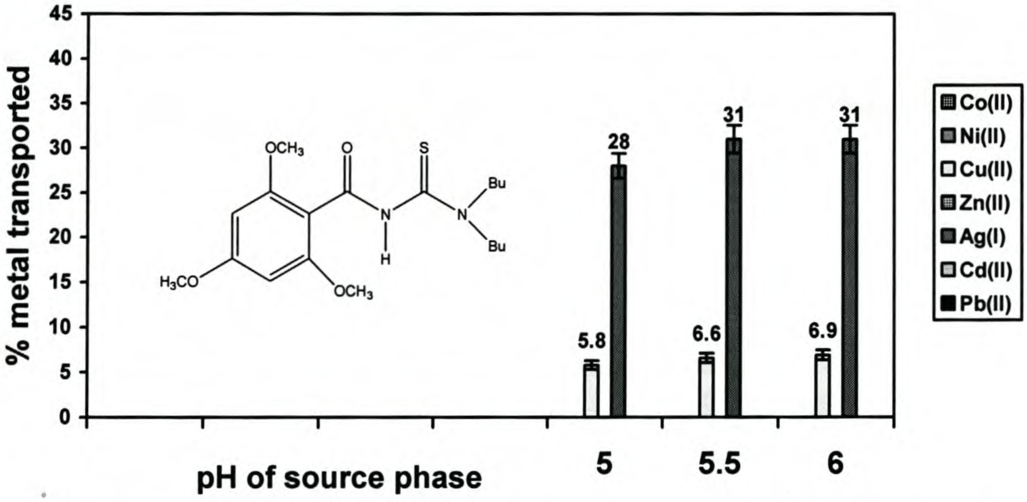

Fig. 3.14: Percentage transport of Ag(I) and Cu(II) ions in competitive transport studies involving **HL^6**. In all cases, the experimental conditions were: **receiving phase pH = 1.0** and **[HL^6] = 2 x 10^{-3} M**. The **pH of the source phase** was varied from **5.0** to **6.0** as shown in the above figure.

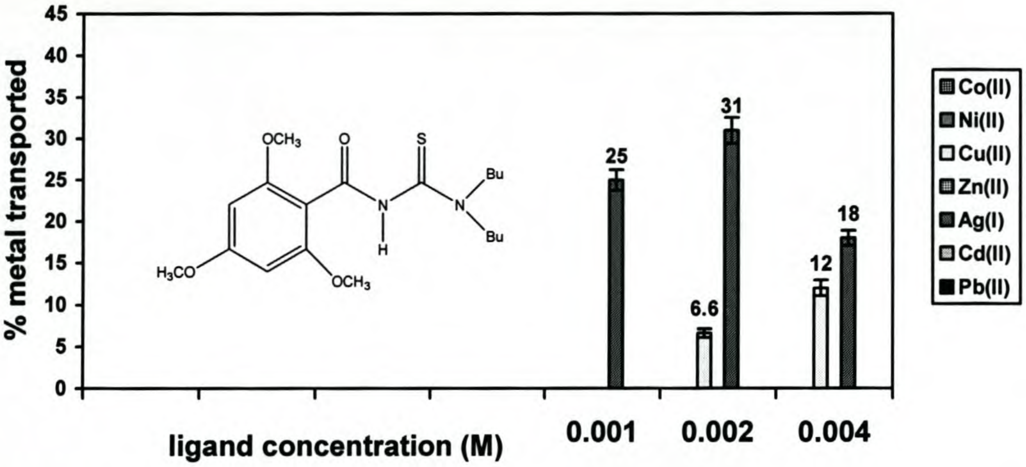

Fig. 3.15: Percentage transport of Ag(I) and Cu(II) ions in competitive transport studies involving **HL^6**. In all cases, the experimental conditions were: **source phase pH = 5.5** and **receiving phase pH = 1.0**. The **concentration of the ligand** was varied from **1 x 10^{-3} M** to **4 x 10^{-3} M** as shown in the above figure.

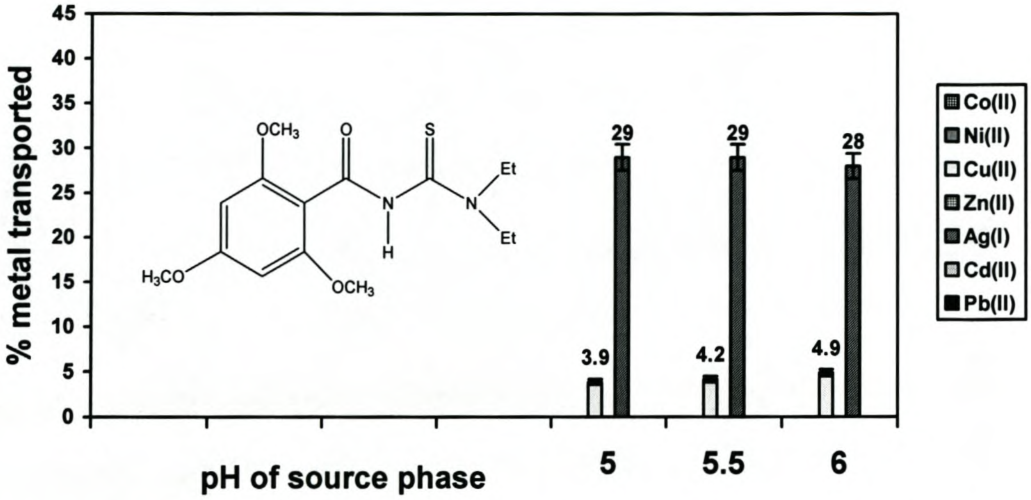

Fig. 3.16: Percentage transport of Ag(I) and Cu(II) ions in competitive transport studies involving **HL⁷**. In all cases, the experimental conditions were: **receiving phase pH = 1.0** and **[HL^7] = 2 x 10^{-3} M**. The **pH of the source phase** was varied from **5.0** to **6.0** as shown in the above figure.

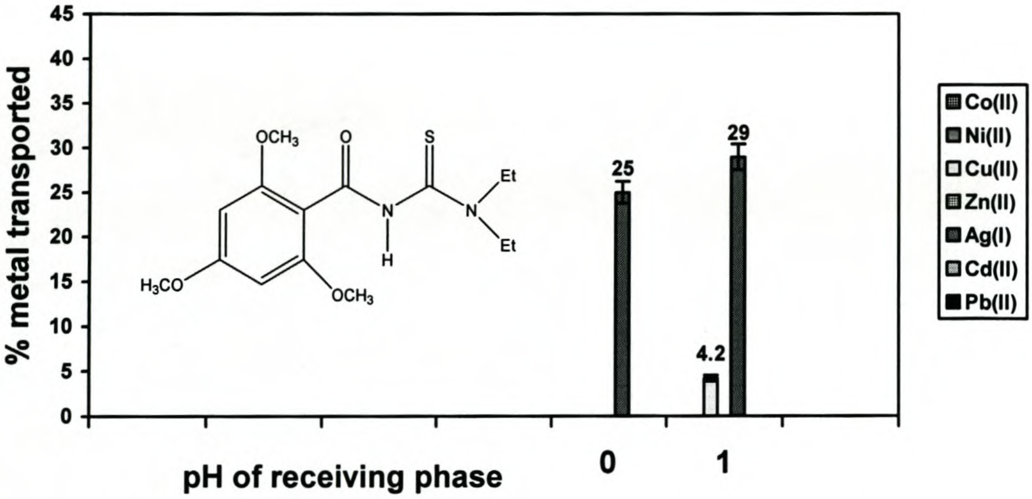

Fig. 3.17: Percentage transport of Ag(I) and Cu(II) ions in competitive transport studies involving **HL^7**. The experimental conditions were: **source phase pH = 5.5** and **[HL^7] = 2 x 10^{-3} M**. The **pH of the receiving phase** was varied from **0** to **1.0** as shown in the above figure.

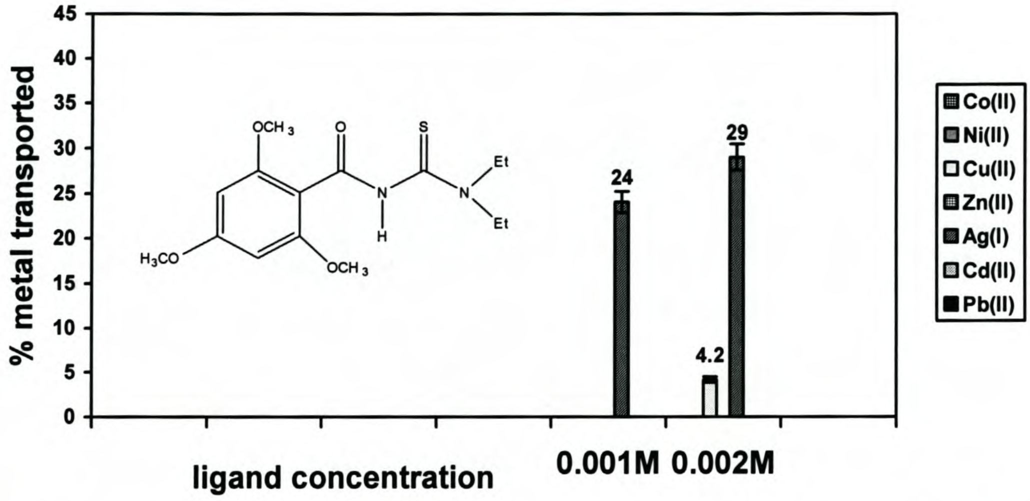

Fig. 3.18: Percentage transport of Ag(I) and Cu(II) ions in competitive transport studies involving **HL^7**. In both cases, the experimental conditions were: **source phase pH = 5.5** and **receiving phase pH = 1.0**. The **concentration of the ligand** was varied from **1 x 10 $^{-3}$ M** to **2 x 10 $^{-3}$ M** as shown in the above figure.

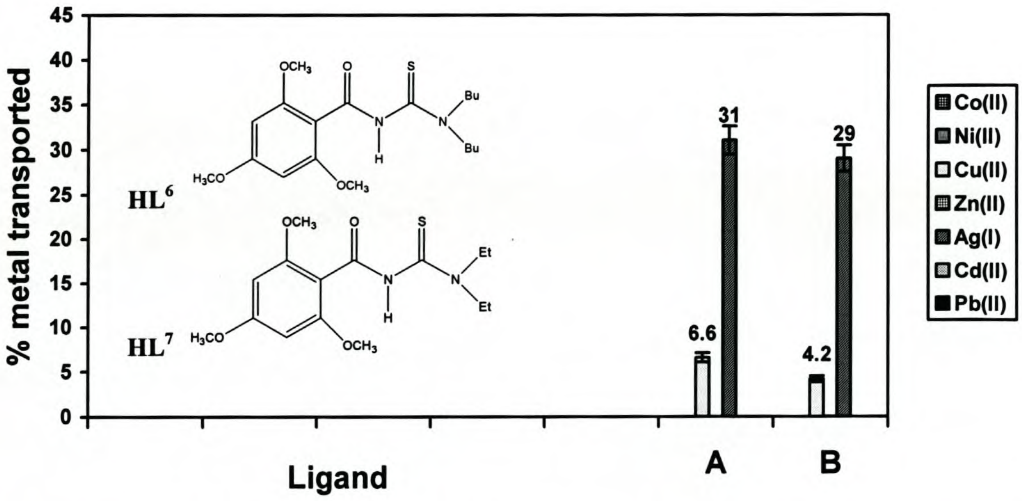

Fig. 3.19: Percentage transport of Ag(I) and Cu(II) ions in competitive transport studies involving **HL^6 and HL^7** ligands. **A** refers to **HL^6** and **B** refers to **HL^7**. In both cases, the experimental conditions were the same: **source phase pH = 5.5**, **receiving phase pH = 1.0** and **concentration of the ligands** were **2 x 10 $^{-3}$ M**.

Table 3.3: J-values for the competitive metal ion transport by **HL^6** and **HL^7** (data includes ± 5% experimental error). The experimental conditions were: pH of source phase = 5.5, pH of receiving phase = 1.0 and concentration of ligand = 0.002 M.

Metal ion transport (J values) in (mol/hr) x 10^{-7}		
	HL^6	**HL^7**
Co(II)	-	-
Ni(II)	-	-
Cu(II)	2.7	1.7
Zn(II)	-	-
Ag(I)	13	12
Cd(II)	-	-
Pb(II)	-	-
$^{Ag}T_r$ %	31	29
$^{Ag}T_M$ %	38	35
$^{Cu}T_r$ %	6.6	4.2
$^{Cu}T_M$%	5.8	2.3
η(Ag(I)/Cu(II))	4.7	6.9

3.7.6 Comparison of metal ion transport by *N,N*-dibutyl-*N'*-2,4,6-trimethoxybenzoyl thiourea (HL^6) and *N,N*-diethyl-*N'*-2,4,6-trimethoxybenzoylthiourea (HL^7) ligands.

The effect of attaching electron releasing substituents to *N,N*-dialkyl-*N'*-benzoylthioureas on transport efficiency and selectivity was studied using HL^6 and HL^7 ligands. As can be seen from their structures, both ligands possess methoxy substituents at positions C_2, C_4 and C_6.

The fact that at room temperature both HL^6 and HL^7 are soluble in chloroform makes these ligands suitable candidates for transport studies. Under the conditions employed, both ligands were selective to Ag(I) with minor amounts of Cu(II) being transported along with Ag(I). The results of the rate of transport of Ag(I) (J-values) for HL^6 and HL^7 are shown in

Table 3.3. The net effect of the bulky electron donating methoxy substituents is to decrease the transport efficiency and selectivity for Ag(I) ion possibly due to steric reasons.

The effect of varying the pH of the source phase on Ag(I) transport by HL^6 and HL^7 was studied. Changing the pH of the source phase from 5.5 to 5.0 or 6.0 did not result in a significant change in the percentage transport of Ag(I) by both ligands (see **Fig. 3.14** and **3.16**). On the other hand, the effect of changing the pH of the receiving phase was studied using HL^7 and it was found that decreasing the pH of the receiving phase from 1.0 to pH = 0 inhibits the transport of Ag(I) (see **Fig. 3.17**), possibly due to the ligand's instability in relatively stronger acidic media. A similar trend was also observed with HL^4.

Under the experimental conditions employed, both HL^6 and HL^7 showed clear selectivity to Ag(I). However, under the same experimental conditions, HL^6 was more efficient than HL^7. This result is consistent with the fact that the longer alkyl substituents (butyl groups) in HL^6 make the ligand more lipophilic compared to the ethyl substituents in HL^7, and hence HL^6 transports better that HL^7. However, as can be seen from **Table 3.3**, the selectivity factor for Ag(I) compared to Cu(II) is higher for HL^7 that HL^6.

The sum of the percentages of Ag(I) transported into the receiving phase ($^{Ag}T_r\%$) and Ag(I) transported into the membrane phase ($^{Ag}T_M\%$) by HL^6 is higher than that of HL^7 **(see Table 3.3).** This suggests that HL^6 may have a higher formation constant with Ag(I) than HL^7. The effect of varying the concentration of HL^6 and HL^7 on transport efficiency and selectivity was also studied. As can be seen from **Fig. 3.15 and 3.18**, the selectivity factor η(Ag(I)/Cu(II)) decreases with an increase in the concentration of the ligands from 1×10^{-3} to 2×10^{-3} M. A further increase in HL^6 concentration from 2×10^{-3} M to 4×10^{-3} M also resulted in a drastic decrease in η (Ag(I)/Cu(II)).

From the results obtained, it is evident that the transport of Ag(I) by HL^6 and HL^7 ligands is optimum when the ligand concentration is 2×10^{-3} M and the pH of the source phase and receiving phase are set at 5.5 and 1.0 respectively.

3.7.7 Metal ion transport by *N*-Piperidyl-*N'*-benzoylthiourea (HL^8), *N*-Piperidyl-*N'*-4-nitrobenzoylthiourea (HL^9) and *N*-Piperidyl-*N'*-2,6-dimethoxybenzoylthiourea (HL^{10}).

Competitive transport experiments involving HL^8, HL^9 and HL^{10} ligands were conducted under conditions where pH of the receiving phase was kept constant, whereas pH of the source phase and concentration of the ligand were systematically varied. The results are presented in **Fig. 3.20 - 3.25.**

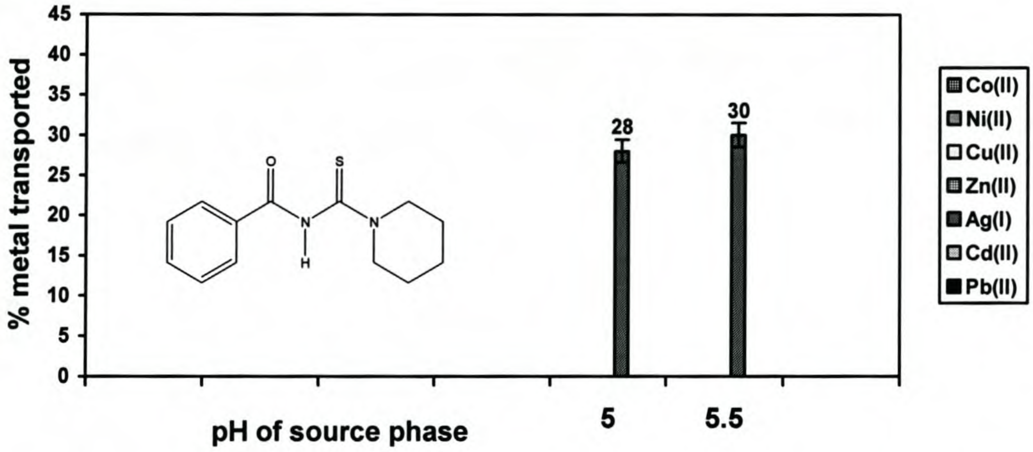

Fig. 3.20: Percentage transport of Ag(I) ion in competitive transport studies involving **HL^8** ligand. In both cases: **pH of the receiving phase = 1.0** and **[HL^8]** = **1 x 10^{-3} M**. The **pH of the source phase** was varied from **5.0** to **5.5** as shown in the above figure.

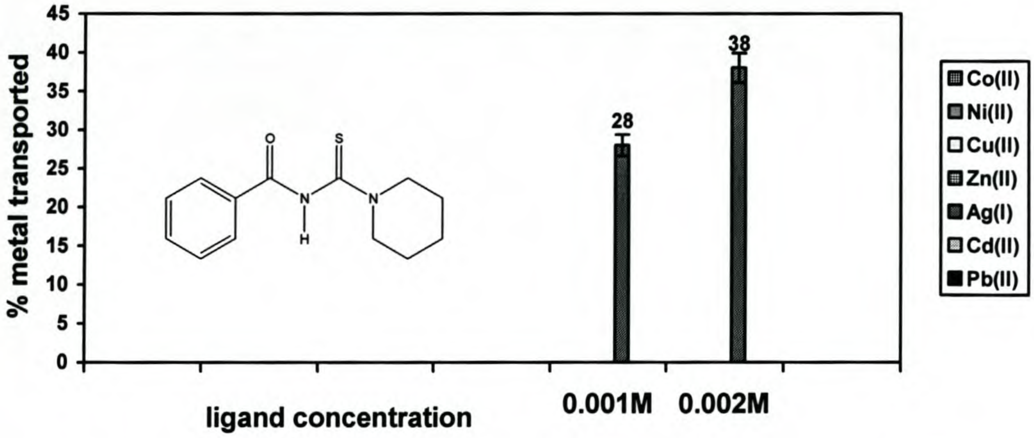

Fig. 3.21: Percentage transport of Ag(I) ion in competitive transport studies involving **HL^8** ligand. In both cases, the experimental conditions were: **source phase pH = 5.5** and **receiving phase pH = 1.0**. The **concentration of the ligand** was varied from **1 x 10^{-3} M** to **2 x 10^{-3} M** as shown in the above figure.

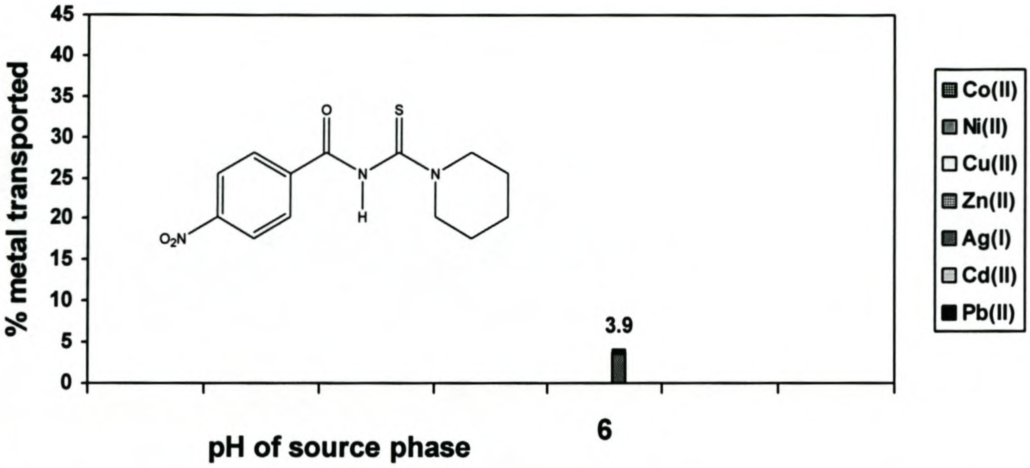

Fig. 3.22: Percentage transport of Ag(I) ion in a competitive transport study involving **HL⁹** ligand. The experimental conditions were: **pH of source phase = 6.0**, **pH of receiving phase = 0.3** and **ligand concentration = 2 x 10 $^{-3}$ M**.

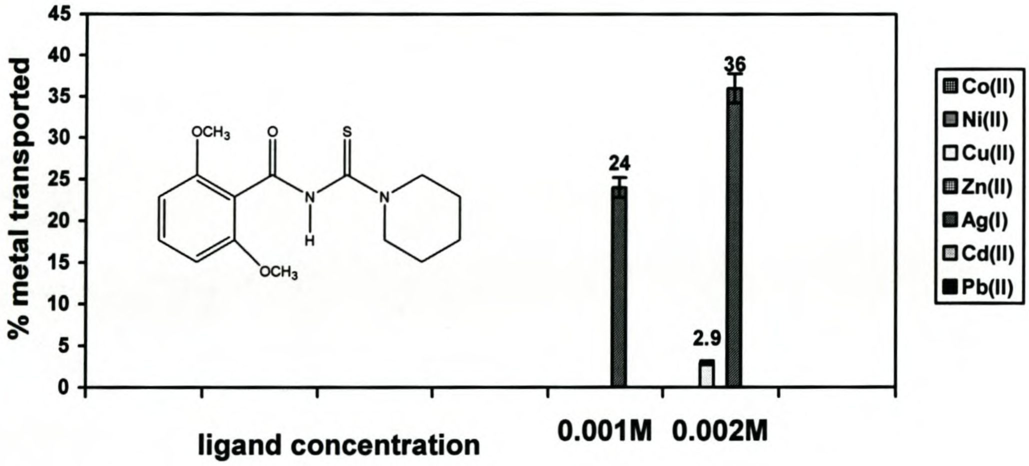

Fig. 3.23: Percentage transport of Ag(I) and Cu(II) ions in competitive transport study involving **HL^{10}**. The experimental conditions were: **source phase pH = 5.5** and **receiving phase pH = 1.0**. The **concentration of the ligand** was varied from **1 x 10 $^{-3}$ M** to **2 x 10 $^{-3}$ M** as shown in the above figure.

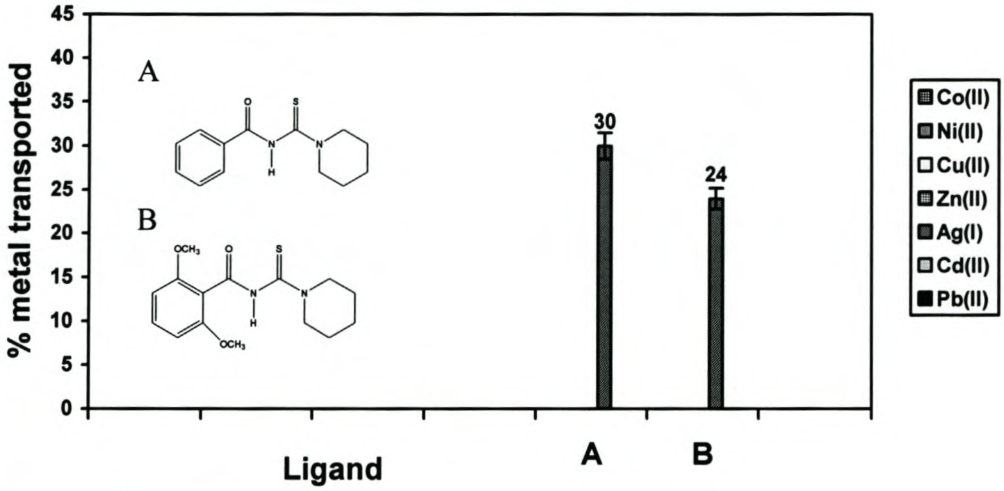

Fig. 3.24: Percentage transport of Ag(I) ion in competitive transport study involving **HL^8** and **HL^{10}**. **A** refers to **HL^8** and **B** refers to **HL^{10}**. In both cases, the experimental conditions were: **pH of source phase = 5.5**, **pH of receiving phase = 1.0** and **concentration of ligand = 1 x 10 $^{-3}$ M**.

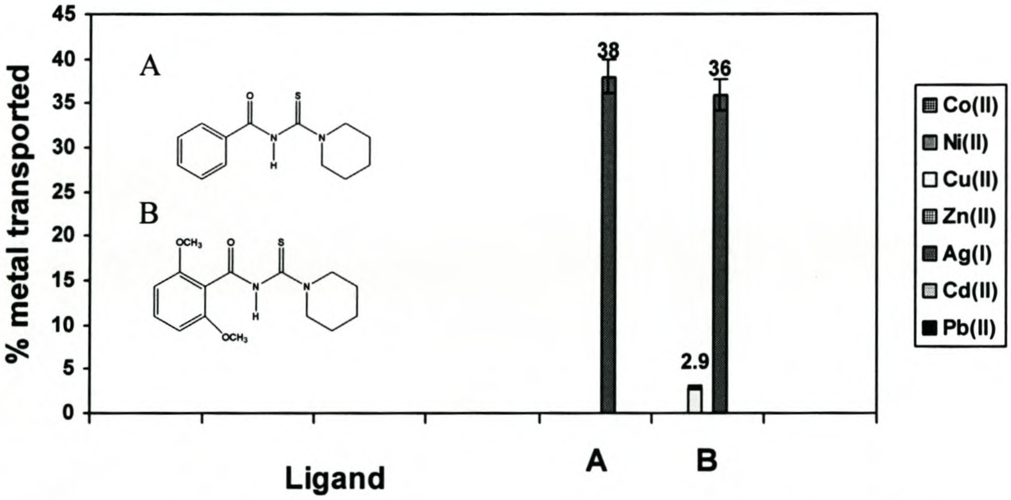

Fig. 3.25: Percentage transport of Ag(I) ion in competitive transport study involving **HL^8** and **HL^{10}**. **A** refers to **HL^8** and **B** refers to **HL^{10}**. In both cases, the experimental conditions were: **pH of source phase = 5.5**, **pH of receiving phase = 1.0** and **concentration of ligand = 2 x 10 $^{-3}$ M**.

Table 3.4: J-values for the competitive metal ion transport involving **HL^8 – HL^{10}** (data includes ± 5% experimental error). The experimental conditions were: pH of source phase = 5.5, pH of receiving phase = 1.0 and concentration of ligand = 0.002 M.

Metal ion transport (J values) in (mol/hr) x 10^{-7}			
	HL^8	**HL^9**	**HL^{10}**
Co(II)	-	-	-
Ni(II)	-	-	-
Cu(II)	-	-	1.2
Zn(II)	-	-	-
Ag(I)	16	-	15
Cd(II)	-	-	-
Pb(II)	-	-	-
$^{Ag}T_r$ %	38	-	36
$^{Ag}T_M$ %	51	9.0	46
$^{Cu}T_r$ %	-	-	2.9
$^{Cu}T_M$%	3.2	2.5	2.1
η(Ag(I)/Cu(II))	$\eta \rightarrow \infty$	no transport	12

3.7.8 Comparison of metal ion transport by *N*-Piperidyl-*N'*-benzoylthiourea (HL^8), *N*-Piperidyl-*N'*-4-nitrobenzoylthiourea (HL^9) and *N*-Piperidyl-*N'*-2,6-dimethoxybenzoyl thiourea (HL^{10}) ligands.

Ligands HL^8 - HL^{10} are grouped together due to the similarity in their structures. These ligands were all soluble in chloroform. The results of the competitive metal ion transport experiments involving these ligands are presented in **Fig. 3.20 – 3.25** and **Table 3.4**. pH = 5.5 and 1.0 were selected as optimum pH conditions for the source and receiving phases respectively.

Comparison of the results of the rate of transport (J values) of Ag(I) by HL^8 and HL^{10} (see **Table 3.4)** show a major preference of both ligands for Ag(I) transport with only minor amounts of Cu(II) being transported. The selectivity factor η (Ag(I)/Cu(II)) for these ligands follows the order **HL^{10}**< **HL^{8}**. Under the experimental conditions studied (see **Fig. 3.22**), HL^{9} did not transport a significant percentage of Ag(I) due to the fact that the ligand bled from the membrane phase into the aqueous phases as was observed in the case of HL^{4}. The receiving phase turned yellow after the 24 hour transport period.

Comparing the sum of Ag (I) transported into the membrane phase "$^{Ag}T_M$%" and Ag(I) transported into the receiving phase "$^{Ag}T_r$ %" for HL^{8} and HL^{10} ligands (see **Table 3.4),** we can see that HL^{8} shows a better interaction with Ag(I) than HL^{10} does. Therefore, based on this we can predict that HL^{8} may have a moderately higher formation constant with Ag(I) than HL^{10} and this in turn implies that HL^{8} is a slightly better transport ionophore for Ag(I) ion. The two-methoxy substituents at carbon positions 2 and 5 in HL^{10} are believed to probably decrease the complex formation ability of the ligand with Ag(I) due to steric effects.

Comparison of the results obtained in these studies shows a selectivity order η(Ag(I)/Cu(II)) of **HL^{8}** > **HL^{10}** > **HL^{9}** for competitive transport and a similar order: **HL^{8}** > **HL^{10}** > **HL^{9}** was also obtained when considering the overall Ag(I)-ligand interaction.

The effect of varying the concentration of HL^{8} and HL^{10} on transport efficiency and selectivity was also studied at the optimum pH conditions. Decreasing the concentration of the ligand from 2×10^{-3} M to 1×10^{-3} M resulted in a decrease in the efficiency of the ligands for Ag(I) transport as expected (see **Fig. 3.24 and 3.25**).

3.7.9 Metal ion transport by *N,N*-Diethyl-*N'*-2,2-dimethylpropanoylthiourea, HL^{11}.

Competitive transport experiments involving HL^{11} as an ionophore was conducted under conditions where pH of the source phase, pH of the receiving phase and concentration of the ligand was systematically varied and the results are summarized in **Fig. 3.26 – 3.28.**

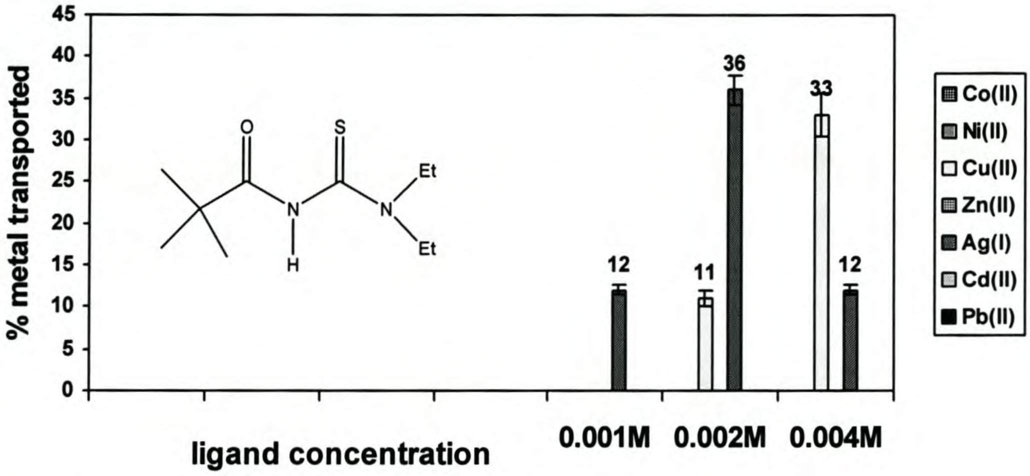

Fig. 3.26: Percentage transport of Ag(I) and Cu(II) ions in competitive transport studies involving HL^{11} ligand. In all cases, the experimental conditions were: **pH of the source phase = 5.5** and **pH of the receiving phase = 1.0**. The **concentration of the ligand** was varied from **1 x 10 $^{-3}$ M** to **4 x 10 $^{-3}$ M** as shown in the above figure.

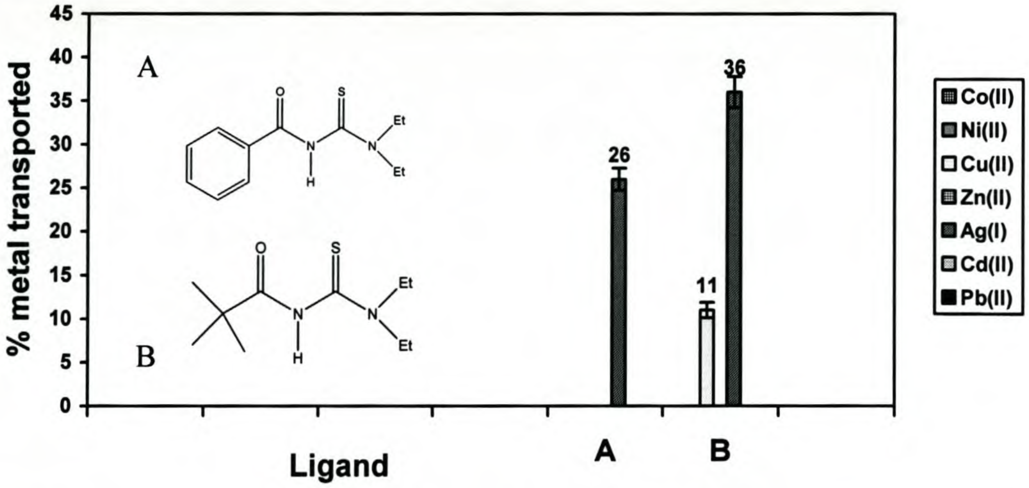

Fig. 3.27: Comparison of percentage transport of Ag(I) and Cu(II) ions in competitive transport studies involving $\mathbf{HL^2}$ and $\mathbf{HL^{11}}$ ligands. **A** refers to HL^2 and **B** refers to HL^{11}. In both cases, the experimental conditions were: **pH of the source phase = 5.5**, **pH of the receiving phase = 1.0** and **concentration of ligand = 2 x 10 $^{-3}$ M**.

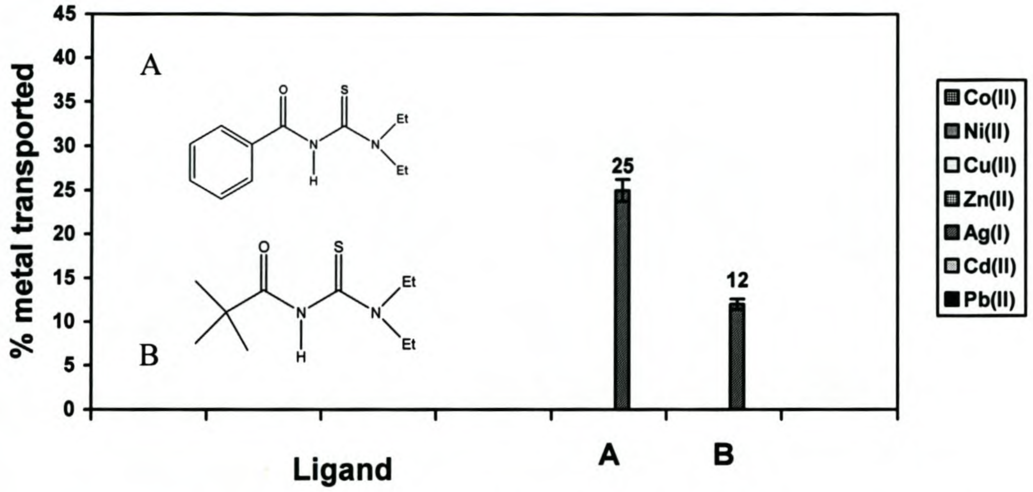

Fig 3.28: Percentage transport of Ag(I) and Cu(II) ions in competitive transport studies involving **HL^2** and **HL^{11}** ligands. **A** refers to HL^2 and **B** refers to HL^{11}. In both cases, the experimental conditions were: **pH of the source phase = 5.5**, **pH of the receiving phase = 1.0** and **concentration of ligand** = **1×10^{-3} M**.

Table 3.5: J-values for the competitive metal ion transport by **HL^{11}** (data includes ± 5% experimental error). The experimental conditions were: pH of source phase = 5.5, pH of receiving phase = 1.0 and concentration of ligand = 0.002 M.

	Metal ions						
	Co(II)	**Ni(II)**	**Cu(II)**	**Zn(II)**	**Ag(I)**	**Cd(II)**	**Pb(II)**
J (mol/hr) x 10^{-7}	-	-	4.7	-	15	-	-
${}^{Ag}T_r$ %	-	-	-	-	36	-	-
${}^{Ag}T_M$ %	-	-	-	-	51	-	-
${}^{Cu}T_r$ %	-	-	11	-	-	-	-
${}^{Cu}T_M$%	-	-	3.9	-	-	-	-
η(Ag(I)/Cu(II))	-	-	-	-	3.3	-	-

3.7.10 Discussion for metal ion transport by *N,N*-Diethyl-*N'*-2,2-dimethylpropanoyl thiourea, HL^{11}, ligand.

In order to study how efficient acyl -thioureas are in selectively transporting Ag(I), we have considered ligand HL^{11} and the results for the competitive metal ion transport using this ligand are summarized in **Table 3.5** and **Fig. 3.26 – 3.28**.

In general, acylthioureas are hydrophilic and therefore such ligands can bleed into the aqueous source and receiving phases before they actually form complexes with the target metal ion(s) in the source phase. However, HL^{11} was soluble in the presaturated chloroform membrane and in fact it was also found to be a good transport ionophore with a pronounced selectivity for Ag(I). As can be seen from **Table 3.5**, the rate of transport (J - value) of Ag(I) by HL^{11} is high which confirms that HL^{11} is an efficient transport ionophore for the transport of Ag(I).

For the transport experiments employing HL^{11}, we have chosen pH = 5.5 for the source phase and pH =1.0 for the receiving phase as our optimum conditions. By keeping these experimental conditions constant, we have studied the effect of varying the ligand concentration on Ag(I) transport. A ligand concentration of 2×10^{-3} M results in maximum efficiency and selectivity for Ag(I) transport (see **Fig. 3.26**). Decreasing the ligand concentration from 4×10^{-3} M to 1×10^{-3} M decreases the efficiency of the ligand to transport Ag(I). On the other hand, the percentage Cu(II) transported by HL^{11} increases with an increase in the ligand concentration from 1×10^{-3} M to 4×10^{-3} M. The large ($^{Ag}T_M\% + {}^{Ag}T_r\%$) sum for HL^{11} is about 87% (see **Table 3.5**) is an indication of the large interaction between the ligand and Ag(I). It is interesting to note that up to a concentration of 2×10^{-3} M, the ligand is selective for Ag(I). However, increasing the concentration of the ligand further to 4×10^{-3} M causes a swing in transport selectivity from Ag(I) to Cu(II). Therefore, Cu(II) must be interacting differently with the ligand at higher ligand concentrations.

Therefore, by varying the ligand concentration, it is possible to transport Ag(I) and/or Cu(II) selectively from a solution containing the seven metal ions. Based on these results, we can say that HL^{11} may probably have a moderately high formation constant with Ag(I) and Cu(II) ions.

3.7.11 Metal ion transport by 3,3,3',3'-Tetraethyl-1,1'-isophthaloylbisthiourea (H_2L^{12}), *N,N*-Diethyl-*N'*-camphanoylthiourea (HL^{13}), *N*-Propyl-*N'*-benzoylthiourea (H_2L^1), *N*-Piperidyl-*N'*-4-heptoxybenzoylthiourea (H_2L^2) and *N*-Phenyl-*N'*-benzoylthiourea (H_2L^3) ligands.

The results for the competitive metal ion transport experiments involving H_2L^{12}, HL^{13} and H_2L^1– H_2L^3 are summarized in **Fig. 3.29 – 3.32 and Table 3.6**. These ligands are all soluble in chloroform. For the purpose of comparison, the mono-alkyl substituted ligands (H_2L^1 - H_2L^3) are grouped together and it was found that under the experimental conditions employed, these ligands are not good at transporting any of the seven metal ions in the source phase.

The transport efficiency and selectivity of the bipodal H_2L^{12} ligand was studied in order to infer the effect of varying ligand structure on metal ion transport. The ligand was previously synthesized and was available in our group.

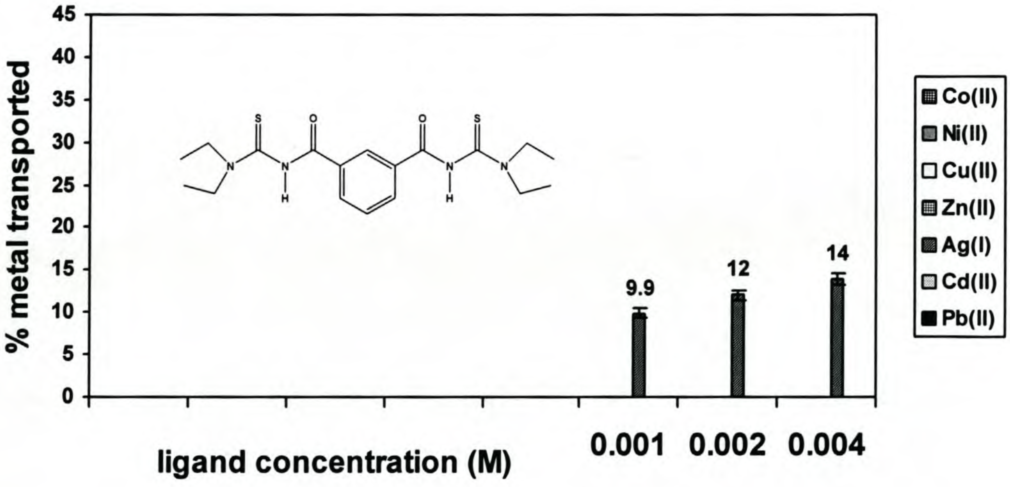

Fig. 3.29: Percentage transport of Ag(I) ion in competitive transport studies involving $\mathbf{H_2L^{12}}$ ligand. The experimental conditions were: **pH of the source phase = 5.5, pH of the receiving phase = 1.0** and the **ligand concentration** varied from $\mathbf{1 \times 10^{-3}}$ **M** to $\mathbf{4 \times 10^{-3}}$ **M**.

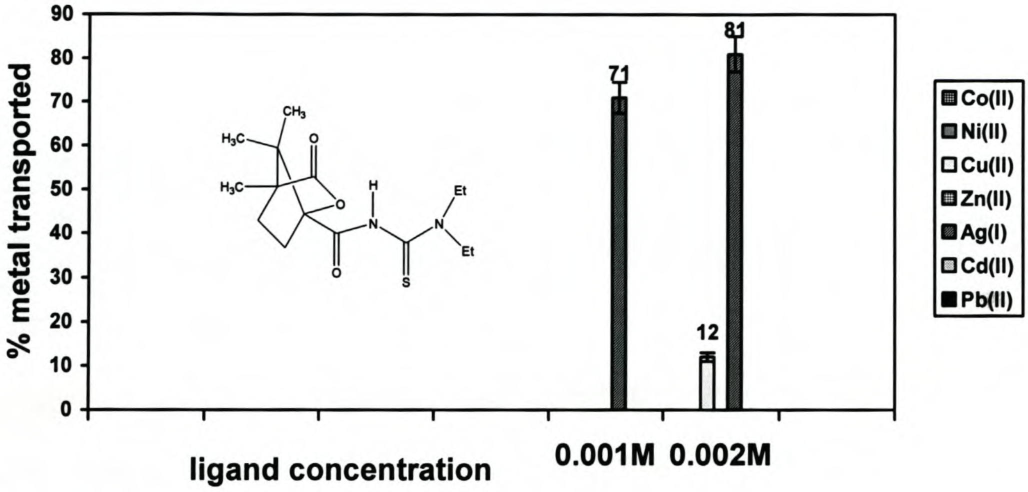

Fig. 3.30: Percentage transport of Ag(I) and Cu(II) ions in competitive transport studies involving HL^{13} ligand. In both cases, the experimental conditions were: **pH of the source phase = 5.0** and **pH of the receiving phase = 1.0**. The **concentration of the ligand** was varied from **1 x 10 $^{-3}$ M** to **2 x 10 $^{-3}$ M** as shown in the above figure.

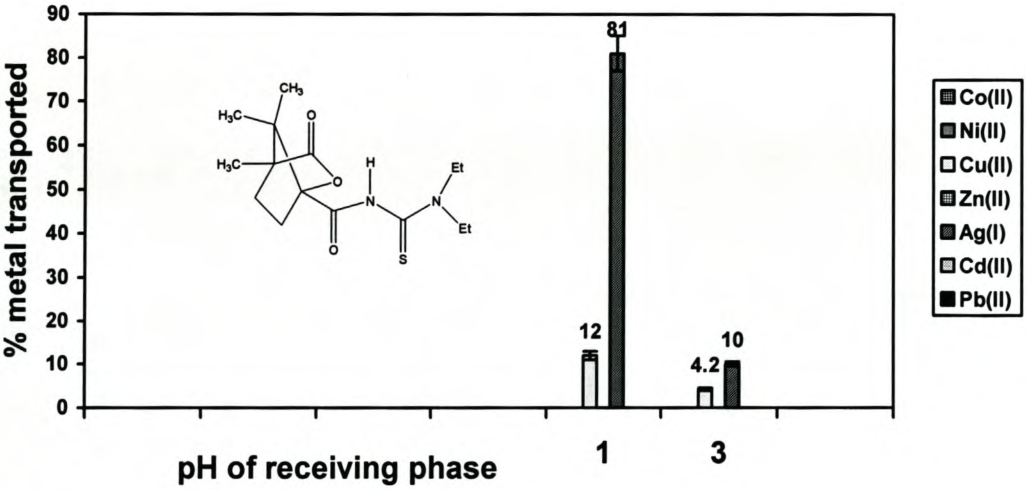

Fig. 3.31: Percentage transport of Ag(I) and Cu(II) ions in competitive transport studies involving HL^{13} ligand. The experimental conditions were: **pH of the source phase = 5.0** and **concentration of the ligand = 2 x 10 $^{-3}$ M**. **pH of the receiving phase** was varied from **1.0** to **3.0** as shown in the above figure.

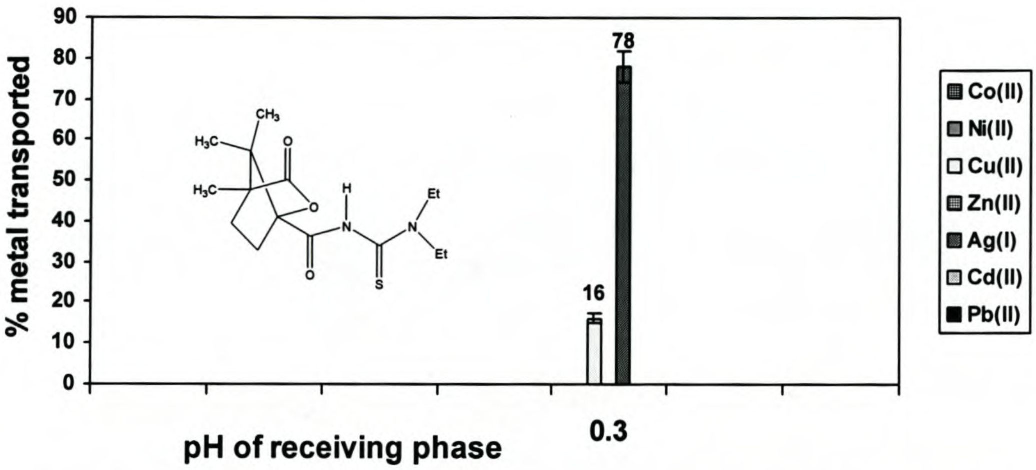

Fig. 3.32: Percentage transport of Ag(I) and Cu(II) ions in a competitive transport study involving HL^{13}. The experimental conditions were: **pH of the source phase = 5.5, pH of the receiving phase = 0.3** and **ligand concentration = 2 x 10^{-3} M**.

Table 3.6: J-values for the competitive metal ion transport by H_2L^{12}, HL^{13} and H_2L^1– H_2L^3 ligands (data includes ± 5% experimental error). The experimental conditions were: pH of source phase = 5.5, pH of receiving phase = 1.0 and concentration of ligand = 0.002 M.

Metal ion transport (J value) in (mol/hr) x 10^{-7}					
	H_2L^{12}	**HL^{13}**	**H_2L^1**	**H_2L^2**	**H_2L^3**
Co(II)	-	-	-	-	-
Ni(II)	-	-	-	-	-
Cu(II)	-	-	-	-	-
Zn(II)	-	-	-	-	-
Ag(I)	5.1	34	0.6	-	-
Cd(II)	-	-	-	-	-
Pb(II)	-	-	-	-	-
$^{Ag}T_r$ %	12	81	1.5	-	-
$^{Ag}T_M$ %	40	12	95	57	45
$^{Cu}T_r$ %	-	12	-	-	-
$^{Cu}T_M$%	-	7.2	-	5.0	-
η (Ag(I)/Cu(II))	η →∞	6.8	η →∞	no transport	no transport

3.7.12 Comparison of metal ion transport by bipodal 3,3,3',3'-Tetraethyl-1,1'-isophthaloylbisthiourea (H_2L^{12}) , *N,N*-Diethyl-*N'*-camphanoylthiourea (HL^{13}), *N*-Propyl-*N'*-benzoylthiourea (H_2L^1), *N*-Piperidyl-*N'*-4-heptoxybenzoylthiourea (H_2L^2) and *N*-Phenyl-*N'*-benzoylthiourea (H_2L^3) ligands.

Under the experimental conditions reported in **Table 3.6**, 95% of the Ag(I) ion that was initially present in the source phase was extracted into the membrane phase using H_2L^1 but only about 1.5% of Ag(I) was stripped into the receiving phase. This indicates that the formation constant (log K value) of Ag(I) with H_2L^1 is probably too high and this inhibits the release of the complexed Ag(I) from the membrane phase into the receiving phase. Therefore, this ligand can be a good extracting reagent but not a good transport ionophore for Ag(I). Ligands H_2L^2 and H_2L^3 did not transport any of the seven metal ions in the source phase, but a large quantity of Ag(I) was found in the membrane.

H_2L^{12} has two sulfur and two oxygen donor atoms. The donor atoms are symmetrically placed around the ligand. We were particularly interested in studying the selectivity and efficiency of H_2L^{12} for the transport of Ag(I). Under the experimental conditions employed, the ligand was found to be selective for Ag(I). However, although H_2L^{12} has two (S, O) bonding sites that could potentially complex to two Ag(I) ions, it has been shown to have less efficiency for transporting Ag(I) than HL^2. The possible reasons that could contribute to the decrease in the Ag(I) transport by H_2L^{12} are:

1. Electronic interaction between the two Ag(I) ions makes it difficult for the ligand to carry two Ag(I) ions through its (*S, O*) donor sets as they are in close proximity to one another.
2. A conformational change within the ligand, that may not favour the binding of the second Ag (I) ion, may be induced and this decreases the efficiency of the ligand to transport Ag(I).

A source phase pH of 5.5 and receiving phase pH of 1.0 were adopted as optimum conditions for transport studies involving H_2L^{12}, HL^{13} and H_2L^1– H_2L^3 ligands. Under these conditions, we have investigated the effect of varying the concentration of H_2L^{12} on the transport of Ag(I). As can be seen from **Fig. 3.29**, the percentage transport of Ag(I) by H_2L^{12} increases with an increase in ligand concentration. However, although H_2L^{12} is selective for Ag(I), the transport is not quantitative. Under the same experimental conditions, the percentage Ag(I) transported by H_2L^{12} is much smaller than that transported by HL^2. The rate of transport (J - value) of Ag(I) using H_2L^{12} (**Table 3.6**) is also small and this shows that the uptake of Ag(I) from the source phase to the membrane phase is relatively small. Therefore, H_2L^{12} is not a good candidate for efficient transport of Ag(I) from a mixture of the seven metal ions.

The results for the competitive metal ion transport by HL^{13} are summarized in **Fig. 3.30 – 3.32**. The effect of varying pH of the source phase and pH of the receiving phase were investigated at the optimum pH conditions: pH = 5.5 for the source phase and pH = 1.0 for the receiving phase. When the ligand concentration at the above pH conditions was kept at 2×10^{-3} M, 81% Ag(I) was transported along with 12% Cu(II). However, the interesting result is that by reducing the ligand concentration to 1×10^{-3} M, 71% of Ag(I) was selectively transported (see **Fig. 3.30**).

The fact that the sum (${}^{Ag}T_M\%$ + ${}^{Ag}T_r\%$) for HL^{13} is large indicates that the ligand may have a moderately high formation constant with Ag(I). This makes the ligand an ideal candidate for efficient and selective transport of Ag(I) from a mixture of the seven metal ions.

3.8 Concluding discussion

The fundamental parameters that influence the transport of Ag(I) have been identified. These are: concentration of ligand, pH of source phase, pH of receiving phase (strippant) and the use of hexadecanoic (palmitic) acid.

In order to study the effect of varying the ligand structure on the transport efficiency and selectivity for Ag(I), we have systematically grouped the ligands into six sections. In each section, ligands with slight variation in structure are grouped together and the transport results obtained under the same conditions are compared. The most efficient ligand for Ag(I) transport is the *N*,*N*-diethyl-*N'*-camphanoylthiourea, HL^{13}, ligand. All the *N*,*N*-dialkyl-*N'*-benzoylthioureas (HL), with the exception of *N*-piperidyl-*N'*-4-nitrobenzoylthiourea, HL^9 and *N*,*N*-di-(2-hydroxyethyl)-*N'*-benzoylthiourea, HL^3, were efficient and selective for Ag(I) transport. The *N*,*N*-di-(2-hydroxyethyl)-*N'*-benzoylthiourea, HL^3 was selective for Cu(II), while the *N*-piperidyl-*N'*-4-nitrobenzoylthiourea, HL^9 transported only a small percentage of Ag(I). The selectivity observed by the *N*,*N*-di-(2-hydroxy)-*N'*-benzoylthiourea, HL^3, for Cu(II) can be due to the presence of the 'hard' oxygen atoms present in the molecule.

Fig 3.33 summarizes the transport of Ag(I) by 12 ligands under the same experimental conditions showing HL^{13} to be the best transport ionophore (ligands HL^9 and H_2L^1-H_2L^3 are not shown). As can be seen from the figure, the percentage of Ag(I) transported by benzoylthiourea ligands varies, which suggests that a slight variation in the structure or substituent groups of the ligand brings about changes in transport efficiency and selectivity of the ligand. The *N*-alkyl-*N'*-benzoylthiourea (H_2L) ligands were good at transporting Ag(I) into the membrane phase, but not into the receiving phase. This suggests that the H_2L ligands may have very high formation constants with Ag(I).

The effect of varying pH of the receiving phase, pH of the source phase and ligand concentration was investigated. In general, keeping all conditions constant, increasing pH of the receiving phase can decrease the percentage transport of Ag(I) into the receiving phase since the pH gradient between the source phase and receiving phase is decreased. Similarly, at higher acid concentration of the receiving phase, the percentage transport of Ag(I) may also decrease, as the ligand may be protonated, form a charged complex and bleed into the aqueous phases. This was observed in the case of *N*,*N*-diethyl-*N'*-4-nitrobenzoylthiourea, HL^4 and *N*-piperidyl-*N'*-4-nitrobenzoylthiourea, HL^9. On the other hand, increasing pH of the source phase (for example from 5.0 to 6.0) results in a decrease in the selectivity of the ligand for Ag(I) as some of the other metal ions in the source phase also start to be co-transported with Ag(I). However, to precisely determine what source phase pH we must use to obtain maximum efficiency and selectivity for Ag(I), the *S*-curves for each ligand with Ag(I) must be studied. The effect of varying ligand concentration on the transport efficiency and selectivity for Ag(I) was also studied. In most cases, the ligand concentration was varied between 1 x 10^{-3} M and 2 x 10^{-3} M. In general, it was found that with an increase in ligand concentration, Cu(II) starts to be co-transported with Ag(I) and in the case of *N*,*N*-diethyl-*N'*-2,2-dimethylpropanoylthiourea, HL^{11} , Cu(II) was favored compared to Ag(I).

Throughout the transport experiments, we have incorporated 4 x 10^{-3} M hexadecanoic acid (palmitic acid) in the membrane phase. We have also proved that, up to a concentration of 4 x 10^{-3} M, palmitic acid does not transport any of the metal ions in the source phase. Palmitic acid is a fatty acid with a long chain alkyl group on its one end and a carboxylic group on its other end. It is soluble in chloroform and due to its strong lipohilicity, it is widely used in transport experiments involving a variety of ligands as ionophores [23,26]. Since the metal ions that we studied are in the form of nitrate salts, NO_3^- may be transported as counter ions along with the divalent metal ions into the receiving phase in order to maintain electro-neutrality through ion pairing or adduct formation. Therefore, in order to avoid the uptake of nitrate ions into the organic phase it becomes important to incorporate hexadecanoic acid into the chloroform membrane. An additional benefit of adding lipophilicity in the form of the long-chain acid is to inhibit any 'bleeding' of 'partially' hydrophilic species (such as the protonated ionophore and / or its corresponding charged metal complex) from the organic membrane phase into either of the aqueous phases [26,70,71].

Finally, we can suggest that the *N*,*N*-diethyl-*N'*-camphanoylthiourea (HL^{13}), *N*,*N*-diethyl-*N'*-4-chlorobenzoylthiourea (HL^5) and *N*,*N*-dibutyl-*N'*-benzoylthiourea (HL^1) are good candidates for further studies aiming at selective and efficient transport of Ag(I) using liquid membranes. Liquid membrane separation is by far more efficient and selective compared to the classical chloride precipitation technique for separating Ag(I) from other metal ions. In fact, in our case, it would also be difficult to separate Ag(I) from Pb(II) using the chloride precipitation method as chloride would not only precipitate Ag(I) as AgCl but it would also precipitate Pb(II) as $PbCl_2$.

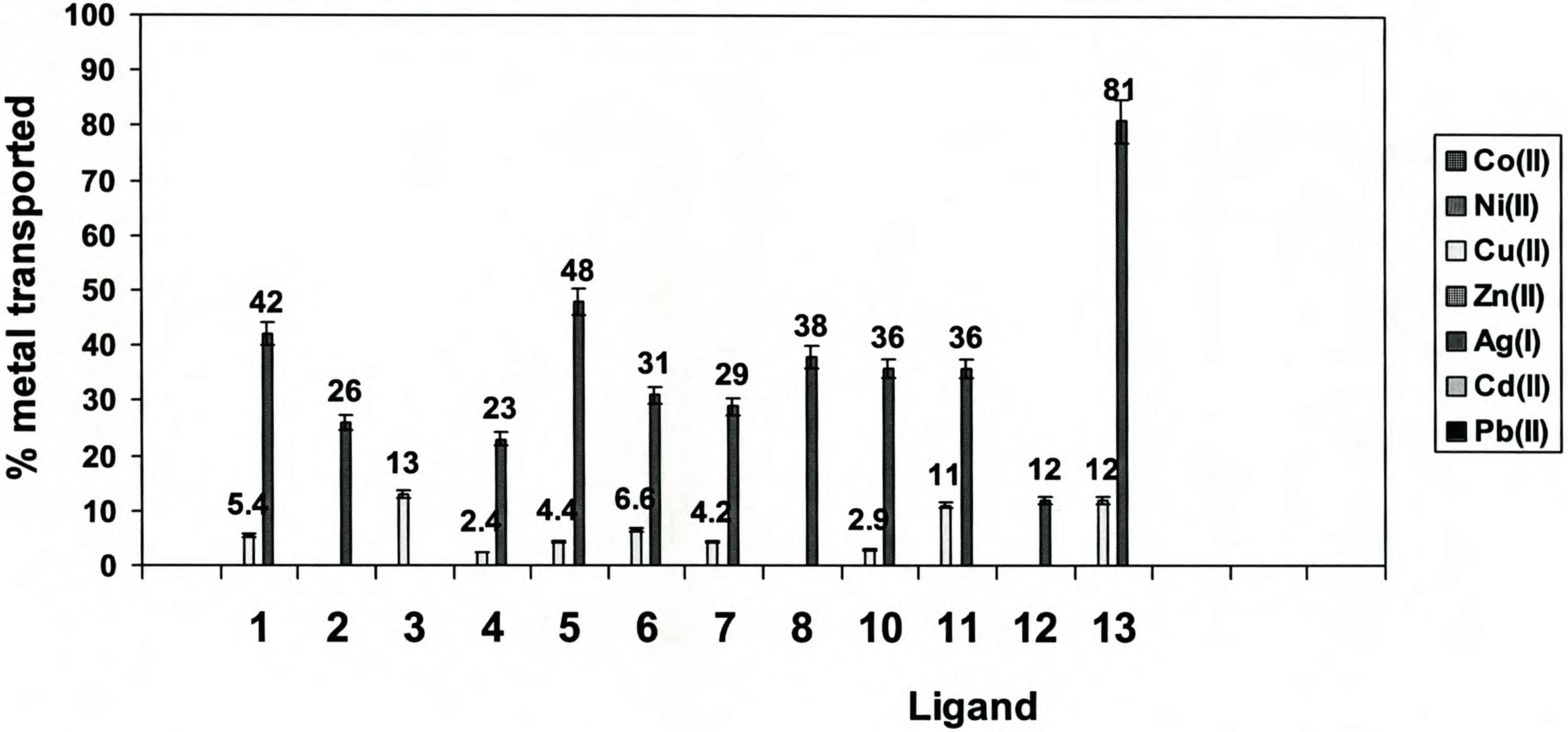

Fig 3.33: Comparison of the percentage transport of Ag(I) and Cu(II) ions in competitive transport studies involving all ligands (except H_2L^1-H_2L^3 and HL^9). **1** refers to **HL^1**, **2** refers to **HL^2**, **3** refers to **HL^3**, **4** refers to **HL^4**, **5** refers to **HL^5**, **6** refers to **HL^6**, **7** refers to **HL^7**, **8** refers to **HL^8**, **10** refers to **HL^{10}**, **11** refers to **HL^{11}**, **12** refers to **H_2L^{12}** and **13** refers to **HL^{13}**. In all cases, the experimental conditions were the same: **source phase pH = 5.5**, **receiving phase pH = 1.0** and **concentration of ligand = 2 x 10 $^{-3}$ M**. The **HL^9** and the mono-alkyl thioureas are not shown in this Figure.

Chapter 4

4 Results for competitive metal ion extraction studies involving *N,N*-dialkyl-*N'*-acyl(aroyl) thioureas

4.1 Introduction

In order to understand the membrane transport results better, a comparative study of liquid-liquid extraction of Ag(I) from a mixture of the metal ions: Co(II), Ni(II), Cu(II), Zn(II), Cd(II) and Pb(II) was conducted. The ligands employed in the transport experiments were used in this study.

Metal ion extraction depends upon a number of parameters, such as: structure of the ligand, stability of the individual metal / ligand complex, type of solvent used, nature of the accompanying anion and pH of the aqueous phase during extraction. However, in this study, we have only focused on the effect of varying the ligand structure on the extraction behaviour of the ligands.

The solvent extraction of a monovalent metal ion (M^+) by *N,N*-dialkyl-*N'*-acyl (aroyl)thioureas (HL) where the complex extracted has a composition of 1:1 metal ion to ligand ratio can be shown by the series of equilibria shown in **scheme 4.1**. There are two formation processes of a metal ion-ligand complex in aqueous and organic phases [72]. These processes are generally competitive and depend considerably on the complexing ability of the ligand in the aqueous phase and its hydrophobicity. Therefore, the species formed in both phases should be carefully considered while evaluating the equilibrium constants.

On the assumption that the complexed salt does not dissociate in the organic phase containing a non-polar solvent, and that the aqueous and organic phases have equal volumes, the following equilibrium constants can be defined.

Scheme 4.1: Equilibrium constants for a metal salt two-phase solvent extraction.

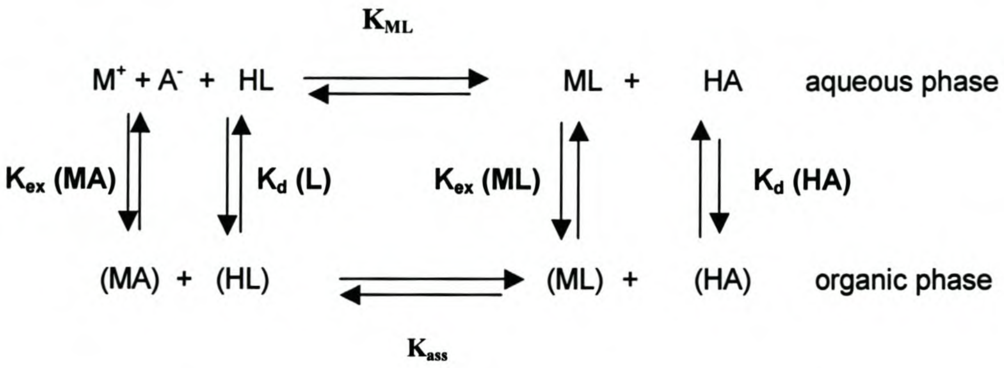

$K_{ML} = [ML]_{aq} [HA]_{aq} / [M^+]_{aq} [A^-]_{aq} [HL]_{aq}$

$K_{ex} (MA) = [MA]_o / [M^+]_{aq} [A^-]_{aq}$

$K_d (L) = [HL]_0 / [HL]_{aq}$

$K_{ass} = [ML]_o [HA]_o / [MA]_o [HL]_o$

$K_{ex} (ML) = [ML]_o / [ML]_{aq}$

$K_d (HA) = [HA]_0 / [HA]_{aq}$

Where K_{ML} is the stability constant of the metal ion-ligand complex in the aqueous phase; K_{ex} (MA) is the distribution constant of the metal salt between the aqueous and organic phases; K_d (L) is the distribution constant of the ligand between the aqueous and organic phase; K_{ass} is the association constant of the metal salt with the ligand in the organic phase; K_{ex} (ML) is the distribution constant of the complex salt between the aqueous and organic phase and K_d (HA) is the distribution constant of the acid (HA) between the aqueous and organic phases. The brackets represent concentrations and the subscripts 'aq' and 'o' refer to the aqueous and organic phases, respectively. A^- stands for the anion of the salt and M^+ for the monovalent metal ion.

The above equilibria can be summarized as:

$$M^{+}_{aq} + A^{-}_{aq} + (HL)_o \rightleftharpoons (ML)_o + (HA)_{aq}$$

$$K_{eq} = \frac{[ML]_o[HA]_{aq}}{[M^{+}]_{aq}\,[A^{-}]_{aq}\,[HL]_o}$$

Assuming no volume change occurs on mixing the two phases, for a system involving M^{n+}, we can write:

$$M^{n+}_{aq} + nA^{-}_{aq} + (HL)_o \rightleftharpoons (MLA_{n-1})_o + (HA)_{aq}$$

$$K_{eq} = \frac{[MLA_{n-1}]_o\,[HA]_{aq}}{[M^{n+}]_{aq}\,[A^{-}]^{n}_{aq}\,[HL]_o}$$

In our case, a detailed solvent extraction study was not undertaken to establish K_{ex} and K_{eq}. However, the overall distribution constant "D" for the Ag(I) extracted can be measured using:

$$D = \frac{\text{Total Ag(I) concentration in the organic phase}}{\text{Total Ag(I) concentration in the aqueous phase}}$$

Experimental conditions

Competitive two-phase solvent extraction experiments were carried out as described in **section 2.3.4**. In order to mimic the experimental conditions employed in the transport experiments, volumes of 3 ml (aq) and 15 ml (org) were used in the extraction studies. This is important, since for comparison purposes, extraction is carried out most of the time using equal volume ratio compared with that of the transport experiments. All extraction experiments were conducted at a fixed source phase pH (pH = 5.0) while the effect of varying the ligand concentration was studied. For effective and convenient comparison, we have grouped the ligands into sections. The results of the two-phase solvent extraction experiments are compared with that of the three-phase transport experiments and an attempt is made to logically relate and explain both sets of results.

The aqueous source phase: 3 ml, contained the seven metal ions each at an initial concentration of 0.01 M prepared in a buffer solution (CH_3COOH/CH_3COONa) of pH = 5.0. The organic phase: 15 ml, contained the ligand dissolved in chloroform. Note that no palmitic acid was used throughout the extraction experiments.

In the extraction experiments, the source phase and organic phase were shaken for 24 hr, at a rate of 120 cycles per minute, on a Labcon oscillating shaker. The experiments were all carried out at 25 °C in duplicate. In all cases, the values between any two duplicate runs did not exceed 2%. Any apparent extraction of small amounts of metal ions (< 2%) may be an artifact rather than a true indication towards a particular metal ion and therefore were ignored from the treatment of our data. The sum of all experimental errors involved in all measurements is assumed to be within ± 5%.

Calculation

The percentage of metal ion extracted was calculated as follows:

$$\text{\% metal ion extracted} = \frac{n_b - n_a}{n_b} \times 100$$

Where:

- n_b refers to the number moles of the metal ion present in the aqueous source phase before the extraction, and
- n_a refers to the number of moles of the metal ion present in the aqueous source phase after the extraction.

Also note that the terms ‘selectivity’ and ‘efficiency’ are used in the same context as defined in chapter 3.

4.2.1 Metal ion extraction by *N,N*-di-n-butyl-*N'*-benzoylthiourea (HL^1), *N,N*-diethyl-*N'*-benzoylthiourea (HL^2) and *N,N*-di-(2-hydroxyethyl)-*N'*-benzoylthiourea (HL^3) ligands.

In this section, ligands HL^1, HL^2 and HL^3 are grouped together and the results for the competitive metal ion extraction studies involving the metal ions: Co(II), Ni(II), Cu(II), Zn(II), Ag(I), Cd(II) and Pb (II) are summarized in **Fig. 4.1 – 4.3**.

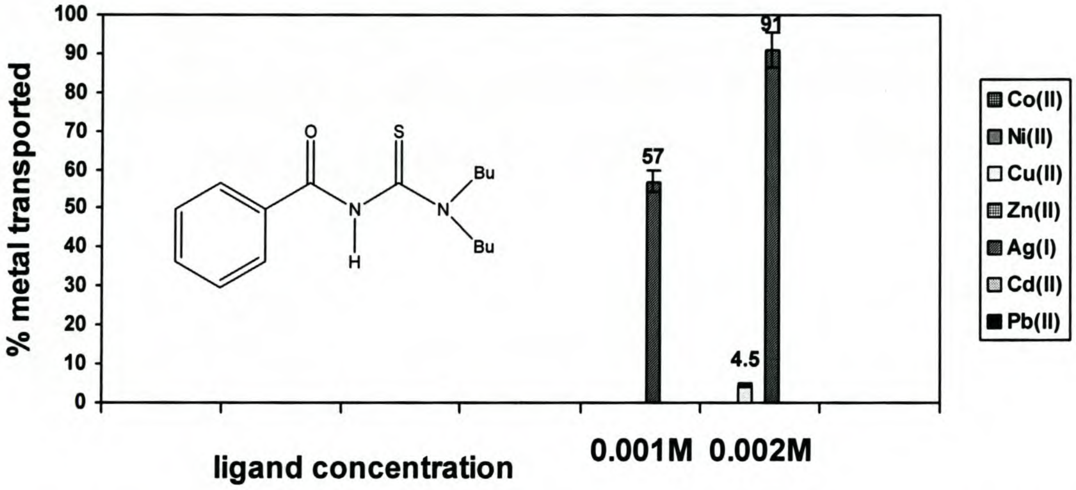

Fig. 4.1: Percentage extraction of Ag(I) and Cu(II) ions in competitive extraction studies involving **HL^1**. **pH of the source phase = 5.0** and the **concentration of the ligand** was varied from **1 x 10 $^{-3}$ M** to **2 x 10 $^{-3}$ M** as shown in the figure.

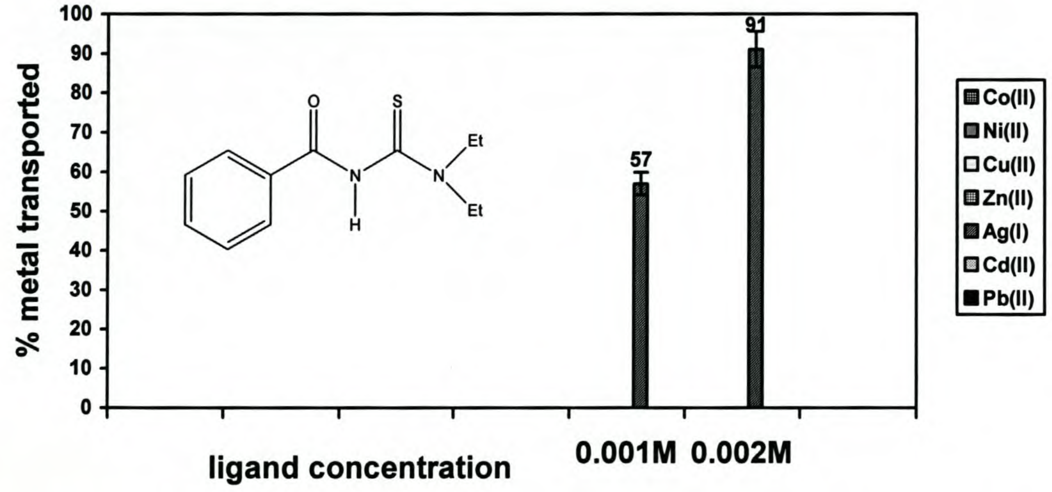

Fig. 4.2: Percentage extraction of Ag(I) in competitive extraction studies involving **HL^2**. **pH of the source phase = 5.0** and the **concentration of the ligand** was varied from **1 x 10 $^{-3}$ M** to **2 x 10 $^{-3}$ M** as shown in the figure.

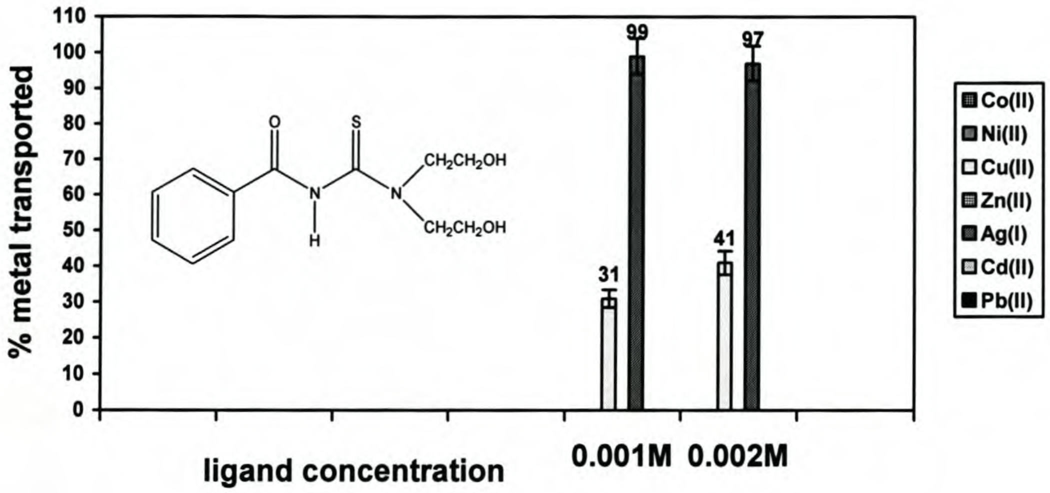

Fig. 4.3: Percentage extraction of Ag(I) and Cu(II) ions in competitive extraction studies involving HL^3. **pH of the source phase = 5.0** and the **concentration of the ligand** was varied from **1×10^{-3} M** to **2×10^{-3} M** as shown in the figure.

4.2.2 Comparison of metal ion extraction by *N,N*-di-n-butyl-*N'*-benzoylthiourea (HL^1), *N,N*-diethyl-*N'*-benzoylthiourea (HL^2) and *N,N*-di-(2-hydroxyethyl)-*N'*-benzoylthiourea (HL^3).

Under the conditions employed, consistent to the transport results, HL^1 and HL^2 showed selective extraction of Ag(I) compared with the other six metal ions (see **Fig 4.1 and 4.2**). At a concentration of 2×10^{-3} M, HL^1 extracted about 91% of Ag(I) and 4.5% of Cu(II). When the ligand concentration was decreased by half, the percentage extraction of Ag(I) by HL^1 was drastically decreased (only about 57% was extracted). Although the decrease in the concentration of HL^1 from 2×10^{-3} M to 1×10^{-3} M resulted in a decrease in the overall extraction efficiency for Ag(I), the selectivity for Ag(I) over Cu(II) was enhanced. A similar trend and percentage of Ag(I) extraction was observed with HL^2. At a ligand concentration of 2×10^{-3} M, HL^2 extracted about 91% of Ag(I). However, with a decrease in ligand concentration by half, the percentage extraction of Ag(I) was decreased to 57%.

The decrease in the percentage extraction of Ag(I) with the decrease in ligand concentration was expected from the crystal structure of HL^1 with Ag(I) (see **section 5.2**). The crystal structure shows a 1:1 mole ratio of ligand to Ag(I) during complex formation. The crystal structure of HL^2 with Ag(I) also shows a similar mode of co-ordination and metal to ligand mole ratio to that of HL^1 with Ag(I) [73]. Therefore, 2×10^{-3} M (3×10^{-5} mol) of the ligands (HL^1 or HL^2) is theoretically required to extract completely the total amount of Ag(I) (1×10^{-3} M, 3×10^{-5} mol) in the source phase. Note that the volumes used in the extraction experiments were 3 ml source phase and 15 ml organic phase. Therefore, in the absence of other determinate and indeterminate errors, we would theoretically expect that decreasing the concentration of HL^1 or HL^2 by half would reduce the total percentage of extraction of Ag(I) by half. However, for both ligands slightly higher percentages of Ag(I) extraction than theoretically expected were obtained.

In the case of HL^3, as can be seen from **Fig. 4.3**, Ag(I) and Cu(II) were selectively extracted. These extraction results are consistent with the transport results obtained in chapter 3, which showed that HL^3 transported more Ag(I) than Cu(II) into the membrane phase (see **Table 3.1**).

Unlike the cases of HL^1 and HL^2, where the decrease in ligand concentration resulted in a sharp decrease in Ag(I) extraction, a decrease in the concentration of HL^3 from 2×10^{-3} M to 1×10^{-3} M did not significantly affect the percentage extraction of Ag(I) but decreased the percentage extraction of Cu(II) from 41% to 31% (see **Fig. 4.3**). In order to explain this result, further studies of ligand HL^3 with Ag(I) and Cu(II) in solution are required.

At a ligand concentration of 2×10^{-3} M, the extraction efficiency and selectivity of ligands HL^1 - HL^3 for Ag(I) follows the order: $\mathbf{HL^3 > HL^2 \cong HL^1}$ for efficiency and $\mathbf{HL^2 > HL^1 > HL^3}$ for selectivity. Therefore, based on the above results, we can say that varying the alkyl end of a benzoylthiourea ligand from butyl to ethyl enhances selectivity for Ag(I) extraction. However, introducing more oxygen donor atoms by adding hydroxyl-groups to the alkyl end of HL^2 to give HL^3 resulted in the extraction of Cu(II) together with Ag(I). Finally, we can conclude that HL^1, HL^2 and HL^3 are very efficient extracting reagents for Ag(I), which may probably be an indication of high formation constants of these ligands with Ag(I).

4.2.3 Metal ion extraction by *N,N*-diethyl-*N'*-4-nitrobenzoylthiourea (HL^4) and *N,N*-diethyl-*N'*-4-chlorobenzoylthiourea (HL^5) ligands.

In this section, ligands HL^4 and HL^5 are grouped together and the results for the competitive metal ion extraction studies involving the metal ions: Co(II), Ni(II), Cu(II), Zn(II), Ag(I), Cd(II) and Pb (II) are summarized in **Fig 4.4 – 4.5**.

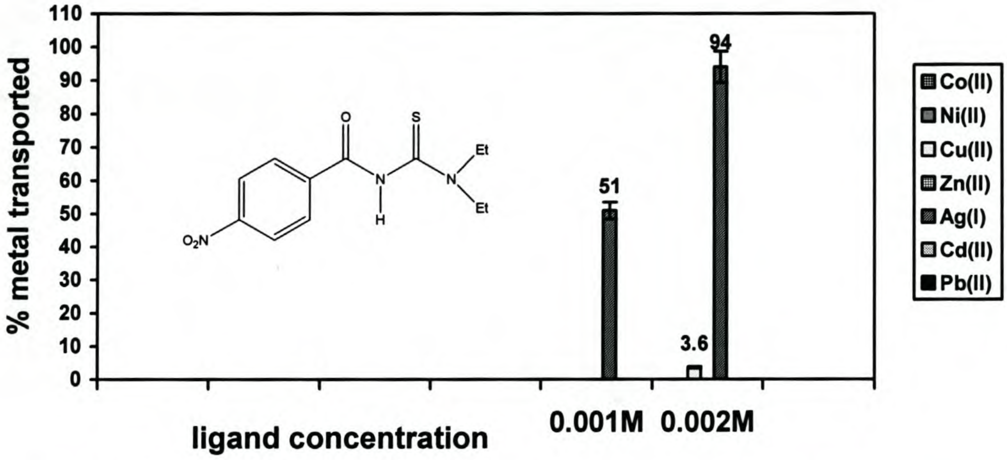

Fig. 4.4: Percentage extraction of Ag(I) and Cu(II) ions in competitive extraction studies involving **HL^4**. **pH of the source phase = 5.0** and the **concentration of the ligand** was varied from **1 x 10 $^{-3}$ M** to **2 x 10 $^{-3}$ M** as shown in the figure.

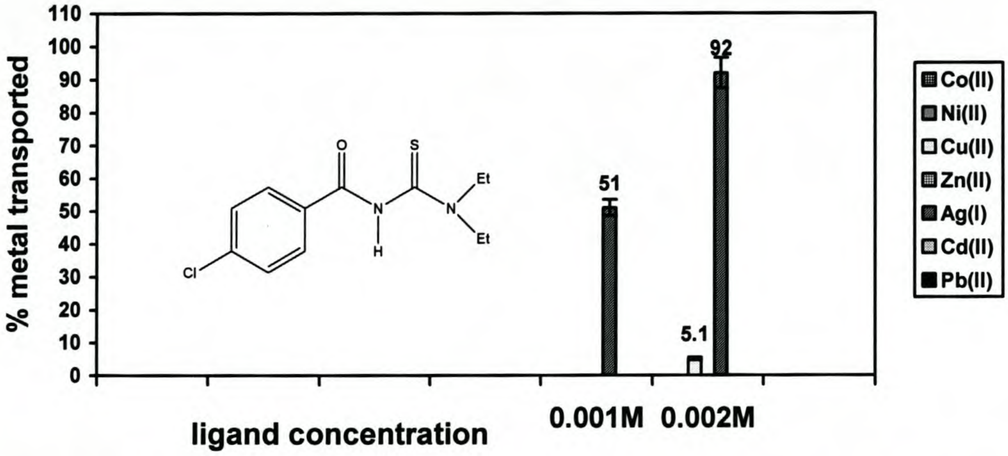

Fig. 4.5: Percentage extraction of Ag(I) and Cu(II) ions in competitive extraction studies involving **HL^5**. **pH of the source phase = 5.0** and the **concentration of the ligand** was varied from **1 x 10 $^{-3}$ M** to **2 x 10 $^{-3}$ M** as shown in the figure.

4.2.4 Comparison of metal ion extraction by *N,N*-diethyl-*N'*-4-nitrobenzoylthiourea (HL^4) and *N,N*-diethyl-*N'*-4-chlorobenzoylthiourea (HL^5) ligands.

As can be seen from their structures, both HL^4 and HL^5 ligands possess electron-withdrawing substituents attached to the benzoyl groups. The substituents (NO_2^- and Cl^-) withdraw electrons from the ring. The benzene ring is also an electron-withdrawing group and therefore withdraws electrons from the carbonyl oxygen of the thiourea moiety, thus making the oxygen softer. This helps the ligand to complex with Ag(I) through both donor atoms, the sulfur and the oxygen.

Under the experimental conditions studied (see **Fig. 4.4** and **4.5**), both ligands were selective for Ag (I). At a ligand concentration of 2 x 10^{-3} M, HL^4 extracted about 94% of Ag(I) and 3.6% of Cu(II). Similarly, HL^5 extracted about 92% of Ag(I) and 5.1% of Cu(II). These results are consistent with the transport results obtained in **section 3.7.3** in that both ligands were selective for Ag(I) and Cu(II), with major preference for Ag(I).

At a ligand concentration of 1 x 10^{-3} M, both ligands extracted selectively about 51% of Ag(I) (see **Fig 4.4 and 4.5**). The decrease in the percentage of extraction for Ag(I) with the decrease in the concentrations of HL^4 and HL^5 can be explained assuming a 1:1 mole ratio in complex formation between Ag(I) and the ligands, as in the case of HL^1 and HL^2. The fact that these results have come down to about 51% is because we have a ratio of 0.5 mol of ligand : 1 mol of metal ion present, so the ligand has extracted as much metal ion as it could extract.

Comparison of the extraction efficiency of HL^4 and HL^5 for Ag(I) at a ligand concentration of 2 x 10^{-3} M shows the order: $\mathbf{HL^4 > HL^5}$. The extraction efficiency of ligands HL^4 and HL^5 can also be compared with that of HL^2 and the following order is obtained: $\mathbf{HL^4 > HL^5 \cong HL^2}$. At a ligand concentration of 2 x 10^{-3} M, the following order of extraction selectivity for Ag(I) compared with Cu(II) was obtained: $\mathbf{HL^2 > HL^4 > HL^5}$. The percentage extraction results for HL^4, HL^5 and HL^2 are very close to one another. This means that the electron withdrawing groups (NO_2^- and Cl^-) did not have a considerable effect on the extraction behavior of the ligands.

4.2.5 Metal ion extraction by *N,N*-dibutyl-*N'*-2,4,6-trimethoxybenzoylthiourea (HL^6) and *N,N*-diethyl-*N'*-2,4,6-trimethoxybenzoylthiourea (HL^7) ligands.

In this section, ligands HL^6 and HL^7 are grouped together and the results of the competitive metal ion extraction studies involving the metal ions: Co(II), Ni(II), Cu(II), Zn(II), Ag(I), Cd(II) and Pb (II) are summarized in **Fig. 4.6 – 4.7**.

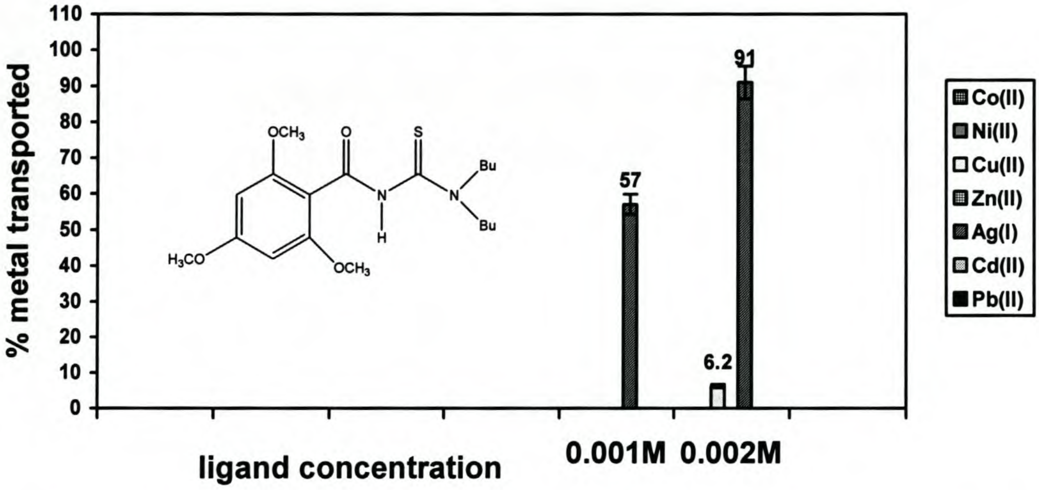

Fig. 4.6: Percentage extraction of Ag(I) and Cu(II) ions in competitive extraction studies involving HL^6. **pH of the source phase = 5.0** and the **concentration of the ligand** was varied from **1 x 10 $^{-3}$ M** to **2 x 10 $^{-3}$ M** as shown in the figure.

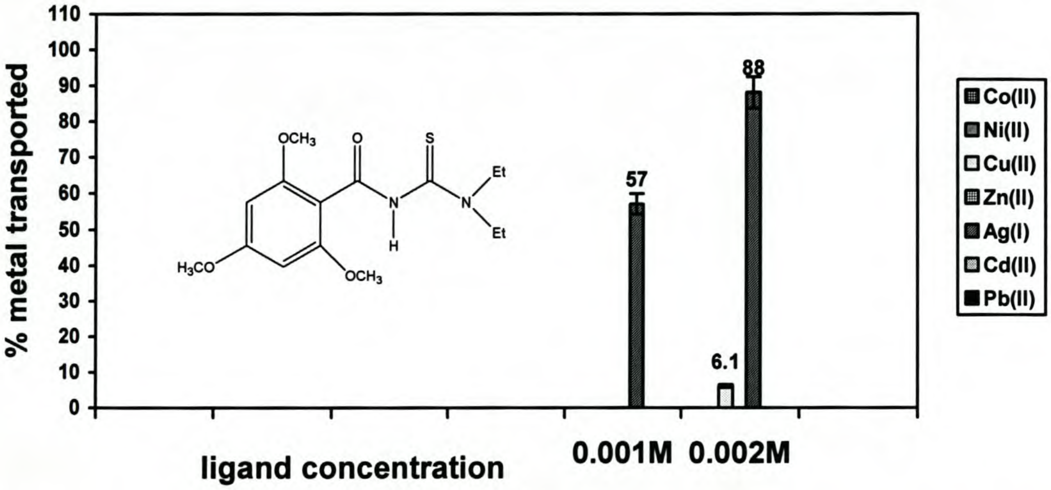

Fig. 4.7: Percentage extraction of Ag(I) and Cu(II) ions in competitive extraction studies involving HL^7. **pH of the source phase = 5.0** and the **concentration of the ligand** was varied from **1 x 10 $^{-3}$ M** to **2 x 10 $^{-3}$ M** as shown in the figure.

4.2.6 Comparison of metal ion extraction by *N,N*-dibutyl-*N'*-2,4,6-trimethoxybenzoyl thiourea (HL^6) and *N,N*-diethyl-*N'*-2,4,6-trimethoxybenzoylthiourea (HL^7) ligands.

As it is evident from their structures, both ligands have electron-releasing methoxy substituents attached to the benzene ring of the ligands at C_2, C_4, and C_6 (see **section 2.1.3** for numbering). The methoxy groups donate electrons to the ring through inductive effects thereby increasing the electron density in the ring.

The results for the competitive metal ion extraction studies involving HL^6 and HL^7 are summarized in **Fig. 4.6 – 4.7**. These results show that both ligands are efficient extraction reagents for Ag(I). Under the conditions employed, consistent to the transport results, the extraction results of these ligands indicate selective extraction of Ag(I) compared with the other six metal ions. The percentages of Ag(I) extraction by both ligands are very close. At a ligand concentration of 2 x 10^{-3} M, 91% of Ag(I) and 6.2% of Cu(II) were extracted by HL^6. When the ligand concentration was decreased by half, the percentage extraction of Ag(I) was drastically decreased to 57%. At a ligand concentration of 2 x 10^{-3} M, 88% of Ag(I) and 6.1% of Cu(II) were extracted by HL^7. However, with a decrease in ligand concentration by half, the percentage extraction of Ag(I) was also decreased to 57%. If we again assume a 1:1 mole ratio of ligand to Ag(I) during complexation, these results are expected. Although a decrease in the ligand concentration from 2 x 10^{-3} M to 1 x 10^{-3} M resulted in a decrease in the percentage extraction of Ag(I) by both ligands, the selectivity for Ag(I) was enhanced. The fact that both HL^6 and HL^7 are very efficient reagents for the extraction of Ag(I) can probably be an indication of high formation constants of these ligands with Ag(I).

Comparison of the extraction efficiency and selectivity of these ligands at ligand concentrations of 2 x 10^{-3} M shows that both ligands display similar efficiency and selectivity for Ag(I). The extraction efficiency of HL^6 and HL^1 ligands for Ag(I) is comparable (about 91%) and comparison of the extraction efficiency for Ag(I) of HL^7 with HL^2, HL^4 and HL^5 shows the order: **HL^4 > HL^5 > HL^2 > HL^7**.

4.2.7 Metal ion extraction by *N*-Piperidyl-*N'*-benzoylthiourea (HL^8), *N*-Piperidyl-*N'*-4-nitrobenzoylthiourea (HL^9) and *N*-Piperidyl-*N'*-2,6-dimethoxybenzoylthiourea (HL^{10}).

In this section, ligands HL^8 - HL^{10} are grouped together and their selectivity and efficiency of extraction for Ag(I) is compared.

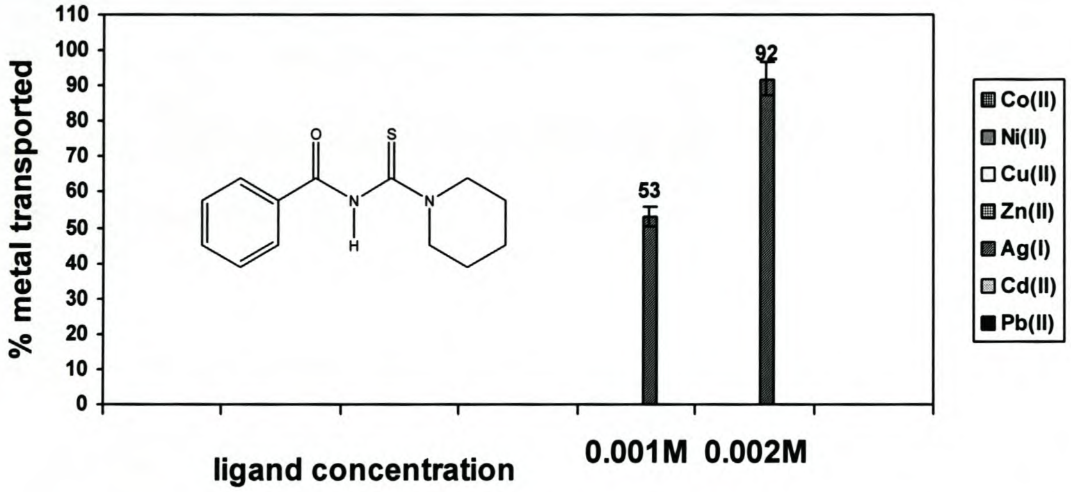

Fig. 4.8: Percentage extraction of Ag(I) in competitive extraction studies involving **HL^8**. **pH of the source phase = 5.0** and the **concentration of the ligand** was varied from **1 x 10 $^{-3}$ M** to **2 x 10 $^{-3}$ M** as shown in the figure.

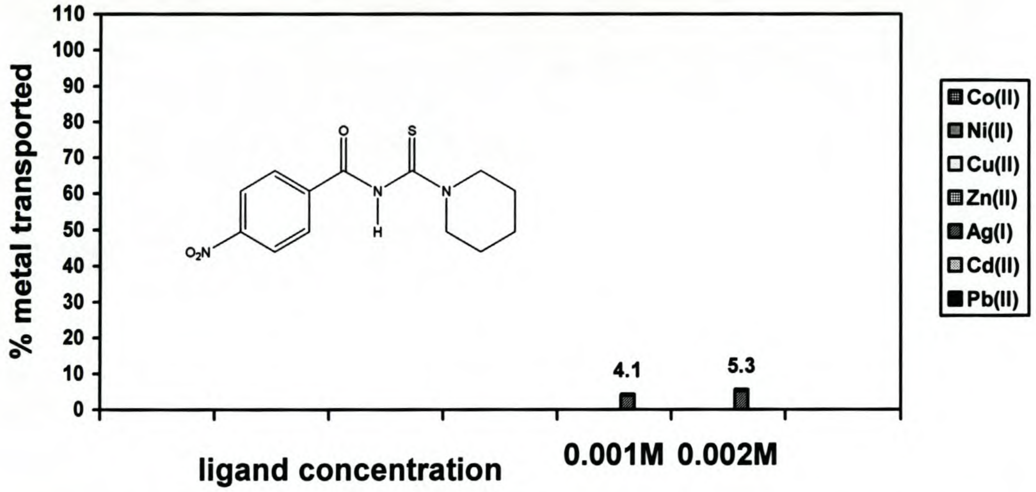

Fig. 4.9: Percentage extraction of Ag(I) in competitive extraction studies involving **HL^9**. **pH of the source phase = 5.0** and the **concentration of the ligand** was varied from **1 x 10 $^{-3}$ M** to **2 x 10 $^{-3}$ M** as shown in the figure.

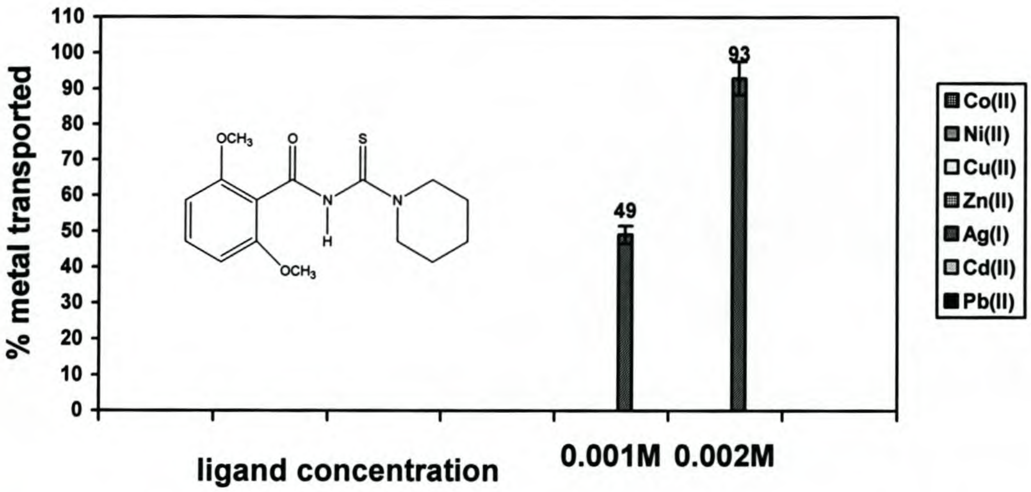

Fig 4.10: Percentage extraction of Ag(I) in competitive extraction studies involving **HL**[10]. **pH of the source phase = 5.0** and the **concentration of the ligand** was varied from **1 x 10 $^{-3}$ M** to **2 x 10 $^{-3}$ M** as shown in the figure.

4.2.8 Comparison of metal ion extraction by *N*-Piperidyl-*N'*-benzoylthiourea (HL[8]), *N*-Piperidyl-*N'*-4-nitrobenzoylthiourea (HL[9]) and *N*-Piperidyl-*N'*-2,6-dimethoxybenzoyl thiourea (HL[10]) ligands.

HL[9] possesses an electron-withdrawing (NO_2^-) group at position C_4, whereas HL[10] possesses two methoxy groups at positions C_2 and C_6. As can be seen from their structures, the three ligands are similar in that each of them possesses a pipyridine ring on one end of the ligand (see **section 2.1.3**).

The results of the competitive metal ion extraction studies involving HL[8] - HL[10] are summarized in **Fig. 4.8 – 4.10**. Under the experimental conditions employed, very efficient and selective extraction of Ag(I) was obtained by HL[8] and HL[10]. However, the extraction efficiency of HL[9] for Ag(I) was poor. As can also be seen from the transport results (**section 3.7.7**), HL[9] was not a good transport ionophore for Ag(I). At a ligand concentration of 1 x 10^{-3} M, the efficiency of extraction of HL[9] for Ag(I) was only 4.1%. Increasing the ligand concentration to 2 x 10^{-3} M did not make a significant change to the percentage extraction of Ag(I) (only 5.3% Ag(I) was extracted).

At a ligand concentration of 2 x 10^{-3}, HL[8] extracted 92% and HL[10] extracted 93% of Ag(I). These results are consistent with the transport results obtained in **sections 3.7.7**, which indicated that both ligands were selective for Ag(I). At a ligand concentration of 1 x 10^{-3} M, The percentages of Ag(I) extracted by HL^8 and HL^{10} were 53% and 49% respectively (see **Fig. 4.8 and 4.10)**. As in the case of HL^1, the decrease in the percentage extraction of Ag(I) with the decrease in ligand concentrations can be explained by assuming a 1:1 mole ratio between Ag(I) and the ligands during complexation. The interesting extraction result with HL^8 and HL^{10} is that, independent of the ligand concentration, they are merely selective for Ag(I). This makes them excellent reagents for selectively extracting Ag(I) from a mixture of the seven metal ions.

Comparison of the extraction efficiency of HL^8 and HL^{10} for Ag(I) at a ligand concentration of 2 x 10^{-3} M shows that both ligands are almost equally efficient. However, comparison of the extraction efficiency of HL^8 - HL^{10} for Ag(I) at a ligand concentration of 1 x 10^{-3} M shows the order: **$HL^8 > HL^{10} >> HL^9$**. The fact that the percentage extraction results for HL^8 and HL^{10} are very close to one another indicates that there was no significant influence of the methoxy substituents in HL^{10} on the extraction efficiency for Ag(I). The transport experiments conducted under the same conditions (**section 3.7.7**) also indicated that both HL^8 and HL^{10} show similar efficiency for Ag(I) transport. However, the fact that HL^9 is a poor extraction reagent for Ag(I) may be an indication of very low formation constant of the ligand with Ag(I). In fact, a similar conclusion was also reached from the transport results involving HL^9 (see **section 3.7.8**).

4.2.9 Metal ion extraction by *N,N*-Diethyl-*N'*-2,2-dimethylpropanoylthiourea (HL^{11}), bipodal 3,3,3',3'-Tetraethyl-1,1'-isophthaloylbisthiourea (H_2L^{12}) and *N,N*-Diethyl-*N'*-camphanoylthiourea (HL^{13}) ligands.

In this section, the results of the competitive metal ion extraction studies involving HL^{11}, HL^{12} and HL^{13} are presented.

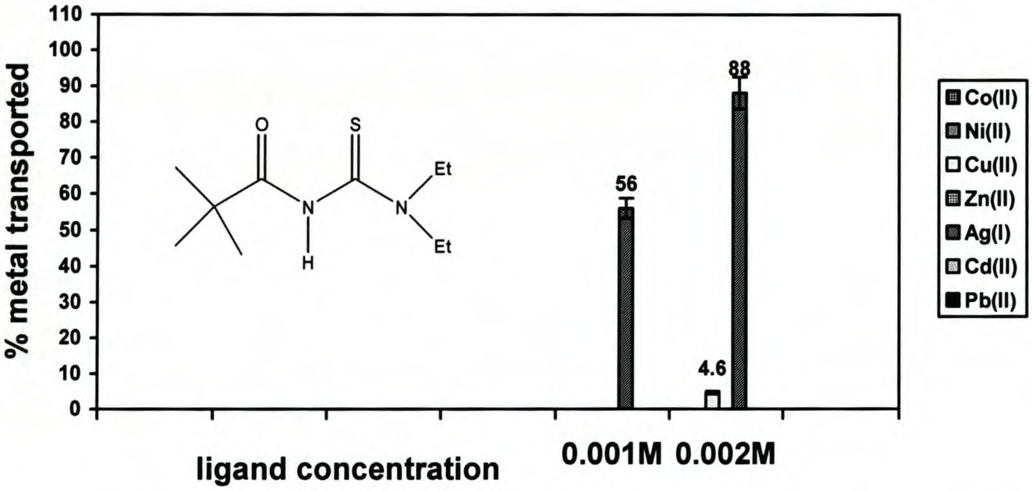

Fig. 4.11: Percentage extraction of Ag(I) and Cu(II) ions in competitive extraction studies involving HL^{11}. **pH of the source phase = 5.0** and the **concentration of the ligand** was varied from **1 x 10 $^{-3}$ M** to **2 x 10 $^{-3}$ M** as shown in the figure.

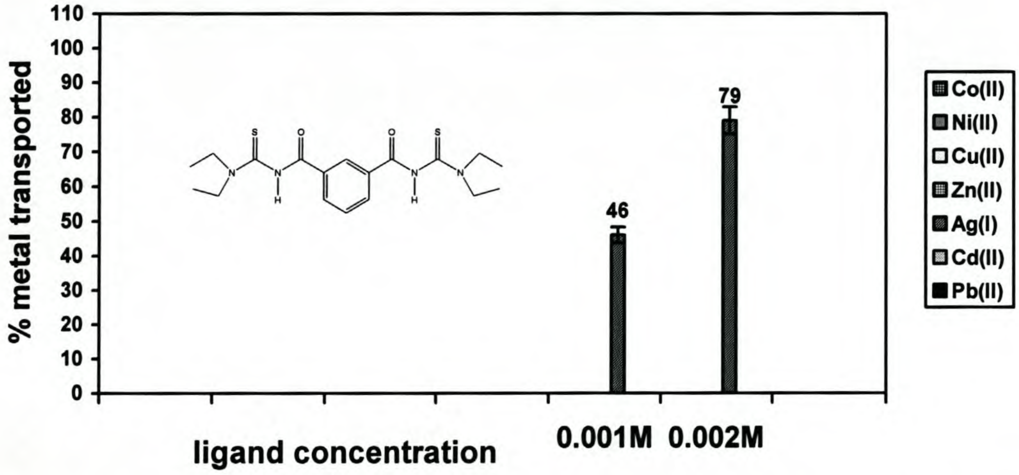

Fig. 4.12: Percentage extraction of Ag(I) in competitive extraction studies involving H_2L^{12}. **pH of the source phase = 5.0** and the **concentration of the ligand** was varied from **1 x 10 $^{-3}$ M** to **2 x 10 $^{-3}$ M** as shown in the figure.

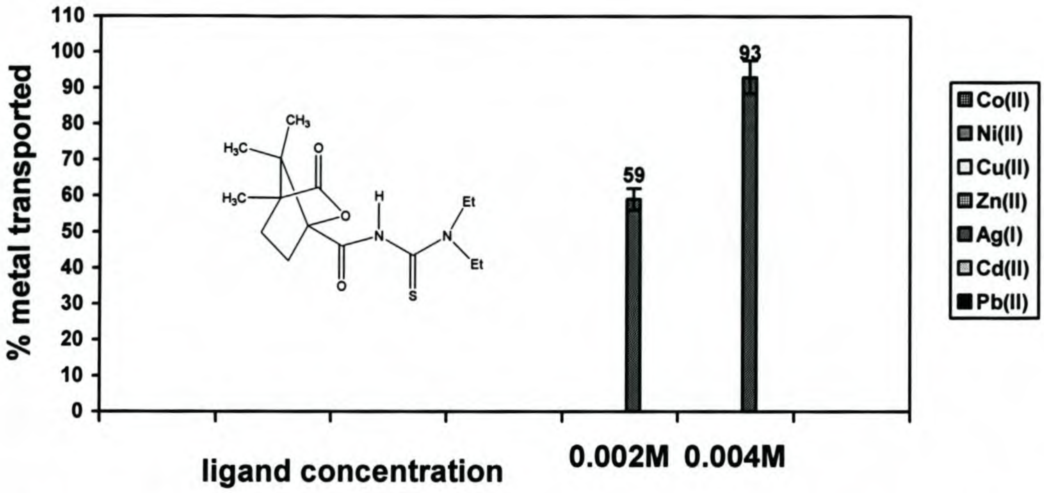

Fig. 4.13: Percentage extraction of Ag(I) in competitive extraction studies involving **HL^{13}**. **pH of the source phase = 5.0** and the **concentration of the ligand** was varied from **2×10^{-3} M** to **4×10^{-3} M** as shown in the figure.

4.2.10 Comparison of metal ion extraction by *N,N*-Diethyl-*N'*-2,2-dimethylpropanoyl thiourea (HL^{11}), bipodal 3,3,3',3'-Tetraethyl-1,1'-isophthaloylbisthiourea (H_2L^{12}) and *N,N*-Diethyl-*N'*-camphanoylthiourea (HL^{13}) ligands.

Under the conditions employed, consistent to the transport results, an efficient and selective extraction of Ag(I) by HL^{11} was obtained. All the ligands that we studied so far were examples of aroyl-thioureas, whereas HL^{11} represents the acyl-thioureas. Investigation of the results of extraction using HL^{11} reveals that at a ligand concentration of 2×10^{-3} M, the ligand extracts 88% of Ag(I) and 4.6% of Cu(II) (see **Fig 4.11**). When the ligand concentration was decreased by half, the percentage extraction for Ag(I) was decreased to 56%. Comparison of the extraction behaviour of HL^{11} with that of HL^2 at a ligand concentration of 2×10^{-3} M shows that the latter is more efficient for the extraction of Ag(I). The reason for this may be attributed to the fact that the oxygen atom of the carbonyl group in the thiourea moiety of the ligand is softer when bonded to an electron withdrawing phenyl group than an electron releasing alkyl group, and hence better efficiency to extract Ag(I).

As can be seen from the structure of H_2L^{12}, it seems that the ligand can accommodate two metal ions thus forming a complex in a 2:1 mole ratio of metal ion to ligand. Based on this prediction, we expected the ligand to be more efficient than HL^2 for extracting Ag(I).

However, the experimental results turned out to be different. In fact, it was found that HL^2 is much more efficient in extracting Ag(I) than H_2L^{12}. Consistent to the transport results obtained in **section 3.7.11**, H_2L^{12} was selective for Ag(I). Furthermore, at a ligand concentration of 2 x 10^{-3} M, 79% of Ag(I) and at a ligand concentration of 1 x 10^{-3} M, 46% of Ag(I) were selectively extracted by H_2L^{12} (see **Fig. 4.12**). Comparison of the extraction efficiency of H_2L^{12} for Ag(I) with that of HL^2 (**Fig. 4.2 and 4.12**) shows the order: $\mathbf{H_2L^{12} < HL^2}$.

HL^{13} is similar to HL^2, except that HL^2 possesses a benzoyl-moiety whereas HL^{13} has a camphanyl group at its one end. Therefore, it becomes interesting to compare the extraction results of these ligands for Ag(I). Comparison of the transport results for HL^2 and HL^{13} shows that HL^{13} was more efficient in transporting Ag(I). However, comparison of the extraction results of these ligands at a ligand concentration of 2 x 10^{-3} M (**Fig. 4.2 and 4.13**) reveals that HL^2 is more efficient in extracting Ag(I). The crystal structure of HL^{13} with Ag(I) [64] shows a 2:1 mole ratio of ligand to Ag(I). Therefore, in order to extract the Ag(I) ion in the source phase completely, 4 x 10^{-3} M of the ligand is required. At a ligand concentration of 4 x 10^{-3} M, 93% and at a ligand concentration of 2 x 10^{-3} M, 59% of Ag(I) was extracted by HL^{13} (see **Fig. 4.13**). The decrease in the percentage of extraction for Ag(I) with a decrease in ligand concentration was expected from the mole ratio calculation.

The selectivity of HL^{13} for Ag(I) is also consistent with the transport result obtained in **section 3.7.11**. The fact that 93% of Ag(I) is selectively extracted by HL^{13} makes this ligand very efficient and selective for extracting Ag(I). Comparison of the extraction efficiency of ligands HL^{11}, H_2L^{12} and HL^{13} for Ag(I) at a ligand concentration of 2 x 10^{-3} M shows the order of: $\mathbf{HL^{11} > H_2L^{12} > HL^{13}}$. However, unless the mole ratios are taken into account, such comparisons must not be confused with the actual extraction efficiency of the ligands. For example, although HL^{13} extracts less that HL^{11} and H_2L^{12} at the specified ligand concentration (2 x 10^{-3} M), we need to realize that this concentration is actually half of the concentration we would theoretically require to extract the total amount of Ag(I) in the source phase. This can be seen from the crystal structure of HL^{13} with Ag(I) [65].

4.2.11 Metal ion extraction by *N*-Propyl-*N'*-benzoylthiourea (H_2L^1), *N*-Piperidyl-*N'*-4-heptoxybenzoylthiourea (H_2L^2) and *N*-Phenyl-*N'*-benzoylthiourea (H_2L^3) ligands.

In this section, H_2L^1 – H_2L^3 are grouped together and their selectivity and efficiency of extraction for Ag(I) is compared.

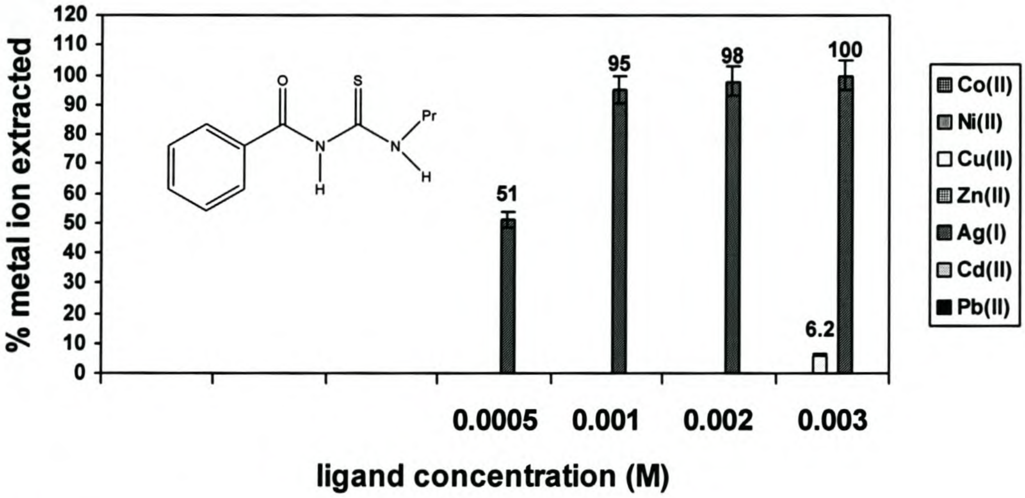

Fig. 4.14: Percentage extraction of Ag(I) and Cu(II) ions in competitive extraction studies involving H_2L^1. **pH of the source phase = 5.0** and **concentration of the ligand** was varied from **5 x 10^{-4} M** to **3 x 10^{-3} M** as shown in the figure.

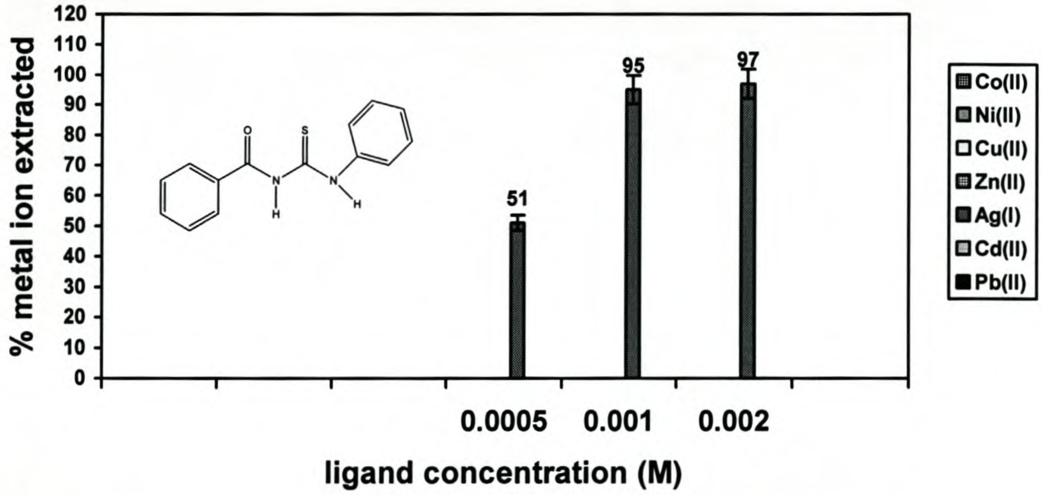

Fig. 4.15: Percentage extraction of Ag(I) in competitive extraction studies involving H_2L^2. **pH of the source phase = 5.0** and **concentration of the ligand** was varied from **5 x 10^{-4} M** to **2 x 10^{-3} M** as shown in the figure.

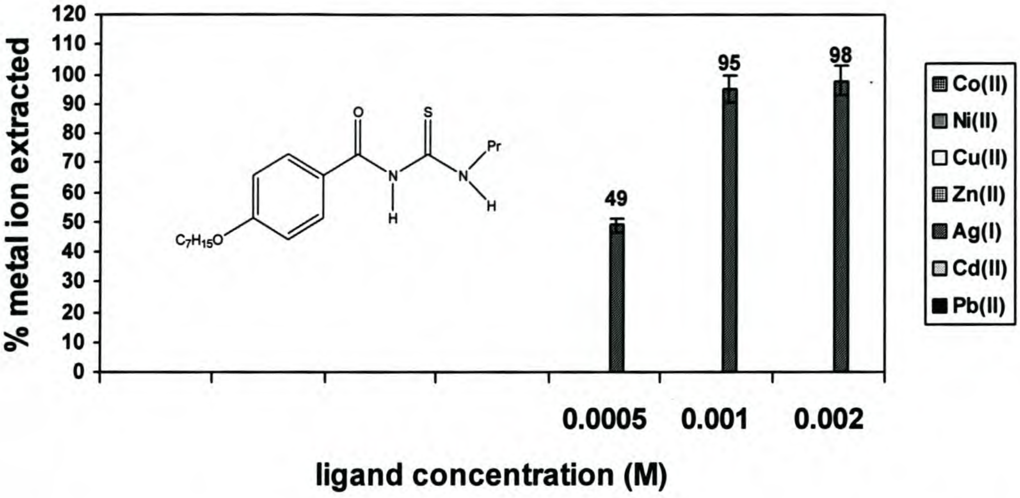

Fig. 4.16: Percentage extraction of Ag(I) in competitive extraction studies involving **H_2L^3**. **pH of the source phase = 5.0** and **concentration of the ligand** was varied from **5×10^{-4} M** to **2×10^{-3} M** as shown in the figure.

4.2.12 Comparison of metal ion extraction by *N*-Propyl-*N'*-benzoylthiourea (H_2L^1), *N*-Piperidyl-*N'*-4-heptoxybenzoylthiourea (H_2L^2) and *N*-Phenyl-*N'*-benzoylthiourea (H_2L^3) ligands.

As it is evident from their structures, these ligands show some similarity in that they are all mono-alkyl substituted ligands. The co-ordination chemistry reviewed by Koch [40] had indicated that the oxygen atom of the carbonyl group in mono-alkyl substituted thioureas is not available for complex formation with metal ions due to the intra-molecular hydrogen bonding. Therefore, based on this argument we can expect H_2L^1 – H_2L^3 ligands to co-ordinate with Ag(I) through only the sulfur donor atom. If this is the case, then we would expect the ligands to extract Ag(I) in a 1:1 ligand to metal mole ratio. In other words, 2×10^{-3} M (3×10^{-5} mol) of the ligand would be theoretically required to extract the total amount of Ag(I) (1×10^{-3} M, 3×10^{-5} mol) in the source phase. Therefore, in the absence of other determinate and indeterminate errors, decreasing the concentration of the ligands by half should theoretically decrease the total percentage of Ag(I) extraction by half. However, inconsistent to our expectation, decreasing the ligand concentration to 1×10^{-3} M had no significant effect on the percentage extraction of Ag(I) by these ligands (see **Fig. 4.14 – 4.16**). However, interestingly, reducing the ligand concentration further to 5×10^{-4} M resulted in a decrease of Ag(I) extraction almost by half. When the concentration of H_2L^1

was increased to 3 x 10^{-3} M, all the Ag(I) and about 6.2% of Cu(II) were extracted. From the above results, it seems that one mole of the ligand (H_2L^1, H_2L^2 or H_2L^3) is extracting almost two moles of Ag(I). In the absence of more evidence (like crystal structure data or further experimentation), it is difficult to discuss these results.

The results of the competitive metal ion extraction studies summarized in **Fig. 4.14 – 4.16** show that H_2L^1 – H_2L^3 ligands are excellent reagents for the extraction of Ag(I). Under the conditions employed, consistent to the transport results, the extraction results indicate that these ligands are very efficient and selective for Ag(I) extraction compared to the other six metal ions. At a ligand concentration of 2 x 10^{-3} M, 98% of Ag(I) was extracted by H_2L^1. When the ligand concentration was decreased to 2 x 10^{-3} M, the extraction of Ag(I) decreased to 95%. A similar trend and percentages of Ag(I) extraction was obtained with H_2L^2 and H_2L^3.

Comparison of the extraction efficiency and selectivity of ligands H_2L^1 – H_2L^3 at ligand concentrations of 2 x 10^{-3} M shows that they have similar efficiency and selectivity behaviours. However, at the experimental conditions studied, comparison of the extraction efficiency of the mono-alkyl substituted thioureas with the dialkyl-substituted analogues shows that the former ligands are more efficient and selective for the extraction of Ag(I).

Ligands H_2L^1 – H_2L^3 were the worst transport ionophores for Ag(I), yet they are the best extraction reagents for Ag(I) since they require low concentrations of ligand and extract selectively and efficiently. The fact that these ligands are very efficient extraction reagents but not good transport ionophores for Ag(I) indicates that these ligands probably have high formation constants with Ag(I).

4.3 Concluding discussion

Although theory does not decree that transport and extraction results should coincide in terms of selectivity and efficiency for a specific metal ion [21], it was nevertheless of interest to see whether the clear Ag(I) transport selectivity observed by most of the thiourea ligands we investigated would be maintained in the extraction studies. This was found to be the case with minor amounts of Cu(II) being co-extracted with Ag(I) by some of the ligands (see **Fig. 4.17**). It has been well documented that both the lipophilicity of a ligand and its binding strength with a particular cation are some of the factors that influence overall extraction efficiencies [21].

In this study, the extraction experiments show that almost all the thiourea ligands investigated as extraction reagents, with the exception of the *N*-piperidyl-*N'*-4-nitrobenzoylthiourea (HL^9), were efficient and selective for the extraction of Ag(I). This may be an indication of high formation constants of the ligands with Ag(I). The percentage of Ag(I) extracted by each thiourea ligand depended on the concentration of the ligand used. The effect of varying the pH of the source phase from 5.0 to 5.5 was also investigated. However, at a source phase pH of 5.5, almost all the other metal ions were also extracted with Ag(I). Therefore, further attempts in this direction were shelved and pH = 5.0 was selected as optimum pH for our study. The selective and efficient extraction of Ag(I) is in agreement with the transport selectivity for Ag(I) obtained in chapter 3.

In conclusion, the high Ag(I) extraction selectivity and efficiency obtained by the ligands we have studied suggests that the ligands can be successfully used in the extraction of Ag(I) from Co(II), Ni(II), Cu(II), Zn(II), Cd(II) and Pb(II) ions.

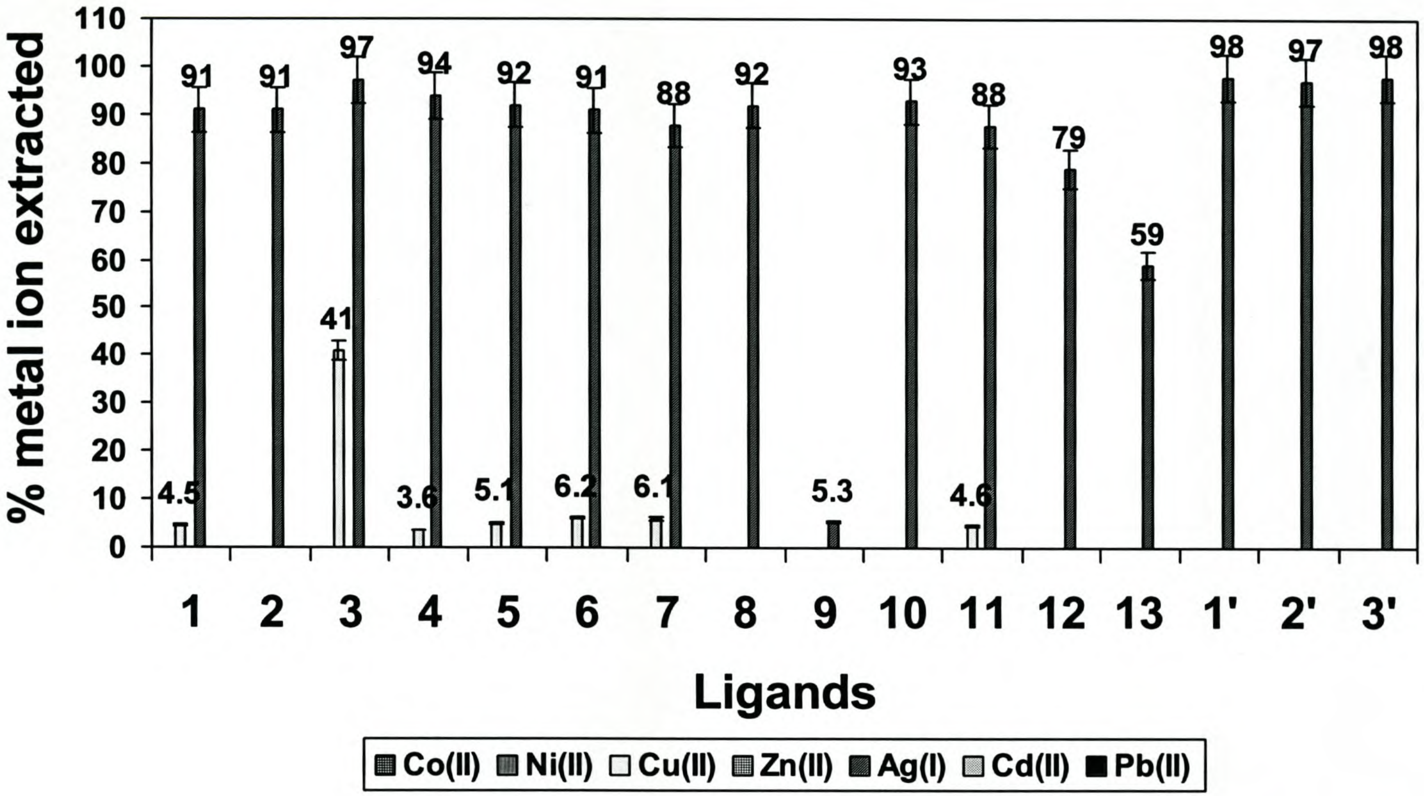

Fig. 4.17: Comparison of the competitive extraction studies involving all ligands studied: **1 = HL^1, 2 = HL^2, 3 = HL^3, 4 = HL^4, 5 = HL^5, 6 = HL^6, 7 = HL^7, 8 = HL^8, 9 = HL^9, 10 = HL^{10}, 11 = HL^{11}, 12 = H_2L^{12}, 13 = HL^{13}, 1' = H_2L^1, 2' = H_2L^2 and 3' = H_2L^3**. The experimental conditions were: pH of the source phase = **5.0** and concentration of ligand = **2×10^{-3} M**.

Chapter 5

5 Crystal and molecular structure of Tetra[(*N,N*-di-n-butyl-*N'*-benzoylthiourea) silver(I)] complex

5.1 Crystallographic data

The tetra[(*N,N*-di-n-butyl-*N'*-benzoylthiourea) silver(I)] complex was synthesized as described in **section 2.2**. Single crystals of the complex were obtained from a 1:1 solvent mixture of acetonitrile/chloroform after 5 days using the slow solvent evaporation method. The crystal and molecular structure of the complex was determined by Prof. S. Bourne (University of Cape Town, Department of Chemistry) and refined by Dr. M.W. Esterhuysen (University of Stellenbosch, Department of Chemistry).

A suitable crystal was mounted on a thin glass fibre and coated in silicone-based oil to prevent decomposition. Data were collected on a Nonius Kappa CCD diffractometer using graphite monochromated Mo Kα radiation (λ=0.7107 Å) with a detector to crystal distance of 45 mm. 663 oscillation frames were recorded, each of width 1° in diameter, followed by 422 frames of 1° width in ω (with $\kappa \neq 0$). Crystals were indexed from the first ten frames using the DENZO package [74] and positional data were refined along with diffractometer constants to give the final cell parameters. Integration and scaling (DENZO, Scalepack [74]) resulted in unique data sets corrected for Lorentz-polarisation effects and for the effects of crystal decay and absorption by a combination of averaging of equivalent reflections and an overall volume and scaling correction. Crystallographic data are recorded in **Table 5.1**. The structure was solved using SHELXS-97 [75] and developed *via* alternating least squares cycles and Fourier difference synthesis (SHELXL-97 [75]) with the aid of the interface program X-SEED [76]. There are two crystallographically independent molecules in the asymmetric unit, giving rise to Z = 8 in $P2_1/n$. All non-hydrogen atoms were modeled anisotropically, except for the carbon atoms in the butyl chains. Since the carbon atoms in the butyl chains have very high thermal motion, they were modeled with isotropic displacement parameters. Hydrogen atoms on the phenyl rings were assigned an isotropic thermal parameter of 1.2 times that of their parent atom and refined using a riding model. No hydrogens were placed on the butyl chains. The different views and sections of the crystal structure are shown in **Fig 5.1- 5.3** and the crystal packing diagrams are shown in **Fig 5.4**.

Table 5.1: The crystallographic data and structure refinement for tetra[(*N*,*N*-di-n-butyl-*N'*-benzoylthiourea) silver(I)] complex.

Empirical formula	$C_{64}H_{92}Ag_4N_8O_4S_4$
Formula weight	1597.216
T/K	193(2)
λ/Å	0.71073
Crystal system and space group	Monoclinic, P2(1)/n
Unit cell dimensions	a = 17.805(4) Å α = 90 deg.
	b = 21.759(4) Å β = 96.34(3) deg.
	c = 36.438(7) Å γ = 90 deg.
V/ $Å^3$	14030 (5)
Z, Calculated density	8, 1.516 g/cm^3
Absorption coefficient.(μ/mm^{-1})	1.269
F(000)	6560
Crystal size	0.12 x 0.20 x 0.25 mm
θ range for data collection	2.85 to 25.00 deg.
Limiting indices	-21<=h<=21, -25<=k<=25, -43<=l<=43
Completeness to θ= 27.87	94.2 %
Max. and min. transmission	0.8626 and 0.7421
Refinement method	Full-matrix least-squares on F^2
Data / restraints / parameters	23275 / 0 / 1334
Goodness-of-fit on F^2	1.030
Reflections collected / unique	41998 / 23275 [R(int) = 0.0265]
Final R indices [I>2σI]	0.0537, 0.0918
R indices (all data)	R1 = 0.1441, wR2 = 0.1692
Largest diff. peak and hole	0.709 and -0.537 e.A^{-3}

5.2 The crystal structure for Tetra[(*N,N*-di-n-butyl-*N'*-benzoylthiourea) silver(I)] complex

The crystal structure of tetra[(*N,N*-di-n-butyl-*N'*-benzoylthiourea)silver(I)] complex is shown in **Fig. 5.1**. Selected bond lengths, bond angles and torsion angles are listed in **Tables 5.2 - 5.4**. The structural analysis for this compound shows an empirical formula of $[AgL]_4$ (L= *N,N*-di-n-butyl-*N'*-benzothiourea). Ag(I) forms a chelate complex with this ligand. The nearly squarely orientated silver atoms in this molecule are alternately bonded to each other with sulfur bridges forming an eight-membered ring of alternating silver and sulfur atoms. The bridging sulfur atoms lie above and below the plane through the silver atoms in this configuration. The Ag-Ag separations lie between 2.9687(9) and 3.0949(9) Å and are thus not significantly longer than in metallic silver (2.889 Å). Since the Ag atoms are close to one another, Ag-Ag contacts are observed. However, these are just contacts and not real bonds. Each Ag-atom is co-ordinated to two *S* - and one *O* - atom and thus has a coordination number of 3. The co-ordination geometry around the silver atom is distorted trigonal as can be seen from the bond angles around each silver atom (see **Table 5.3**). The Ag atoms are not in the same plane with the coordinated *O* and *S* atoms of the ligands. Ag1 lies 0.0288 Å from the plane defined by S1S4O41, Ag2 lies 0.0667 Å from the plane defined by S1S2O11, Ag3 lies 0.0462 Å from the plane defined by S2S3O21 and Ag4 lies 0.0033 Å from the plane defined by S3S4O31.

The ligands are co-ordinated as bidentate monoanions. The conformation of the molecule with respect to the thio-carbonyl and carbonyl moieties is definitely twisted as reflected by the torsion angles (see **Table 5.4**). The S-Ag-S angles are between 138.27(6) and 148.63 (6)°. The usual Ag-S separations for thiourea Ag(I) complexes are in the range of 2.45 – 2.54 Å [77]. In our case, they vary within the ligand chelate rings from 2.457(2) to 2.510(2) Å and are significantly longer than those that do not form part of the ligand chelates [2.399(2) to 2.4304(9) Å]. The Ag-O separations in the chelate rings vary from 2.312(4) to 2.359(4) Å.

Within the chelate rings, there is only partial delocalization of the bond order. Even though all the C-S, C-O and C-N separations lie between the values for single and double bond order, the C-S separations are longer [1.752(6) to 1.783(7) Å)] compared to those found in other thioureas [78-80] and thioamides [81,82]. The C-N distances do not show the usually observed equality and are all shorter than the average single C-N bond length of 1.472(5) Å [36]. They are significantly longer on the acyl side [1.330(9) to 1.392(19) Å] than on the thiourea side [1.296(10) to 1.330 (9) Å]. The C-O bond lengths [1.226(7) to 1.249(8) Å)] suggest co-ordination of the oxygen atom.

The C-N bonds between the chelate ring and the amino group [1.330(9) to 1.392(9) Å] show, like in all *N*,*N*-dialkyl-*N'*-acylthioureas and their complexes, partial double bond character in the C-N(C_4H_9)$_2$ group. The phenyl groups are rotated by 9.29(0.87), 8.98(0.64), 3.69(0.47) and 6.04(0.60) with respect to the planes defined by C12N11O11, C22N21O21, C32N31O31 and C42N41O41 respectively.

The presence of the disorder makes it difficult to predict intermolecular interactions within the sum of the van der Waals radii of the atoms involved in this crystal structure. However, for the positions of the atoms that were well determined, no van der Waals interactions were reported. The determined bond lengths show that the bonding situation of the ligands in the current Ag-complex shows a widespread bond delocalization in the chelate ring.

The bonding mode for the tetra[(*N*,*N*-di-n-butyl-*N'*-benzoylthiourea) Ag(I)] complex is very similar to the one reported earlier for Ag(I) complex with HL^2 (HL^2 = *N*,*N*-diethyl-*N'*-benzoylthiourea) [73] but different from the other reported Ag(I) complex with *N*,*N*-diethyl-*N'*-benzoylthiourea, [Ag(HL)$_3$SH] [83]. In the latter case, the ligands act as neutral monodentate sulfur ligands and form a distorted tetrahedral Ag(I) complex in which the bond lengths in the ligands remain largely unchanged upon co-ordination. The fourth co-ordination site is occupied by a hydrogen sulfide ion that is formed from the ligand during complex formation. Similar monodentate sulfur ligand co-ordination to silver through the sulfur atom had also been reported previously [84]. A comparison of the important bond lengths for the molecular structure of tetra[(*N*,*N*-di-n-butyl-*N'*-benzoylthiourea) Ag(I)] complex with the previously published Ag(I) complexes with *N*,*N*-diethyl-*N'*-benzoylthiourea is presented in **Table 5.5**.

Table 5.2: Selected bond lengths [Å] for tetra[(*N*,*N*-di-n-butyl-*N'*-benzoylthiourea) Ag(I)] complex.

Bond	Length	Bond	Length
Ag1-Ag2	3.0510(9)	Ag5-Ag6	3.0806(9)
Ag1-Ag4	2.9687(9)	Ag5-Ag8	3.0398(10)
Ag1-S4	2.4616(17)	Ag5-S5	2.4266(17)
Ag1-S1	2.4064(16)	Ag5-S8	2.4819(19)
Ag1-O41	2.359(4)	Ag5-O81	2.342(5)
C41-N41	1.313(8)	C81-N82	1.330(9)
C41-N42	1.343(7)	C81-N81	1.324(9)
C41-S4	1.774(6)	C81-S8	1.776(8)
C42-O41	1.242(7)	C82-O81	1.231(8)
C42-N41	1.341(8)	C82-N81	1.343(9)
Ag2-Ag3	3.0161(10)	Ag6-Ag7	2.9752(10)
Ag2-S2	2.399(2)	Ag6-S6	2.4304(19)
Ag2-S1	2.457(2)	Ag6-S5	2.4944(19)
Ag2-O11	2.316(5)	Ag6-O51	2.332(4)
C11-N11	1.315(8)	C51-N51	1.303(8)
C11-N12	1.352(8)	C51-N52	1.351(8)
C11-S1	1.783(7)	C51-S5	1.768(7)
C12-O11	1.249(8)	C52-O51	1.239(7)
C12-N11	1.338(8)	C52-N51	1.342(8)
Ag3-Ag4	3.0949(9)	Ag7-Ag8	3.0413(9)
Ag3-S3	2.4190(18)	Ag7-S7	2.4034(17)
Ag3-S2	2.482(2)	Ag7-S6	2.4562(18)
Ag3-O21	2.354(4)	Ag7-O61	2.345(4)
C21-N21	1.296(10)	C61-N61	1.306(8)
C21-N22	1.392(19)	C61-N62	1.347(8)
C21-S2	1.779(9)	C61-S6	1.775(7)
C22-O21	1.249(8)	C62-O61	1.248(7)
C22-N21	1.337(9)	C62-N61	1.313(8)
Ag4-S4	2.4230(19)	Ag8-S8	2.402(2)
Ag4-S3	2.510(2)	Ag8-S7	2.4581(19)
Ag4-O31	2.312(4)	Ag8-O71	2.324(4)
C31-N31	1.323(8)	C71-N71	1.306(8)
C31-N32	1.335(8)	C71-N72	1.350(8)
C31-S3	1.752(6)	C71-S7	1.777(7)
C32-O31	1.239(8)	C72-O71	1.226(7)
C32-N31	1.336(8)	C72-N71	1.360(8)

Table 5.3: Selected bond angles [deg] for tetra[(*N*,*N*-di-n-butyl-*N'*-benzoylthiourea) Ag(I)] complex.

Bond	Angle	Bond	Angle
Ag1 Ag4 Ag3	79.40(3)	Ag5 Ag8 Ag7	80.36(3)
Ag2 Ag3 Ag4	78.67(3)	Ag6 Ag7 Ag8	79.36(2)
Ag3 Ag2 Ag1	79.37(3)	Ag7 Ag6 Ag5	80.75(3)
Ag4 Ag1 Ag2	80.10(2)	Ag8 Ag5 Ag6	77.76(2)
S1 Ag1 S4	148.63(6)	S5 Ag5 S8	146.26(6)
S2 Ag2 S1	143.37(7)	S6 Ag6 S5	141.56(6)
S3 Ag3 S2	148.03(6)	S7 Ag7 S6	146.31(6)
S4 Ag4 S3	138.27(6)	S8 Ag8 S7	145.16(7)
O11 Ag2 S2	122.94(13)	O51 Ag6 S6	129.75(12)
O11 Ag2 S1	92.26(13)	O51 Ag6 S5	88.56(12)
O21 Ag3 S3	123.86(13)	O61 Ag7 S7	123.90(12)
O21 Ag3 S2	87.39(13)	O61 Ag7 S6	89.33(12)
O31 Ag4 S4	133.11(13)	O71 Ag8 S8	121.95(12)
O31 Ag4 S3	88.61(13)	O71 Ag8 S7	91.49(12)
O41 Ag1 S1	123.24(11)	O81 Ag5 S5	124.67(12)
O41 Ag1 S4	87.85(11)	O81 Ag5 S8	88.70(12)
Ag1 S1 Ag2	77.70(5)	Ag5 S5 Ag6	77.50(5)
Ag2 S2 Ag3	76.30(6)	Ag6 S6 Ag7	75.01(5)
Ag3 S3 Ag4	77.76(6)	Ag7 S7 Ag8	77.44(5)
Ag4 S4 Ag1	74.85(5)	Ag8 S8 Ag5	76.97(5)
C11 S1 Ag1	105.1(2)	C51 S5 Ag5	105.2(2)
C11 S1 Ag2	98.5(2)	C51 S5 Ag6	96.8(2)
C21 S2 Ag2	100.9(3)	C61 S6 Ag6	102.4(2)
C21 S2 Ag3	103.2(3)	C61 S6 Ag7	99.8(2)
C31 S3 Ag3	104.2(2)	C71 S7 Ag7	104.7(2)
C31 S3 Ag4	94.5(2)	C71 S7 Ag8	99.1(2)
C41 S4 Ag4	103.9(2)	C81 S8 Ag8	103.1(3)
C41 S4 Ag1	102.0(2)	C81 S8 Ag5	101.0(3)
C12 O11 Ag2	117.3(4)	C52 O51 Ag6	124.0(4)
C22 O21 Ag3	121.6(4)	C62 O61 Ag7	121.2(4)
C32 O31 Ag4	124.6(4)	C72 O71 Ag8	119.1(4)
C42 O41 Ag1	124.4(4)	C82 O81 Ag5	121.5(4)
C11 N11 C12	129.6(6)	C51 N51 C52	128.5(6)
C21 N21 C22	126.6(7)	C61 N61 C62	128.3(5)
C31 N31 C32	128.0(6)	C71 N71 C72	129.1(6)
C41 N41 C42	128.1(5)	C81 N81 C82	128.0(6)
N11 C11 S1	125.0(5)	N51 C51 S5	125.7(5)
N21 C21 S2	128.6(6)	N61 C61 S6	126.5(5)

N31 C31 S3	124.5(5)	N71 C71 S7	126.2(5)
N41 C41 S4	127.1(5)	N81 C81 S8	124.4(6)
N12 C11 S1	116.0(5)	N52 C51 S5	116.9(5)
N22 C21 S2	114.3(9)	N62 C61 S6	116.7(6)
N32 C31 S3	117.4(5)	N72 C71 S7	116.9(5)
N42 C41 S4	116.3(5)	N82 C81 S8	116.5(7)
N11 C11 N12	118.6(6)	N51 C51 N52	117.0(6)
N21 C21 N22	113.5(10)	N61 C61 N62	116.6(6)
N31 C31 N32	117.9(6)	N71 C71 N72	116.8(6)
N41 C41 N42	116.3(5)	N82 C81 N81	118.8(7)
O11 C12 N11	125.5(6)	O51 C52 N51	126.9(6)
O21 C22 N21	126.3(7)	O61 C62 N61	125.9(6)
O31 C32 N31	125.3(6)	O71 C72 N71	125.5(6)
O41 C42 N41	127.3(6)	O81 C82 N81	125.6(7)
O11 C12 C13	119.4(6)	O51 C52 C53	118.7(6)
O21 C22 C23	118.0(7)	O61 C62 C63	118.5(6)
O31 C32 C33	118.9(6)	O71 C72 C73	120.4(6)
O41 C42 C43	117.0(6)	O81 C82 C83	118.8(7)
N11 C12 C13	115.0(6)	N51 C52 C53	114.1(6)
N21 C22 C23	115.6(7)	N61 C62 C63	115.4(6)
N31 C32 C33	115.7(6)	N71 C72 C73	113.8(6)
N41 C42 C43	115.4(5)	N81 C82 C83	115.5(7)

Table 5.4: Selected torsion angles [deg] for tetra[(*N*,*N*-di-n-butyl-*N'*-benzoylthiourea) Ag(I)] complex.

Bond	Angle	Bond	Angle
O11 C12 N11 C11	-26.3(10)	O51 C52 N51 C51	20.9(11)
S1 C11 N11 C12	-41.2(9)	S5 C51 N51 C52	40.5(10)
O21 C22 N21 C21	26.9(14)	O61 C62 N61 C61	-23.7(11)
S2 C21 N21 C22	34.0(15)	S6 C61 N61 C62	-40.5(10)
O31 C32 N31 C31	-19.1(11)	O71 C72 N71 C71	25.4(10)
S3 C31 N31 C32	-46.8(10)	S7 C71 N71 C72	39.9(10)
O41 C42 N41 C41	22.8(10)	O81 C82 N81 C81	-19.9(12)
S4 C41 N41 C42	34.0(9)	S8 C81 N81 C82	-44.5(11)

Table 5.5: Comparison of the relevant bond lengths [Å] in Ag(I)-*N*,*N*-dialkyl-*N'*-benzoylthiourea complexes. {AgL}$_4$ represents for the tetra[(*N*,*N*-di-n-butl-*N'*-benzoyl thiourea) Ag(I)]complex.

Complex	C_s-S	C_o-N	C_s-N	C_o-O	Reference
AgL$_4$ (L=*N*,*N*-diethyl-*N'*-benzoyl thiourea)	1.776	1.302	1.341	1.247	[73]
AgL$_3$.SH(L=*N*,*N*-diethyl-*N'*-benzoylthiourea)	1.681	1.381	1.417	1.218	[83]
{AgL}$_4$ (L=*N*,*N*-di-n-butyl-*N'*-benzoylthiourea)	1.768	1.313	1.361	1.238	this work

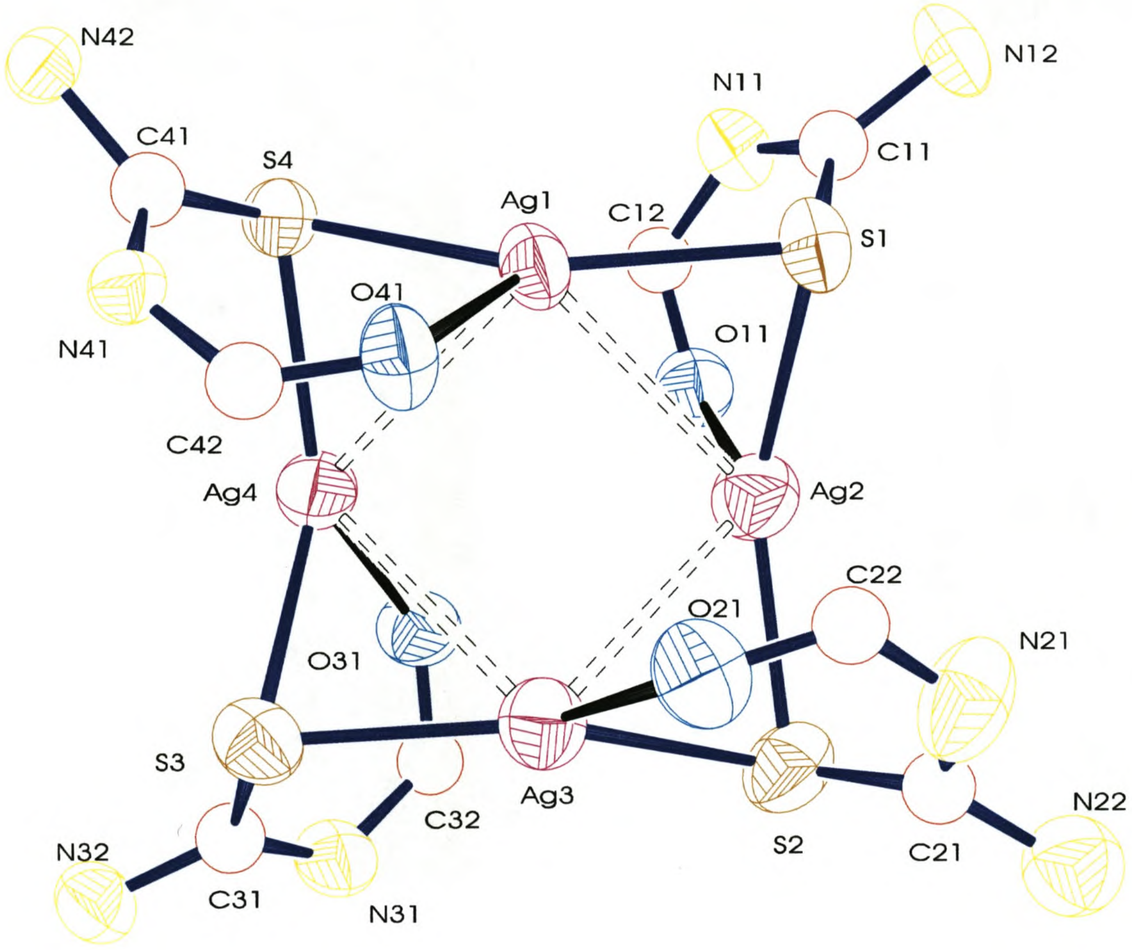

Fig 5.1: The partial molecular structure and numbering scheme of Ag-HL^1 complex. The phenyl and butyl groups are omitted.

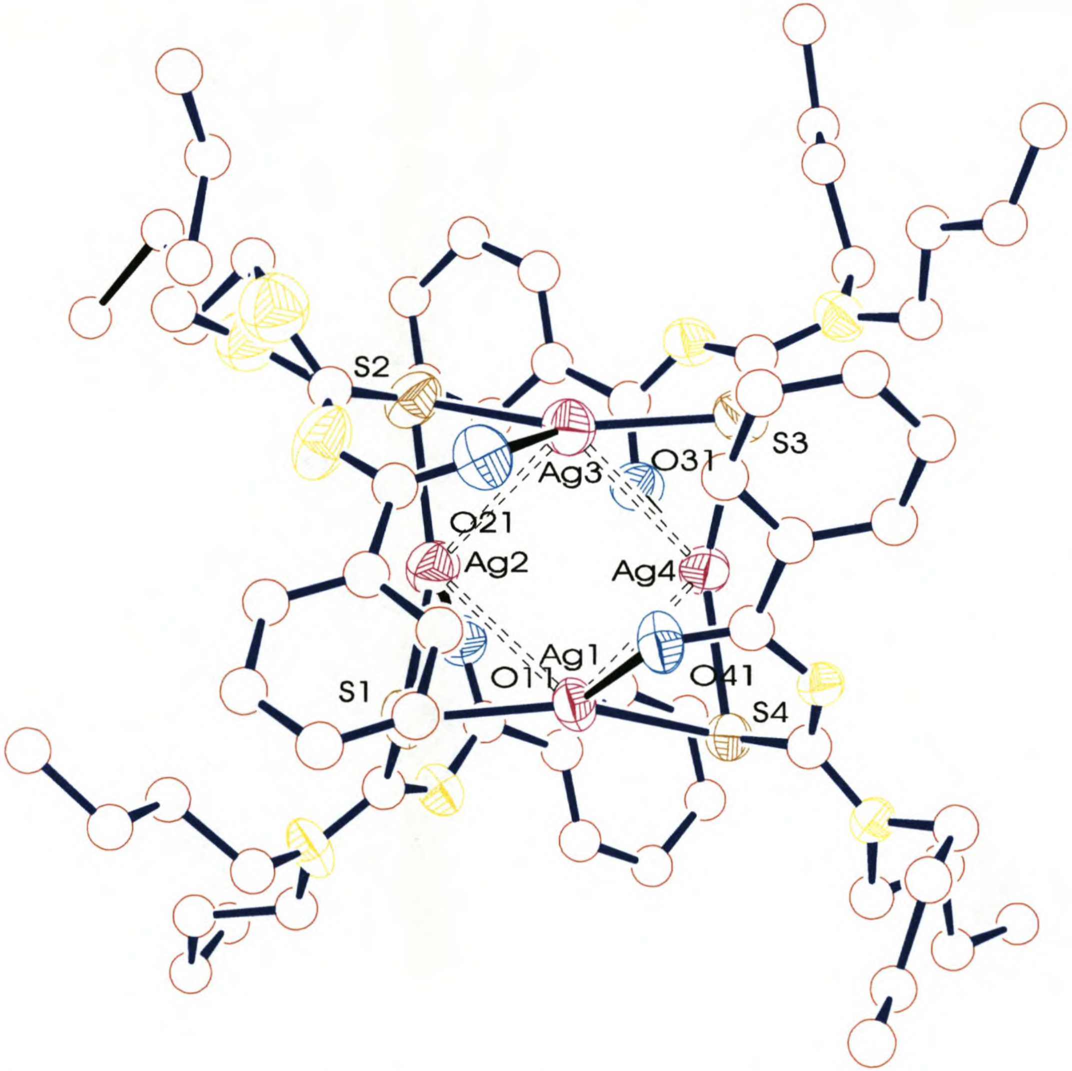

***Fig 5.2**: The molecular structure of Ag-HL^1 complex showing one of the two molecules in the asymmetric unit.*

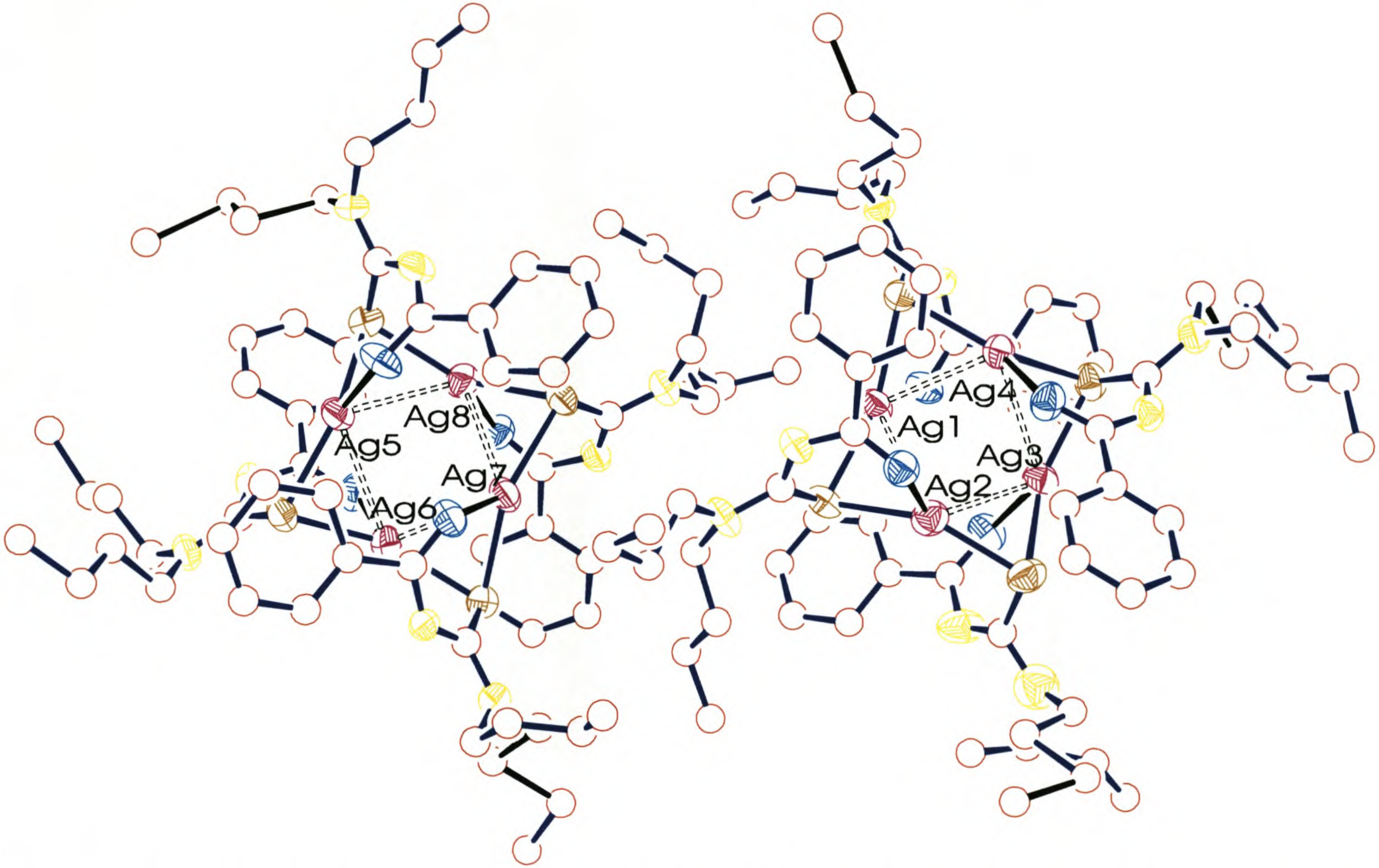

***Fig 5.3**: The molecular structure of Ag-HL^1 complex showing the two crystallographically independent molecules in the asymmetric unit.*

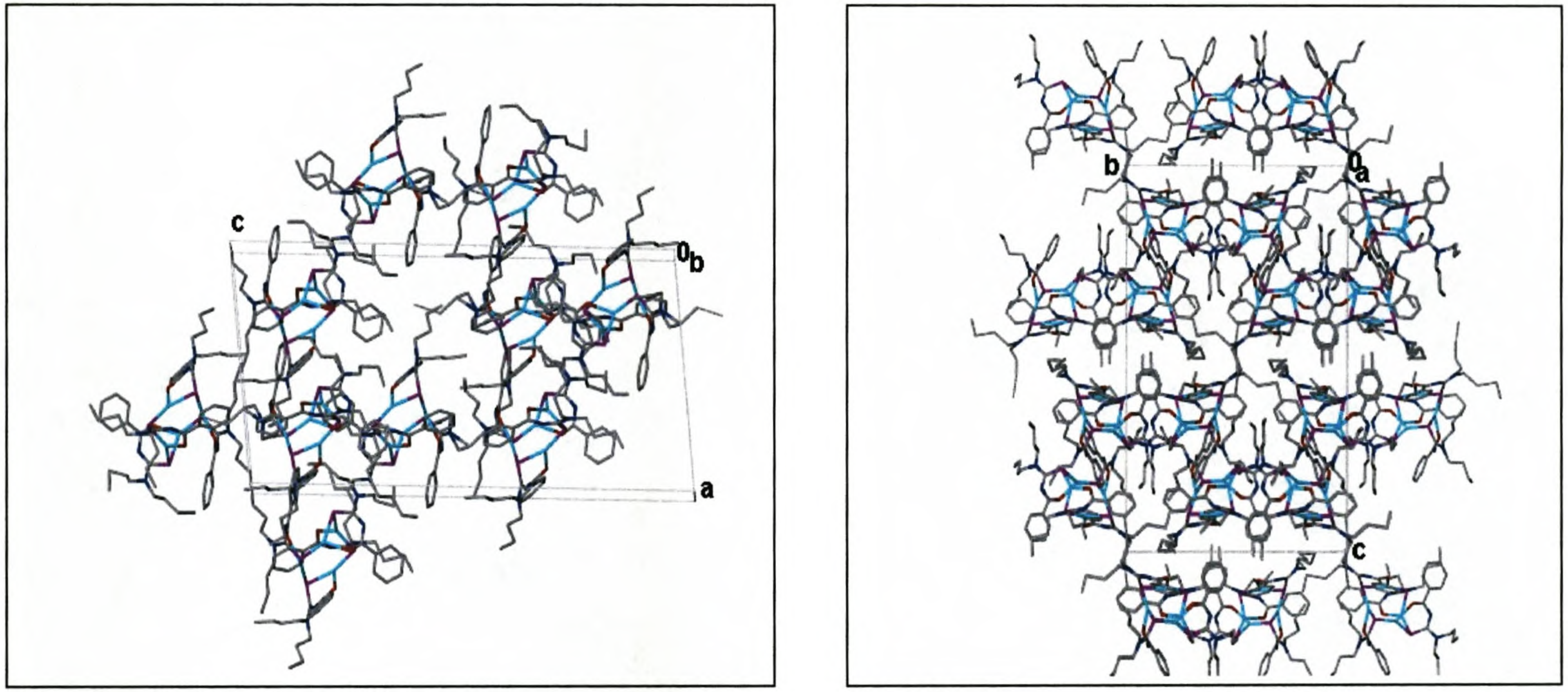

Fig 5.4*: Crystal packing diagrams of the molecules within the cell.*

Chapter 6

6 Conclusion

A number of *N*,*N*-dialkyl-*N'*-(HL) and *N*-alkyl-*N'*-aroylthiourea (H_2L) ligands were studied for potential application as specific carriers (ionophores) for the transport of Ag(I) through a bulk liquid membrane set up. In addition to these ligands, the *N*,*N*-diethyl-*N'*-camphanoyl thiourea (HL^{13}) and the 3,3,3',3'-tetraethyl-1,1'-isophthaloylbisthiourea (H_2L^{12}) ligands were also investigated.

Ligands of the type *N*-alkyl-*N'*- (H_2L) and *N*,*N*-dialkyl-*N'*-acyl(aroyl)thioureas (HL) are prepared in high yield from readily available and inexpensive starting materials. These ligands were previously synthesized and their co-ordination chemistry with Pt(II) and Pd(II) was extensively studied. However, in this study we were particularly interested in investigating the potential use of these group of thioureas for the selective transport as well as extraction of Ag(I) from a mixture of the metal ions: Co(II), Ni(II), Cu(II), Zn(II), Cd(II) and Pb(II).

The *N*,*N*-diethyl-*N'*-camphanoylthiourea (HL^{13}) was the most efficient ligand for Ag(I) transport. About 81% Ag(I) was transported using this ligand. However, although we expected that the 3,3,3',3'-tetraethyl-1,1'-isophthaloylbisthiourea (H_2L^{12}) would also be an efficient ligand for Ag(I) transport by complexing bidentately to two silver ions through its two *S* and two *O* atoms, it was actually found that the percentage of Ag(I) transported by this ligand is very low (only 14%) compared to the Ag(I) transported by a similar ligand HL^2 (26%). We believe that electronic repulsions between the two silver atoms after complexation with H_2L^{12} may be responsible for the low Ag(I) transport by H_2L^{12} compared to HL^2.

Under the experimental conditions employed, the dialkyl substituted benzoylthioureas, with the exception of HL^3 and HL^9, were found to be efficient and selective in transporting Ag(I). The highest transport percentages were obtained by ligands HL^1, HL^5 and HL^{13} in which 42%, 47% and 81% of Ag(I) were transported by the ligands respectively. However, small percentages of Cu(II) were also co-transported by these ligands. The high degree of transport selectivity for Ag(I) by these ligands has significant implications. Incorporation of these ligands into liquid membranes may be used to remove Ag(I) from a mixture of the seven metal ions. In a broader sense, these transport experiments demonstrate the potential application of these ligands for the selective removal, concentration and purification of Ag(I) from contaminated samples.

HL^3 was selective for Cu (II), while HL^9 was not good at either transporting or extracting Ag(I) to a significant amount. The transport efficiency and selectivity of HL ligands for the softer Ag(I) compared to the other borderline metal ions is in accordance with Pearson's hard soft acid base principle [68,69]. The soft donor atom, *S*, coordinates well to soft metal ions. However, the selectivity of HL^3 for Cu(II) compared to Ag(I) may be due to the presence of the - OH groups attached to the alkyl end of the ligand. The transport results showed that HL^3 carries both Ag(I) and Cu(II) ions into the membrane phase, however only Cu(II) was stripped into the receiving phase. These results would probably mean that HL^3 has a moderately high formation constant with Cu(II), while its formation constant with Ag(I) may be too high to allow the release of Ag(I) from the membrane phase into the receiving phase.

Parallel to the transport studies, competitive metal ion extraction experiments were also performed under similar conditions. The results show that the *N*-alkyl-*N'*-benzoylthioureas, *N*,*N*-dialkyl-*N'*-(acyl)aroylthioureas (with the exception of HL^9) and *N*,*N*-diethyl-*N'*-camphanoylthiourea are very efficient in selectively extracting Ag(I) from a mixture of the seven metal ions. The percentages of Ag(I) extracted by these ligands varied with the ligand concentrations. The mono-alkyl substituted aroylthioureas (H_2L^1 – H_2L^3) were not good at transporting Ag(I) or any of the other six metal ions. However, these ligands showed a profound selectivity and efficiency for the extraction of Ag(I). A possible reason for this could be *N*-alkyl-*N'*-benzoylthioureas possess a very high formation constant with Ag(I) and this makes transport of Ag(I) difficult as the stripping of Ag(I) from the membrane phase into the receiving phase is inhibited.

The transport and extraction results show that a slight variation in the structure of the ligand brings about a significant change in the transport behavior. The reason for this is different ligand structures have different formation constants (log *K* values) with metal ions. A higher formation constant results in a stronger complexation of a carrier with a metal ion and this in turn would imply enhanced uptake of the metal ion from the source phase into the membrane phase. However, it is required that the formation constant (log K) for a cation-ligand interaction should not be too high as this would inhibit the recovery of the metal ion from the membrane phase into the receiving phase and not too low as this would inhibit the uptake of the metal ion into the chloroform phase. Therefore, it is important to note that log *K* for the cation-ligand interaction is a very crucial parameter for determining cation transport efficiency and selectivity. The effective transport behavior of a ligand is controlled by a subtle balance between metal uptake and metal loss into and out of the respective membrane phase.

Metal ion concentration measurements in the transport and extraction experiments were carried out by Atomic Absorption Spectroscopy (AAS) and the results were later confirmed by Inductively Coupled Plasma-Optical Emission Spectroscopy (ICP-OES). The crystal structure of Ag(I) complex with *N*,*N*-di-n-butyl-*N'*-benzoylthiourea ligand, HL^1, was determined. The structure shows that there are four silver ions bonded to four molecules of the ligand.

Attempts could be made in the future to get crystals of other metal ligand complexes to shed more light on their solid state co-ordination geometry and stoichiometry. Furthermore, the *N,N*-diethyl-*N'*-camphanoylthiourea ligand could be comprehensively studied with Ag(I), where an *S* -curve could be determined and an attempt be made at determining its protonation and formation constants. Finally, the design of more chiral ligands similar to the *N*,*N*-diethyl-*N'*-camphanoylthiourea (HL^{13}) ligand which could produce "better" transport results for Ag(I) would also be an interesting route for further study.

7 References

1. Mishara, D. and Sharma, U., *Sep. and Purif. Technol.*, 2002, **27**, 51.
2. Alizadeh, N., Salimi, S. and Jabbari, A., *Sep. and Purif. Technol.*, 2002, **28**, 174.
3. Chia, P. S. K., Lindoy, L. F., Walker, G. W. and Everett, G. W., *Pure Appl. Chem.,* 1993, **65**, 521.
4. Danesi, P. R., *Sep. Sci. Technol.,* 1984, **19**, 857.
5. Izatt, R. M., Clark, J. K. and Christensen, J. J., *J. Membr. Sci.*, 1985, **24**, 1.
6. Cox, J. A., Bhatnagar, A. and Francis, W. R., *Talanta,* 1990, **37**, 1037.
7. Shamsipur, M., Azimi, G., Mashhadizadeh, M. H. and Madaeni, S. S., *Analytical Sciences*, 2001, **17**, 491-494.
8. Shamsipur, M., Azimi, G. and Madaeni, S. S., *J. Membr. Sci.*, 2000, **165**, 217.
9. Alexander, P. R. and Callahan, R. W., *J. Membr. Sci.*, 1987, **35**, 67.
10. Shamsipur, M., Kazemi, S. Y., Azimi, G., Madaeni, S. S., Lippolis, V., Garau, A. and Isaia, F., *J. Membr. Sci.*, 2003, **5550**, 1-7.
11. Gherrou, A., Kerdjoudj, H., Molinari, R. and Drioli, E., *Sep. and Purif. Technol.*, 2002, **28**, 235-244.
12. Bradshaw, J. S., Maas, J. D., Izatt, R. M. and Christensen, J. J., *J. Am. Chem. Soc.*, 1980, **102**, 467.
13. Lamb, J. D., Izatt, R. M., Robertson, P. A. and Christensen, J. J., *J. Am. Chem. Soc.,*1980, **102**, 2452.
14. Izatt, R. M., Dearden, D. V., Brown, P. R., Bradshaw, J. S., Lamb, J. D. and Christenson, J. J., *J. Am. Chem. Soc.,* 1983, **105**, 1785.
15. Tsubeke, H., *Tetrahedron lett.*, 1982, **23**, 2109.
16. Wakita, R., Matsumoto, M., Nakatsuji, Y. and Okahara, M., *J. Membr. Sci.,* 1991, **57**, 297.
17. Ameerunisha, S. and Zacharias, P. S., *J. Chem. Soc., Perkin Trans. 2*, 1995, 1679.

18. Lee, S. S., Yoon, I. I., Park, K., Jung, J. H., Lindoy, L. F., Nezhadali, A. and Rounaghi, G., *J. Chem. Soc., Dalton Trans.*, 2002, 2180-2182.
19. Shamsipur, M. and Mashhadizadeh, M. H., *Sep. and Purif. Technol.*, 2000, **20**, 147.
20. Lindoy, L. F., *The Chemistry of Macrocyclic Ligand Complexes*, Cambridge University Press, 1989, 9.
21. Chartres, Jy. D., Groth, A. M., Lindoy, L. F. and Meehan, G. M., *J. Chem. Soc., Dalton Trans.,* 2002, 371-375.
22. Lindoy, L. F., *Pure Appl. Chem.*, 1997, **69**, 2179.
23. Kim, J., Leong, A. J., Lindoy, L. F., Kim, J., Nachbaur, J., Nezhadali, A., Rounaghi, G. and Wei, G., *J. Chem. Soc., Dalton Trans.*, 2000, 3453.
24. Dadfarnia, S. and Shamsipur, M., *J. Membr. Sci.*, 1992, **75**, 61.
25. Akhond, M. and Shamsipur, M., *Sep. Sci. Technol.*, 1995, **30**, 3061.
26. Akhond, M. and Shamsipur, M., *J. Membr. Sci.*, 1996, **117**, 221.
27. Safavi, A. and Shams, E., *J. Membr. Sci.*, 1998, **144**, 37.
28. Saito, K., Murakami, S. and Muromatsu, A., *Polyhedron*, 1993, **12**, 1587.
29. Sakamoto, H., Ishikawa, J., Mizuno, T., Doi, K. and Otomo, M., *Chem. Lett.,* 1993, 609.
30. Lachowicz, E., Rozanska, B., Teixidor, F., Meliani, H., Barboiu, M. and Hovnanian, N., *J. Membr. Sci.*, 2002, **210**, 279-290.
31. Cho, M. H., Lee, S. C., yang, S. C., Shin, S. S. and Kim, K., *Bull. Korean Chem. Soc.,* 1996, **17**, no 12, 1109-1111.
32. Aamrani, F. Z., Kumar, A., Beyer, L., Florido, A. and Sastre, A. M., *J. Membr. Sci.,* 1999, **152**, 263-275.
33. Muhammed, G. Z., *Sep. Sci. Technol.,* 1990, **25**, 1785.
34. Dominguez, M., Antico, E., Beyer, L., Aguirre, A., Granda, S. and Salvado, V., *Polyhedron*, 2002, **21**, 1429-1437.

35. Koch, K. R., Grimmbacher, T. and Sacht, C., *Polyhedron*, 1998, **17**, 267-274.

36. Koch, K. R., Sacht, C., Grimmbacher, T. and Bourne, S., *S. Afr. J. Chem.*, 1995, **48**, 71-77.

37. Koch, K. R., Sacht, C. and Bourne, S., *Inorg. Chem. Acta*, 1995, **232**, 109-115.

38. Koch, K. R. and Matoetoe, M. C., *Magnetic resonance in Chem.*, 1991, **29**, 1158-1160.

39. Douglass, I. B. and Dain, F. B., *J. Am. Chem. Soc.*, 1934, **56**, 719.

40. Koch, K. R., *Coord. Chem. Rev.*, 2001, 473-477.

41. Schuster, M., *Fresenius J. Anal. Chem.*, 1992, **342**, 791.

42. Koch, K., R. and Bourne, S., *Journal of Molec. Structure,* 1998, **441**, 11.

43. Koch, K. R., Wang, Y. and Coetzee, A., *J. Chem. Soc., Dalton Trans.*, 1999, 1013-1014.

44. Dago, A., Shepelev, Yu., Fajardo, F., Alvarez, F. and Pomes, R., *Acta Crystallogr. Sect. C.*, 1989, **45**, 1192.

45. Miller, J., PhD thesis, University of Cape Town, 2000, 102-103.

46. Bourne, S. and Koch, K. R., *J. Chem. Soc., Dalton Trans.*, 1993, 2071.

47. Koch, K. R., Bourne, S. S., Coetzee, A. and Miller, J., *J. Chem. Soc., Dalton Trans.,* 1999, 3156-3160.

48. Schroder, U., Beyer, L. and Sieler, J., *Inorg. Chem. Commun.*, 2000, **3**, 630-632.

49. Unterreitmaier, E. and Schster, M., *Anal. Chim. Acta*, 1995, **309**, 339.

50. Vest, P. and Konig, M., *Fresenius Z. Anal. Chem.*, 1989, **339**, 142.

51. Campo, R. D., Criado, J. J., Garcia, E., Hermosa, M. R., Sanchez, A. J., Manzano, J. L., Monte, E., Fernandez, E. R. and Sanz, F., *J. Inorg. Biochem.,* 2002, **89**, 74.

52. Koch, K. R., *J. Chem. Soc., Dalton Trans.,* 1991, 1.

53. Muller, H. and Rother, R., *Anal. Chim. Acta*, 1973, **66**, 49.

54. Cantle, J. E., *Atomic absorption spectrometry*, 1982, Elsevier Science Publishing Company, Netherlands, 1.

55. Christian, G. D., *Atomic absorption spectroscopy: Applications in agriculture, biology and medicine*, 1970, John Wiley and sons, USA, 114.

56. Skoog, D. A., West, D. M. and Holler, F. J., *Fundamentals of analytical chemistry*, 1992, Saunders College Publishing, USA, 625-626.

57. Christian, G. D., *Analytical chemistry*, 1994, John Wiley and sons, USA, 466-474.

58. Tyler, G., ICP-ES instrument at work, 1991, **3**, 1-4.

59. Merensky Institute of Physics, *Handbook of ICP-ES*, University of Stellenbosch, 2000.

60. Mtongana, S., MSc dissertation, University of Stellenbosch, 2002, 28.

61. Konig, K.H, Schuster, M., Steinberech, B., Schneeweis, G. and Schlodder, R., *Fresenius Z. Anal. Chem*., 1985, **321**, 457.

62. Beyer, L., Hoyer, E., Hennig, H., Kirmse, R., Hartmann, H. and Liebscher, J., *J. Prakt. Chem*., 1975, **317**, 829.

63. Miller, J., PhD thesis, University of Cape Town, 2000.

64. Berhe, H., MSc thesis, University of Stellenbosch, 2003.

65. Perkin, D. D. and Dempsey, B., *Buffers for pH and Metal Ion Control*, Chapman and Hall, 1974, 135.

66. Varian Techtron Pty. Ltd., *Analytical methods for flame spectroscopy: Operation Manual for AA-1275 and AA-1475,* Australia, 1979, 1-65.

67. Varian Australia Pty Ltd., *ICP-ES Liberty series II specifications*, Australia, 1991, 1.

68. Pearson, R. G., *J. Am. Chem. Soc.,* 1963, **85**, 3533.

69. Wulfsberg, G., *Principles of descriptive inorganic chemistry*, 1987, Brooks/Cole Publishing Company, USA, 266-271.

70. Safavi, A. and Rastegarzadeh, S., *Talanta*, 1995, **42**, 2039.

71. Kim, J., Ahn, T. H., Lee, M., Leong, A. J., Lindoy, L. F., Rumbel, B. R., Skelton, B. W., Strixner, T., Wei, G. and White, A. H., *J. Chem. Soc., Dalton Trans.,* 2002, 3994.

72. Shin, H. S., Bannard, R. A. B., Purdon, J. G. and Cox, B. G., *Talanta*, 1984, **31**, 585.

73. Richter, R., Dietze, F., Schmidt, S. and Hoyer, E., *Z. anorg. allg. Chem.*, 1997, **623**, 138.

74. Otwinowski, Z. and Minor, W., *Methods Enzymol.*, 1996, **276**, 307.

75. Sheldrick, G. M., SHELX-97, Programme for the refinement of Crystal Structures, University of Göttingen, 1997.

76. Barbour, L. J., X-SEED (http://www.lbarbour.com/xseed/) University of Missouri-Columbia, 1999.

77. Orpen, A. G., Brammer, L., Allen, F. H., Kennard, O., Watson, D. G. and Taylor, R., *J. Chem. Soc., Dalton Trans.*, 1989, 51.

78. Kunchur, N. R. and Truter, M. R., *J. Chem. Soc.*, 1958, 2551.

79. Elcombe, M. M. and Taylor, J. C., *Acta Crystallogr.*, A 24, 1968, 410.

80. Dias, H. W. and Truter, M. R., *Acta Crystallogr.*, A17, 1964, 937.

81. Truter, M. R., *J. Chem. Soc.*, 1960, 997.

82. Walter, W., Harter, S. and Voss, J., *Acta Crystallogr.*, B 32, 1976, 2876.

83. Braun, U., Richter, R. and Sieler, J., *Z. anorg. allg. Chem.*, 1985, **529**, 201-208.

84. Banarjee, S. N. and Sukthankar, A. C., *J. Indian chem. Soc.*, 1963, **40**, 573.

8 Appendices

Table 8.1: Atomic coordinates (x 10^4) and isotropic displacement parameters (A^2 x 10^3). U(eq) is defined as one third of the orthogonalized U_{ij} tensor.

	x	y	z	U(eq)
C11	0.8929(3)	0.4062(3)	0.2190(2)	0.0513(17)
C12	0.7648(4)	0.3965(3)	0.2330(2)	0.0463(16)
C13	0.7243(4)	0.3649(3)	0.26041(19)	0.0492(16)
C14	0.7611(4)	0.3461(4)	0.2940(2)	0.075(2)
H14	0.8136	0.3539	0.2994	0.090
C15	0.7226(6)	0.3160(5)	0.3198(3)	0.105(3)
H15	0.7486	0.3028	0.3426	0.126
C16	0.6450(6)	0.3054(5)	0.3118(3)	0.102(3)
H16	0.6180	0.2844	0.3290	0.122
C17	0.6094(5)	0.3247(4)	0.2800(3)	0.078(2)
H17	0.5564	0.3184	0.2750	0.094
C18	0.6479(4)	0.3540(3)	0.2537(2)	0.0612(19)
H18	0.6212	0.3666	0.2309	0.073
C19	1.0266(4)	0.4367(3)	0.2138(2)	0.0631(19)
C21	0.7641(5)	0.4424(4)	0.0626(2)	0.083(3)
C22	0.8440(4)	0.3562(4)	0.0704(2)	0.0621(19)
C23	0.9241(4)	0.3418(3)	0.08247(19)	0.0581(18)
C24	0.9434(4)	0.2839(4)	0.0936(2)	0.066(2)
H24	0.9052	0.2535	0.0941	0.079
C25	1.0181(5)	0.2685(5)	0.1044(2)	0.087(3)
H25	1.0301	0.2276	0.1121	0.104
C26	1.0727(5)	0.3090(6)	0.1043(3)	0.095(3)
H26	1.1235	0.2974	0.1118	0.114
C27	1.0564(5)	0.3672(6)	0.0935(3)	0.104(4)
H27	1.0961	0.3963	0.0935	0.124
C28	0.9802(5)	0.3861(4)	0.0820(2)	0.087(3)
H28	0.9687	0.4270	0.0744	0.104
C31	0.5174(4)	0.2537(3)	0.10568(19)	0.0518(16)
C32	0.5391(4)	0.3509(3)	0.1354(2)	0.0497(16)
C33	0.5229(3)	0.4169(3)	0.1290(2)	0.0513(17)
C34	0.4786(4)	0.4364(3)	0.0980(2)	0.075(2)
H34	0.4573	0.4072	0.0805	0.090
C35	0.4648(6)	0.4976(5)	0.0921(3)	0.109(3)
H35	0.4340	0.5109	0.0706	0.131
C36	0.4972(6)	0.5410(4)	0.1184(3)	0.110(3)
H36	0.4870	0.5837	0.1153	0.131
C37	0.5419(5)	0.5207(4)	0.1476(3)	0.094(3)
H37	0.5650	0.5495	0.1648	0.113
C38	0.5556(4)	0.4594(3)	0.1533(2)	0.070(2)
H38	0.5881	0.4464	0.1743	0.084
C39	0.3810(4)	0.2378(4)	0.1033(2)	0.074(2)
C41	0.7718(3)	0.1349(3)	0.19761(18)	0.0432(15)
C42	0.7821(3)	0.1513(3)	0.13362(18)	0.0437(15)
C43	0.7529(3)	0.1246(3)	0.09628(17)	0.0429(15)
C44	0.7664(4)	0.1541(3)	0.06458(19)	0.0530(17)
H44	0.7942	0.1915	0.0660	0.064
C45	0.7401(4)	0.1305(3)	0.0306(2)	0.065(2)

H45	0.7494	0.1516	0.0087	0.078
C46	0.7001(4)	0.0757(4)	0.0282(2)	0.070(2)
H46	0.6830	0.0588	0.0047	0.084
C47	0.6852(4)	0.0461(3)	0.0598(2)	0.066(2)
H47	0.6564	0.0092	0.0582	0.079
C48	0.7122(3)	0.0699(3)	0.09401(19)	0.0516(16)
H48	0.7028	0.0489	0.1159	0.062
C49	0.7957(4)	0.0257(3)	0.21135(19)	0.0583(18)
C51	1.4858(3)	0.4525(3)	0.38887(17)	0.0501(16)
C52	1.4596(3)	0.3583(3)	0.35660(19)	0.0494(16)
C53	1.4784(4)	0.2911(3)	0.36160(19)	0.0539(17)
C54	1.4433(4)	0.2499(3)	0.3367(2)	0.070(2)
H54	1.4072	0.2633	0.3172	0.084
C55	1.4621(5)	0.1887(4)	0.3408(3)	0.092(3)
H55	1.4395	0.1596	0.3236	0.111
C56	1.5125(5)	0.1694(4)	0.3693(3)	0.092(3)
H56	1.5243	0.1269	0.3718	0.110
C57	1.5461(5)	0.2102(4)	0.3939(2)	0.083(2)
H57	1.5816	0.1967	0.4137	0.099
C58	1.5284(4)	0.2707(4)	0.3902(2)	0.0644(19)
H58	1.5511	0.2993	0.4077	0.077
C59	1.6225(4)	0.4633(4)	0.3948(2)	0.076(2)
C61	1.2314(3)	0.5775(3)	0.2967(2)	0.0514(17)
C62	1.2196(3)	0.5630(3)	0.35989(18)	0.0462(15)
C63	1.2553(3)	0.5844(3)	0.39621(19)	0.0508(16)
C64	1.2453(4)	0.5503(3)	0.4276(2)	0.0567(18)
H64	1.2127	0.5156	0.4257	0.068
C65	1.2827(4)	0.5670(4)	0.4614(2)	0.071(2)
H65	1.2775	0.5425	0.4826	0.086
C66	1.3273(4)	0.6186(4)	0.4646(2)	0.074(2)
H66	1.3518	0.6305	0.4880	0.089
C67	1.3363(4)	0.6529(3)	0.4339(2)	0.069(2)
H67	1.3675	0.6884	0.4360	0.083
C68	1.3006(4)	0.6361(3)	0.4004(2)	0.0569(18)
H68	1.3069	0.6605	0.3794	0.068
C71	1.0998(4)	0.3143(3)	0.27395(19)	0.0508(16)
C72	1.2289(4)	0.3206(3)	0.26036(19)	0.0448(15)
C73	1.2700(4)	0.3482(3)	0.23137(19)	0.0488(16)
C74	1.3464(4)	0.3610(3)	0.2390(2)	0.0593(18)
H74	1.3713	0.3529	0.2630	0.071
C75	1.3864(5)	0.3852(4)	0.2123(3)	0.076(2)
H75	1.4388	0.3937	0.2180	0.091
C76	1.3526(5)	0.3970(4)	0.1788(3)	0.092(3)
H76	1.3813	0.4134	0.1606	0.111
C77	1.2773(6)	0.3858(5)	0.1699(3)	0.107(3)
H77	1.2533	0.3952	0.1460	0.129
C78	1.2366(4)	0.3607(4)	0.1964(2)	0.074(2)
H78	1.1844	0.3519	0.1902	0.088
C79	1.0320(4)	0.2547(3)	0.2237(2)	0.0625(19)
C81	1.2339(5)	0.2730(3)	0.4327(2)	0.065(2)
C82	1.1534(4)	0.3616(3)	0.42401(19)	0.0618(19)
C83	1.0714(4)	0.3777(4)	0.4128(2)	0.069(2)
C84	1.0509(5)	0.4350(4)	0.4018(2)	0.079(2)
H84	1.0886	0.4656	0.4008	0.095
C85	0.9760(5)	0.4502(5)	0.3921(3)	0.098(3)
H85	0.9636	0.4919	0.3867	0.118

C86	0.9202(6)	0.4087(6)	0.3901(4)	0.121(4)
H86	0.8696	0.4196	0.3816	0.146
C87	0.9386(5)	0.3515(6)	0.4005(4)	0.132(5)
H87	0.8998	0.3214	0.3998	0.159
C88	1.0146(5)	0.3335(4)	0.4127(3)	0.102(3)
H88	1.0260	0.2925	0.4205	0.122
Ag1	0.82399(3)	0.27685(2)	0.178506(15)	0.05267(16)
Ag2	0.76579(3)	0.40072(2)	0.148161(16)	0.06385(17)
Ag3	0.68314(3)	0.31468(3)	0.092705(16)	0.06247(17)
Ag4	0.65960(3)	0.25025(2)	0.166290(15)	0.05560(16)
Ag5	1.31499(3)	0.39737(2)	0.402255(15)	0.05876(17)
Ag6	1.33868(3)	0.46154(2)	0.329054(15)	0.05543(16)
Ag7	1.17281(3)	0.44026(2)	0.316026(16)	0.05576(16)
Ag8	1.22647(3)	0.31516(2)	0.345502(15)	0.05857(16)
N11	0.8400(3)	0.3987(2)	0.24106(16)	0.0554(14)
N12	0.9560(3)	0.4376(2)	0.23173(17)	0.0614(16)
N21	0.8288(4)	0.4152(3)	0.0626(2)	0.084(2)
N31	0.5025(3)	0.3123(3)	0.11120(16)	0.0562(15)
N32	0.4592(3)	0.2149(3)	0.09992(16)	0.0601(15)
N41	0.7682(3)	0.1177(2)	0.16293(15)	0.0465(13)
N42	0.7873(3)	0.0907(2)	0.22303(14)	0.0469(13)
N51	1.4992(3)	0.3953(3)	0.38104(15)	0.0566(14)
N52	1.5464(3)	0.4888(3)	0.39833(15)	0.0575(15)
N61	1.2377(3)	0.5942(2)	0.33128(16)	0.0526(14)
N62	1.2147(3)	0.6221(3)	0.27145(15)	0.0578(15)
N71	1.1525(3)	0.3204(2)	0.25197(15)	0.0517(13)
N72	1.0369(3)	0.2835(2)	0.26053(16)	0.0548(14)
N81	1.1677(4)	0.3018(3)	0.43061(17)	0.0658(16)
N82	1.2481(4)	0.2289(3)	0.45749(18)	0.079(2)
O11	0.7282(2)	0.4213(2)	0.20576(14)	0.0580(12)
O21	0.7981(3)	0.3126(2)	0.06647(14)	0.0668(13)
O31	0.5817(3)	0.33552(19)	0.16311(14)	0.0602(12)
O41	0.8213(2)	0.19855(19)	0.13359(12)	0.0583(12)
O51	1.4148(3)	0.3742(2)	0.32982(13)	0.0614(12)
O61	1.1725(2)	0.5205(2)	0.35901(12)	0.0580(12)
O71	1.2635(2)	0.2960(2)	0.28739(13)	0.0546(11)
O81	1.2003(3)	0.4033(2)	0.42798(14)	0.0679(14)
S1	0.89344(9)	0.37112(7)	0.17482(5)	0.0551(4)
S2	0.69175(11)	0.42852(9)	0.09157(6)	0.0668(5)
S3	0.60766(9)	0.22444(8)	0.10126(5)	0.0576(5)
S4	0.74983(9)	0.20850(7)	0.21452(5)	0.0479(4)
S5	1.39599(9)	0.48449(8)	0.39317(5)	0.0543(4)
S6	1.25120(10)	0.50360(8)	0.27946(5)	0.0537(4)
S7	1.10006(9)	0.34761(8)	0.31851(5)	0.0539(4)
S8	1.30187(10)	0.28381(8)	0.40108(5)	0.0605(5)

Table 8.2: Anisotropic displacement parameters (A^2 x 10^3). The anisotropic displacement factor exponent takes the form: $-2\,pi^2\,[h^2 a^{*2}\,U11 + ... + 2\,h\,k\,a^*\,b^*\,U^{12}]$

	U11	U22	U33	U23	U13	U12
C11	0.042(4)	0.038(3)	0.073(5)	-0.003(3)	-0.001(4)	-0.002(3)
C12	0.049(4)	0.034(3)	0.057(5)	-0.018(3)	0.010(4)	-0.005(3)
C13	0.053(4)	0.051(4)	0.046(4)	-0.014(3)	0.015(3)	0.001(3)
C14	0.058(5)	0.105(6)	0.066(6)	-0.005(5)	0.017(4)	0.009(4)
C15	0.096(7)	0.161(10)	0.063(6)	0.024(6)	0.026(6)	0.016(7)
C17	0.063(5)	0.088(6)	0.088(7)	-0.015(5)	0.025(5)	-0.014(4)
C18	0.056(4)	0.063(4)	0.066(5)	-0.012(4)	0.010(4)	-0.020(3)
C21	0.105(7)	0.075(5)	0.071(6)	0.039(5)	0.016(5)	0.004(5)
C22	0.068(5)	0.067(5)	0.057(5)	-0.003(4)	0.029(4)	-0.003(4)
C23	0.058(4)	0.070(5)	0.050(5)	-0.006(4)	0.019(4)	-0.004(4)
C24	0.056(5)	0.083(6)	0.063(5)	-0.002(4)	0.024(4)	0.000(4)
C25	0.064(6)	0.118(7)	0.082(7)	-0.001(5)	0.023(5)	-0.007(5)
C26	0.073(6)	0.129(9)	0.085(7)	-0.025(7)	0.015(5)	0.013(7)
C27	0.065(6)	0.145(10)	0.106(8)	-0.063(7)	0.036(6)	-0.049(6)
C28	0.086(6)	0.088(6)	0.092(7)	-0.031(5)	0.032(5)	-0.023(5)
C31	0.048(4)	0.052(4)	0.054(4)	0.002(3)	0.001(3)	0.001(3)
C32	0.040(4)	0.051(4)	0.059(5)	-0.005(4)	0.007(4)	0.000(3)
C33	0.040(4)	0.054(4)	0.062(5)	0.008(4)	0.011(3)	0.012(3)
C34	0.077(5)	0.055(5)	0.093(7)	0.006(4)	0.004(5)	0.016(4)
C35	0.099(7)	0.096(8)	0.127(9)	0.034(7)	-0.011(6)	0.024(6)
C36	0.128(9)	0.057(5)	0.140(10)	0.011(6)	-0.003(8)	0.021(6)
C37	0.105(7)	0.063(6)	0.111(8)	-0.006(5)	-0.003(6)	0.009(5)
C38	0.073(5)	0.044(4)	0.091(6)	-0.008(4)	0.003(4)	0.007(4)
C41	0.040(3)	0.039(3)	0.049(4)	0.003(3)	-0.002(3)	-0.003(3)
C42	0.038(3)	0.040(3)	0.053(4)	-0.004(3)	0.005(3)	0.006(3)
C43	0.040(3)	0.041(3)	0.047(4)	-0.002(3)	0.001(3)	0.011(3)
C44	0.065(4)	0.046(4)	0.050(5)	-0.002(3)	0.014(4)	0.002(3)
C45	0.076(5)	0.070(5)	0.049(5)	0.009(4)	0.003(4)	0.009(4)
C46	0.082(5)	0.069(5)	0.055(5)	-0.011(4)	-0.003(4)	0.024(4)
C47	0.076(5)	0.055(4)	0.063(5)	-0.011(4)	-0.008(4)	-0.002(4)
C48	0.055(4)	0.049(4)	0.050(4)	0.001(3)	0.001(3)	0.003(3)
C51	0.044(4)	0.069(5)	0.035(4)	0.004(3)	-0.003(3)	-0.010(3)
C52	0.037(4)	0.067(4)	0.044(4)	-0.001(3)	0.003(3)	-0.007(3)
C53	0.043(4)	0.070(5)	0.048(4)	-0.005(4)	0.008(3)	0.000(3)
C54	0.066(5)	0.071(5)	0.067(5)	-0.007(4)	-0.013(4)	0.003(4)
C55	0.108(7)	0.069(6)	0.093(7)	-0.011(5)	-0.021(6)	0.008(5)
C56	0.115(7)	0.069(5)	0.089(7)	0.012(5)	0.002(6)	0.023(5)
C57	0.085(6)	0.085(6)	0.074(6)	0.005(5)	-0.010(5)	0.012(5)
C58	0.056(4)	0.080(6)	0.056(5)	-0.003(4)	0.000(4)	0.001(4)
C61	0.044(4)	0.050(4)	0.056(5)	0.016(4)	-0.011(3)	-0.012(3)
C62	0.047(4)	0.042(4)	0.047(4)	-0.002(3)	-0.004(3)	0.000(3)
C63	0.047(4)	0.046(4)	0.059(5)	-0.007(3)	0.009(3)	0.002(3)
C64	0.058(4)	0.062(4)	0.052(5)	-0.007(4)	0.010(4)	-0.005(3)
C65	0.069(5)	0.092(6)	0.053(5)	-0.004(4)	0.004(4)	-0.006(4)
C66	0.073(5)	0.089(6)	0.058(5)	-0.010(4)	-0.009(4)	-0.015(5)
C67	0.073(5)	0.063(5)	0.068(6)	0.000(4)	-0.006(4)	-0.023(4)
C68	0.063(4)	0.049(4)	0.058(5)	-0.001(3)	0.003(4)	-0.008(3)
C71	0.047(4)	0.052(4)	0.052(4)	-0.001(3)	0.001(3)	-0.014(3)
C72	0.046(4)	0.045(4)	0.043(4)	-0.012(3)	0.006(3)	-0.008(3)
C73	0.050(4)	0.046(4)	0.049(4)	-0.008(3)	0.002(3)	0.002(3)
C74	0.057(4)	0.059(4)	0.062(5)	-0.013(4)	0.008(4)	-0.008(3)

C75	0.072(5)	0.086(6)	0.074(6)	-0.009(5)	0.026(5)	-0.017(4)
C76	0.077(6)	0.121(8)	0.087(8)	0.027(6)	0.044(6)	0.007(5)
C77	0.091(7)	0.165(10)	0.068(7)	0.044(6)	0.019(5)	0.020(7)
C78	0.058(5)	0.100(6)	0.064(6)	0.012(5)	0.014(4)	0.013(4)
C81	0.072(5)	0.066(5)	0.054(5)	0.005(4)	-0.003(4)	-0.027(4)
C82	0.075(5)	0.065(5)	0.051(5)	-0.002(4)	0.032(4)	-0.012(4)
C83	0.059(5)	0.080(6)	0.074(6)	-0.015(4)	0.031(4)	-0.019(4)
C84	0.069(6)	0.077(6)	0.097(7)	-0.003(5)	0.034(5)	-0.009(4)
C85	0.072(6)	0.104(7)	0.126(9)	-0.001(6)	0.042(6)	0.006(6)
C86	0.081(7)	0.103(8)	0.185(13)	-0.018(8)	0.034(7)	0.009(7)
C87	0.052(6)	0.145(11)	0.204(14)	-0.039(10)	0.038(7)	-0.021(6)
C88	0.078(6)	0.083(6)	0.150(10)	-0.022(6)	0.038(6)	-0.009(5)
Ag1	0.0455(3)	0.0400(3)	0.0716(4)	-0.0032(2)	0.0025(3)	-0.0056(2)
Ag2	0.0720(4)	0.0544(3)	0.0643(4)	0.0014(3)	0.0033(3)	0.0026(3)
Ag3	0.0559(3)	0.0715(4)	0.0614(4)	0.0031(3)	0.0123(3)	-0.0045(3)
Ag4	0.0432(3)	0.0553(3)	0.0673(4)	0.0093(3)	0.0014(3)	0.0033(2)
Ag5	0.0554(3)	0.0676(3)	0.0534(4)	0.0030(3)	0.0063(3)	-0.0192(3)
Ag6	0.0445(3)	0.0635(3)	0.0569(4)	0.0072(3)	-0.0006(2)	-0.0033(2)
Ag7	0.0475(3)	0.0503(3)	0.0678(4)	-0.0032(3)	-0.0012(3)	-0.0103(2)
Ag8	0.0677(4)	0.0597(3)	0.0472(3)	0.0008(2)	0.0012(3)	-0.0036(3)
N11	0.047(3)	0.060(3)	0.060(4)	-0.007(3)	0.006(3)	-0.008(3)
N12	0.039(3)	0.054(3)	0.091(5)	-0.015(3)	0.006(3)	-0.011(3)
N21	0.072(4)	0.077(5)	0.111(6)	0.031(4)	0.041(4)	0.015(4)
N31	0.038(3)	0.057(4)	0.072(4)	0.002(3)	-0.003(3)	0.008(3)
N32	0.050(3)	0.057(3)	0.070(4)	-0.001(3)	-0.005(3)	-0.004(3)
N41	0.056(3)	0.039(3)	0.042(4)	0.002(3)	-0.005(3)	-0.002(2)
N42	0.058(3)	0.039(3)	0.042(3)	0.003(2)	-0.002(3)	-0.003(2)
N51	0.043(3)	0.076(4)	0.049(4)	-0.005(3)	-0.004(3)	-0.003(3)
N52	0.048(3)	0.076(4)	0.047(4)	-0.005(3)	0.001(3)	-0.020(3)
N61	0.068(4)	0.039(3)	0.047(4)	0.001(3)	-0.011(3)	-0.010(3)
N62	0.058(3)	0.063(4)	0.051(4)	0.009(3)	-0.002(3)	-0.010(3)
N71	0.050(3)	0.061(3)	0.045(3)	-0.004(3)	0.005(3)	-0.013(3)
N72	0.043(3)	0.053(3)	0.068(4)	-0.008(3)	0.005(3)	-0.008(3)
N81	0.065(4)	0.072(4)	0.062(4)	0.008(3)	0.014(3)	-0.025(3)
N82	0.076(4)	0.090(5)	0.067(4)	0.038(4)	-0.009(3)	-0.035(4)
O11	0.052(3)	0.055(3)	0.067(3)	0.001(2)	0.005(3)	0.003(2)
O21	0.057(3)	0.072(3)	0.074(4)	-0.008(3)	0.019(3)	-0.001(3)
O31	0.062(3)	0.049(3)	0.067(3)	-0.003(2)	-0.006(3)	0.011(2)
O41	0.068(3)	0.051(3)	0.058(3)	-0.009(2)	0.017(2)	-0.017(2)
O51	0.066(3)	0.061(3)	0.053(3)	-0.007(2)	-0.013(3)	0.004(2)
O61	0.052(3)	0.066(3)	0.056(3)	-0.008(2)	0.007(2)	-0.012(2)
O71	0.055(3)	0.066(3)	0.043(3)	0.001(2)	0.005(2)	0.002(2)
O81	0.062(3)	0.061(3)	0.084(4)	-0.005(3	0.024(3)	-0.025(3)
S1	0.0506(10)	0.0455(9)	0.0707(13)	-0.005 (8)	0.0136(9)	-0.0103(7)
S2	0.0658(12)	0.0636(11)	0.0720(14)	0.0170(10)	0.0122(10)	0.0119(9)
S3	0.0494(10)	0.0548(10)	0.0675(13)	-0.0075(9)	0.0010(9)	0.0056(8)
S4	0.0511(9)	0.0417(8)	0.0503(11)	-0.0022(7)	0.0032(8)	0.0002(7)
S5	0.0488(10)	0.0574(10)	0.0558(11)	-0.0025(8)	0.0020(8)	-0.0127(8)
S6	0.0570(10)	0.0542(10)	0.0486(11)	0.0015(8)	0.0005(8)	-0.0059(8)
S7	0.0472(9)	0.0578(10)	0.0575(11)	-0.0050(8)	0.0089(8)	-0.0132(8)
S8	0.0625(11)	0.0623(11)	0.0562(12)	0.0115(9)	0.0040(9)	-0.0040(9)